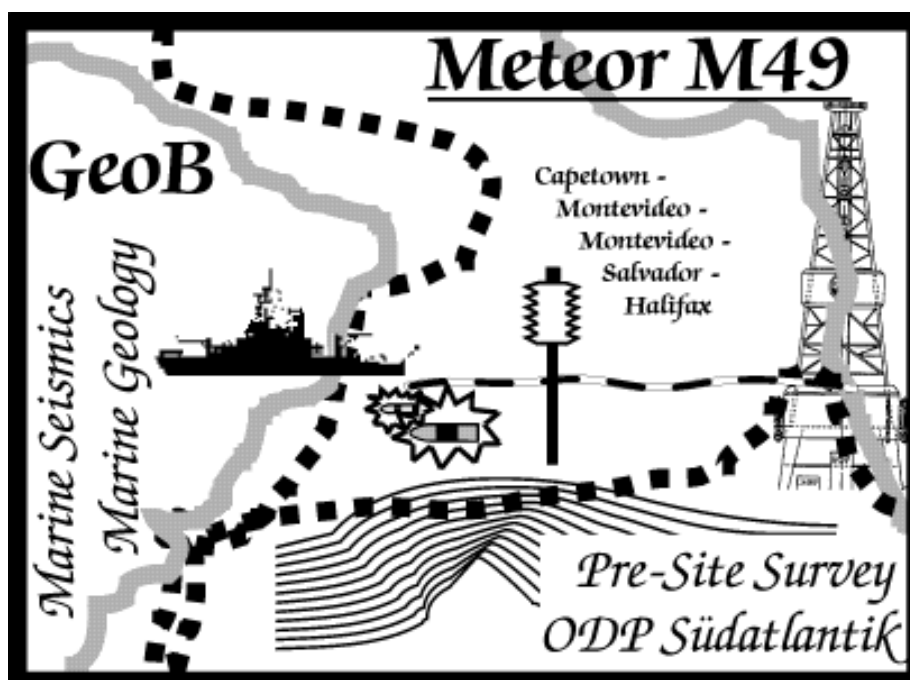


METEOR-Berichte 02-1
ODP Südatlantik 2001

Part 2

Cruise No. 49, Leg 2

13 February – 7 March 2001, Montevideo – Montevideo



V. Spieß, N. Albrecht, T. Bickert, M. Breitzke, M. Brüning, A. Dreyzehner, U. Groß,
D. Krüger, H. von Lom-Keil, H.-J. Möller, M. Nimrich, W.-T. Ochsenhirt,
T. Rudolf, C. Seiter, T. Truscheit, R. Violante, T. Westerhold

Editorial Assistance:

Frank Schmieder, Hanno von Lom-Keil
Fachbereich Geowissenschaften, Universität Bremen

Leitstelle METEOR
Institut für Meereskunde der Universität Hamburg

2.1 Participants

Name	Discipline	Institution
Spieß, Volkhard, Prof. Dr., Chief Scientist	Geophysics	GeoB
Albrecht, Nicole, Student	Geophysics	GeoB
Bickert, Torsten, Dr.	Marine Geology	GeoB
Breitzke, Monika, Dr. habil.	Geophysics	GeoB
Brüning, Markus, Student	Geophysics	GeoB
Dreyzehner, Anke, Student	Geophysics	GeoB
Groß, Ulrike, Student	Marine Geology	GeoB
Krüger, David, Student	Geophysics	GeoB
von Lom-Keil, Hanno, Dipl.-Geophys.	Geophysics	GeoB
Möller, Hans-Joachim, Dipl.-Meteor.	Meteorology	DWD
Nimrich, Mirja, Student	Geophysics	GeoB
Ochsenhirt, Wolf-Thilo, Technician	Meteorology	DWD
Rudolf, Thessa, Student	Geophysics	GeoB
Seiter, Christian, Student	Geophysics	GeoB
Truscheit, Torsten, Technician	Meteorology	DWD
Violante, Roberto, Dr.	Geology/Argentine Observer	SHN
Westerhold, Thomas, Dipl.-Geol.	Marine Geology	GeoB

DWD	Deutscher Wetterdienst – Seewetteramt - Bernhard-Nocht-Straße 76, 20359 Hamburg, Germany
GeoB	Fachbereich Geowissenschaften, Universität Bremen Klagenfurter Straße, 28334 Bremen, Germany
SHN	Servicio de Hidrografia Naval Departamento Oceanografia, Geologia Marina Av. Montes de Oca 2124, C1270ABV Buenos Aires, Argentina

2.2 Research Program

Synopsis

R/V METEOR Cruise M49 combined four legs of the 'ODP South Atlantic 2001' expedition to the Walvis Ridge, to the eastern South American continental margin off central to northern Argentina, Uruguay, and southern Brazil and to the equatorial Atlantic. All cruises were entirely or in major parts dedicated to pre-site surveys for active Ocean Drilling Program (ODP) proposals aiming at documenting and reconstructing the Paleogene and Neogene palaeoceanographic history from sedimentary deposits in various key regions of the South Atlantic.

This second leg M49/2 concentrated with multichannel reflection seismic, sediment echosounder and bathymetric swath sounder surveying as well as with geologic sampling on the Argentine and Uruguayan continental margin. Investigations were pursued during leg M49/3 further to the north. Both cruises are to support the ODP proposal '*Brazil – Falkland (Malvinas) Confluence: Palaeoceanography of a Mixing Region*' (Wefer et al., 1999) by identifying appropriate drill sites to recover continuous undisturbed Neogene sedimentary sequences allowing a detailed reconstruction of the past oceanographic and climatic evolution.

Scientific Background

The Neogene palaeoceanography of the south western South Atlantic is of principal importance to understand the past global oceanic circulation system and its link to the geologic record. Wefer et al. (1999) have proposed an ODP scientific drilling campaign in this region, for the first time comprising a number of transects on the Atlantic margin of South America at the boundary of the Argentine Basin between the Falkland Islands (Malvinas) and the Rio Grande Rise. Main target is the Brazil Current and the Falkland (Malvinas) Current. The dynamics of this region are consequential in several contexts: for the heat budget of the South Atlantic, for the production of intermediate water, and for the efficacy of regional biologic productivity.

Due to the well known complexity of depositional regimes at the Atlantic South American continental margin, two R/V METEOR cruises employing geophysical methods of multichannel reflection seismics, PARASOUND sediment sounding and HYDROSWEEP swath bathymetry sounding combined with geologic sampling of the water column and the sedimentary deposits were assigned to the task of identifying a series of suitable ODP deep drilling sites.

During the cruise M49/2 pre-site surveys were carried out in two different sectors off Argentina (working areas A and B) and off Uruguay (working area C). The consecutive cruise M49/3 was to operate off southern Brazil (working areas D and E). Relatively sparse information about the Cenozoic history of these regions is available from previous investigations, mainly because of the extraordinary heterogeneity of topography and sedimentary structures and the strong influence of bottom currents limiting the lateral continuity and extent of reflectors and sediment units. Knowledge of the near surface Quaternary sedimentation was improved during several R/V METEOR Cruises: M23/2 (Bleil et al., 1994), M29/1 (Segl et al., 1994), M29/2 (Bleil et al., 1994), M46/2 (Schulz et al., 2001) and M46/3 (Bleil et al., 2001). Of primary interest for the present cruise M49/2 are the upper 200 to 600 m of the sediment cover that cannot be explored with sediment echosounding nor sampled by conventional coring techniques. While the structural and stratigraphic resolution of standard seismic instrumentation is on the order of 10 m or less, the Bremen equipment allows for much more detailed insight.

Methods

Geophysical activities particularly focus on seismic and echographic surveys using the Bremen high-resolution multichannel seismic equipment to depict small scale sedimentary structures and closely spaced layers which cannot be resolved with conventional seismic systems. The alternating operation of a small volume watergun (200 – 1600 Hz) and two larger chamber GI airguns (100 – 500 Hz) simultaneously produces two seismic data sets, one of deeper penetration contributing extended insight into the structural and temporal context of near surface depositional processes and a second revealing details of the upper about 200 m of sediment cover.

Seismic measurements are complemented by high frequency digital recordings with the shipboard PARASOUND sediment echosounder and HYDROSWEEP swath sonar systems. The broad signal frequency spectrum of the seismoacoustic data sets acquired secures an optimum morphologic and structural resolution at all depth levels of the sedimentary formations. Both shipboard echographic systems are permanently operated on a 24 hours watch schedule during the cruise for the best possible selection and positioning of sediment sampling locations. Furthermore, multiple frequency recordings of the PARASOUND sediment echosounder are performed at geologic sampling sites for a direct comparison with sedimentological parameters and detailed shore based physical properties core log measurements which are later performed in the University of Bremen laboratories.

Working Plan

In the three projected working areas A, B and C seismic surveys were accomplished with the primary objective to locate appropriate sites for deep drilling operations. The investigations concentrate on water depths between 1000 and 4000 m to cover the influences of different major water masses such as North Atlantic Deep Water (NADW) and Antarctic Bottom Water (AABW) on depositional regimes and sedimentation processes.

Already during the cruise seismic data sets are processed to support further planning and particularly to define crossing points on recorded lines, where promising structures were encountered that may be selected as potential drill sites. The analysis of sediment layering shall ensure that deposition was as continuous as possible and that major hiatuses can be avoided.

The main objective of geological work is the sampling of Quaternary sediments on the Argentine and Uruguayan continental margin. The materials are analysed for the stratigraphic and sedimentologic characterization of the top sequences at potential ODP coring sites. Moreover, they will be used to continue and extend palaeoceanographic studies in the scope of a long-term program aimed at reconstructing the mass budget and current systems of the South Atlantic during late Quaternary established as a Special Research Project (SFB 261) at the University of Bremen since 1989. Along the proposed transects over the continental margin sediments are recovered from different water depths with multicorer and gravity corer devices. Their detailed investigation with sedimentological, geochemical and micropalaeontological methods will yield information about the history of water mass fluctuations and sustain the understanding of past ocean circulation and the mechanisms of late Quaternary climatic changes. Wherever structural settings should provide an opportunity, also older deposits rising to near surface will be recovered to date deeper reflectors.

2.3 Narrative of the Cruise

R/V Meteor Cruise M49/2 started in Montevideo, Uruguay, on February, 13th, to carry out marine geophysical studies at the Argentine and Uruguayan continental margin. The cruise was dedicated to a pre-site survey for the drilling proposal “Brazil-Falkland (Malvinas) Confluence: Paleooceanography of a Mixing Region” for the Ocean Drilling Program (ODP), which includes multichannel seismics and geologic sampling. From departure at 10 am we headed to the southernmost working area at 45°S. The transit time of two days was just sufficient to prepare the new scientific crew for the watchkeeping operations, to set up the sampling devices as gravity corer, multicorer and box corer, to prepare the laboratories and to make a plan for the first few survey lines. The seismic survey started on February, 15th, in the afternoon.

The first survey area was chosen in the vicinity of a system of large canyons, some with a depth of more than 1000 meters. Since the continental margin was shaped by strong contour currents passing in North-South direction as part of the North Atlantic Deep Water as well as in South-North direction originating from the Antarctic Bottom Water and shallow water masses, the survey focused on locations, where sedimentation was protected or enhanced. In the vicinity of large canyons we could observe drift deposits on both flanks, which seemed to provide more complete sedimentary sections than anywhere else near 45°S. Since the drift deposits revealed a limited lateral and downslope extent, a narrow grid of survey lines was required to identify individual depocenters. A few seismic lines towards the southern part of the working area indicated a transition to a purely erosive character at all water depths, and suitable drilling locations could not be identified. After 5 days of surveying, in the morning of February, 20th, we started a sampling program at 4 locations, before seismic surveying was continued around midnight of February, 21st. After another 18 hours, where seismic lines were collected along a dense grid near a large drift deposit on the northern flank of a large canyon, we finished the survey and collected sediment material with gravity corer from another 4 locations, partly at steep flanks to date deeper reflectors and older sediments. At this stage, we had collected sufficient data to map out depositional patterns, to trace reflectors of regional significance, but stratigraphic identification must await further shorebased analyses.

In the early morning of February, 22nd, we completed our program in the southernmost working area and moved to a box between 40°S and 41°S, reaching it for deployment of the seismic equipment around midnight of February, 23rd. To reach the goals of the proposed drilling campaign, which plans a reconstruction of the warm and cold water confluence near the coast and their evolution through geologic time as well as their impact on biologic productivity and depositional style, it would be necessary to drill a latitudinal transect. Therefore, the original proposed drilling plan was targeted to five areas from 45°S through 25°S, where it would be ideal to identify roughly evenly spaced suites of appropriate drilling locations for Neogene sediments. The area near 40°S reveals a steeper morphology than further south, but it is located on the North-South transect in a critical position just south of the Rio de la Plata depocenter. Also here, the margin is shaped by numerous canyons, drift and slump deposits, showing sediment waves and wedge shaped units and pronounced unconformities. But sediment units are much thinner, and erosional features more pronounced. The 4-day seismic survey, ending in the afternoon of February, 26th, revealed a complex depositional style, where potential drilling locations were more difficult to find than in the South. After a small sampling program at 3 locations we therefore decided in the evening of February, 26th, to continue our work - after a 14 hour transit - off the mouth of the Rio de la Plata river near the Mar del Plata Canyon, where our Argentine colleagues had recently carried out a seismic survey.

The Mar del Plata Canyon, revealing steep flanks of more than 1000 m height, is located seaward of the Rio de la Plata mouth. In its vicinity, accumulation rates seemed to be significantly higher and in particular on a plateau from 900 m through 1300 m water depth sediment packages with parallel layering were

found. On the other hand, large areas of older sediments were exposed, partly caused by massive slumping and partly by strong erosive currents in medium water depth. Seaward of the exposed Miocene sequences undulating reflectors were observed indicating drift deposits. The seismic survey, ranging from 39°S through 37°S, was planned to cover both the northern and southern flanks of the canyon and to run a sufficient number of slope parallel and downslope profiles to characterize the plateau, the exposed units and the transition to drift sediments, and to map out reflectors of regional significance. Profiling was continued over 5 days and finished in the morning of March, 3rd.

Based on observations of our Argentine colleagues, on our own survey and some results from early sampling campaigns we were able to locate sediment units of early Neogene age within this complex, which were subsequently sampled at 6 locations with gravity corer.

During a 9 hour transit we moved from Argentine to Uruguayan waters to carry out only seismic investigations in the last survey box between 36°40'S and 36°S, beginning in the early morning of March, 4th. This area had been visited already during the Meteor Cruise M29/2 in 1994, and sediments of Pleistocene age were well known from several sampling sites to be fine-grained and organic rich. They derive from the suspended matter transported by the Rio de la Plata, which is moved northward by coastal currents into the working area. High water content and low rigidity supported frequent destabilization of slope sediments and mass flow deposits extending over wide areas. The seismic data revealed that the continental slope deeper than 1500 m water depth was heavily affected by slumping and suitable drilling locations could not be identified. Only at the upper slope, candidate locations for drilling were chosen, but geologic sampling was not appropriate due to the lack of exposed sections older than latest Neogene. 18 hours before arrival in port we finished the survey program in the northernmost area of the Meteor M49/2 Cruise around noon on March, 6th. In the night we headed towards the port of Montevideo to arrive in the morning of March, 7th. Port activities were limited to crew exchange only, since the following cruise should continue the survey program for the drilling proposal. However, the successful cruise was complemented by a very successful reception with more than 50 guests on March, 8th, expressing the thanks to the friendly welcome in Uruguay, crew and scientists had received several times in Uruguay in recent years.

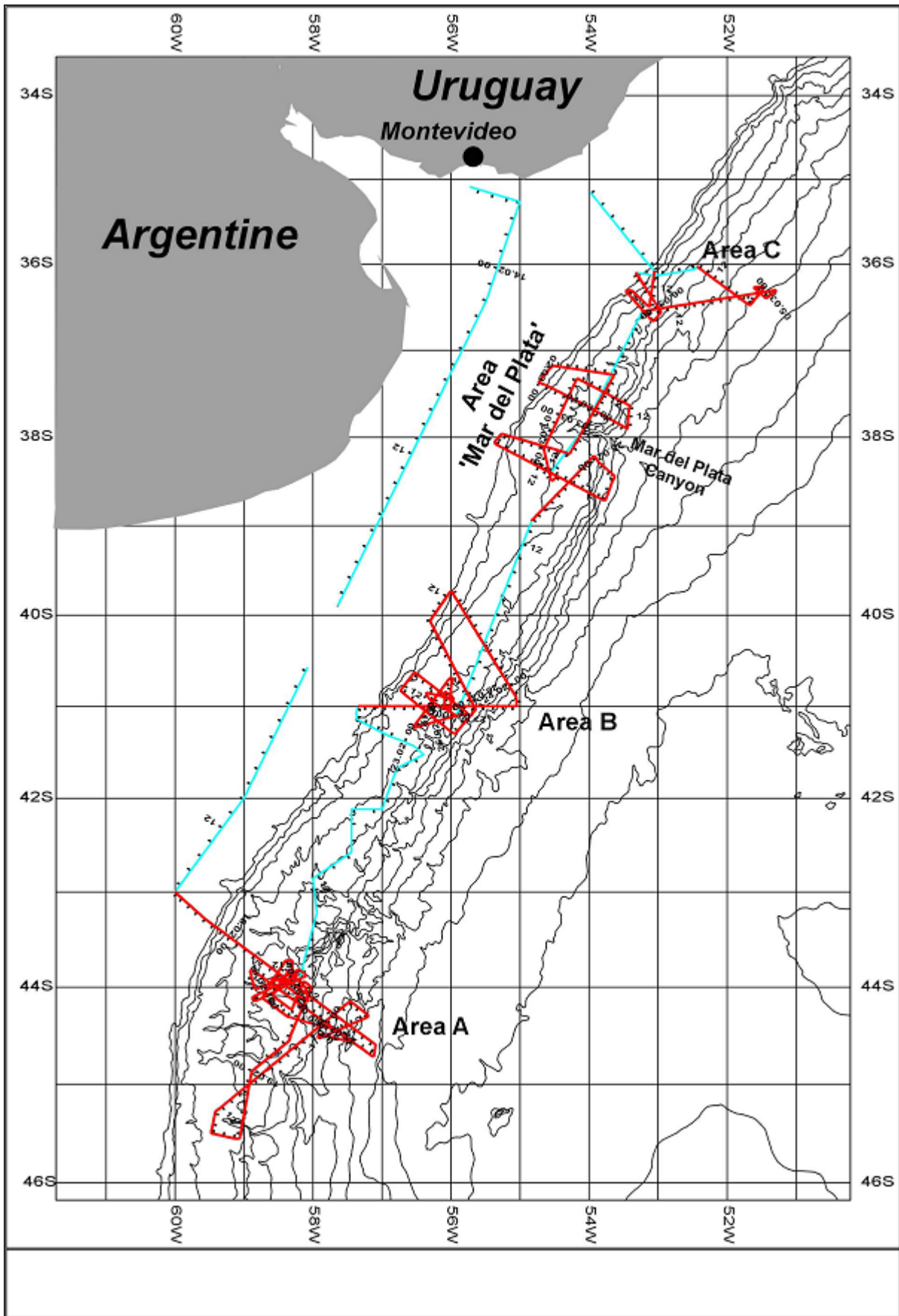


Fig. 2.1: Track Chart of R/V METEOR Cruise M49/2 with seismic lines indicated in red, HYDROSWEEP/PARASOUND survey lines in blue. Bathymetry from Gebco Digital Atlas.

2.4 Preliminary Results

2.4.1 Underway Geophysics

(M. Breitzke, N. Albrecht, M. Brüning, A. Dreyzehner, D. Krüger, H. v. Lom-Keil, M. Nimrich, T. Rudolf, C. Seiter, V. Spieß)

2.4.1.1 Study Areas

The Argentine, Uruguayan and Southern Brazilian continental margins between Falkland Plateau in the south and Rio Grande Rise in the north lie at the western boundary of the central subtropical gyre. The warm southward flowing water masses of the Brazil Current join the cold northward flowing water masses of the Falkland (Malvinas) Current at about 40°S, where the latter is retroflected and both water masses begin to mix on their way southward [Peterson and Stramma, 1991]. Knowledge about the paleoceanographic history of this region and about the sedimentation processes and sedimentary structures on the continental margin of the southwestern South Atlantic is sparse and not well resolved, particularly for the Neogene sedimentation history [e.g. Hinz et al., 1999]. Up to now, ODP drill holes, where modern coring techniques like APC coring have been applied to recover high quality cores for paleoceanographic reconstructions are located in the eastern South Atlantic from equatorial latitudes to the South African Cape (Legs 108, 159, 175), in the Southern Ocean (Legs 113, 114, 177) and in the western equatorial Atlantic (Legs 154, 155), but are still lacking on the Argentine, Uruguayan and Brazilian continental margins in the southwestern South Atlantic. Only few DSDP sites exist here, but are mostly located either on the Falkland Plateau (DSDP 328, 511, 512), in the Argentine and Brazil Basins (DSDP 331, 358, 515), on the Rio Grande Rise (DSDP 516, 517, 518) or on the Sao Paulo Ridge (DSDP 356) far away from the eastern South American coast, and thus far away from the region where western boundary currents dominate and affect the composition and structures of the sediment coverage.

R/V Meteor Cruise M49/2 together with the subsequent cruise M49/3 was dedicated to a pre-site survey for ODP Proposal 556 "Brazil-Falkland (Malvinas) confluence: Paleoceanography of a Mixing Region" of Wefer et al.. Both cruises had the primary goal to collect high-resolution multichannel seismic, sediment echosounder and bathymetric swath sounder data from totally five study areas A - E proposed as potential drilling targets for a reconstruction of the Neogene paleoceanographic history of the Brazil-Falkland (Malvinas) confluence.

The three southern areas A, B and C are located off southern, central and northern Argentina and Uruguay at about 44°S, 41°S and between 39° - 34°S and were surveyed during R/V Meteor Cruise M49/2. Ewing and Lonardi [1971] and Lonardi and Ewing [1971] in former studies have shown that the continental slope in these areas is very steep and dissected by deeply incised furrows, channels and canyons probably originated by rivers and/or currents and now acting as conduits for downslope sediment transport. As a consequence extensive mass wasting occurs and slides, slumps, debris flow and turbidite deposits often interrupt an undisturbed, continuous sedimentation as record of the paleoenvironmental conditions. Additionally, high current intensities of the northward flowing Antarctic Bottom Water (AABW), of the southward flowing North Atlantic Deep Water (NADW) and of shallow water masses have produced rough sea floor topographies, erosional zones and hiatuses that prevent the recovery of continuous sediment sequences for paleoceanographic reconstructions as well, so that the search for undisturbed sediment sequences as potential drilling targets is a difficult task in these areas.

Additionally, in the northern part of area C off Uruguay and off southern Brazil a huge amount of terrigenous material is delivered by the Rio de la Plata and mixed with biogenic components so that sedimentation rates are very high. However, the high water content of these sediments facilitate downslope sediment transport processes along the steep Uruguayan margin, too.

The two northern areas D and E are located between 34° - 31°S and 29° - 25°S off southern and central Brazil on the Rio Grande Cone and on the Sao Paulo Plateau. They were surveyed during the subsequent R/V Meteor Cruise M49/3 [Bleil et al, 2001].

2.4.1.2 PARASOUND, HYDROSWEEP and Navigation

The Parasound system works as both a low-frequency narrow-beam sediment echosounder and a high-frequency narrow-beam echosounder to determine the water depth. It makes use of the parametric effect, which produces waves with secondary frequencies through nonlinear acoustic interaction of finite amplitude waves. If two sound waves of similar frequencies (here 18 kHz and e.g. 22 kHz) are emitted simultaneously, a signal of the difference frequency (e.g. 4 kHz) is generated for sufficiently high primary amplitudes. The new component is traveling within the emission cone of the original high frequency waves, which is limited to an angle of only 4° for the equipment used. Therefore, the footprint size of 7% of the water depth is much smaller than for conventional systems and both vertical and lateral resolution are significantly improved.

The Parasound system is permanently installed on the ship. The hull-mounted transducer array has 128 elements on an area of approximately 1 m². It requires up to 70 kW of electric power due to the low degree of efficiency of the parametric effect. In 2 electronic cabinets, beam forming, signal generation and separation of primary (18, 22 kHz) and secondary frequencies (4 kHz) is carried out. With the third electronic cabinet in the echosounder control room, the system is operated on a 24 hour watch schedule.

Since the two-way travel time in the deep sea is long compared to the length of the reception window of up to 266 ms, the Parasound System sends out a burst of pulses at 400 ms intervals, until the first echo returns. The coverage of this discontinuous mode depends on the water depth and produces non-equidistant shot distances between bursts. On average, one seismogram is recorded per second providing a spatial resolution on the order of a few meters on seismic profiles at 6.0 - 6.5 knots.

The main tasks of the operators are system and quality control and the adjustment of the start of the reception window. Because of the limited penetration of the echosounder signal into the sediment, only a short window close to the sea floor is recorded.

In addition to the analog recording features of the b/w DESO 25 device, which we did not use any more, the Parasound System is equipped with the digital data acquisition system PARADIGMA, which was developed at the University of Bremen [Spieß, 1993]. The data are stored on two exchangeable disc drives of 4 GByte capacity, allowing continuous recording between 5 and 10 days dependent on water depth and shot rate. The Pentium-processor based PC allows the buffering, transfer and storage of the digital seismograms at very high repetition rates. From the emitted series of pulses usually every second pulse is digitized and stored, resulting in recording intervals of 800 ms within a pulse sequence. The seismograms were sampled at a frequency of 40 kHz, with a typical registration length of 266 ms for a depth window of about 200 m. The source signal was a band limited, 2 - 6 kHz sinusoidal wavelet of 4 kHz dominant frequency with a duration of 2 periods (~500 µs total length).

Already during the acquisition of the data an online processing was carried out. For all profiles, Parasound sections were plotted with a vertical scale of several hundred meters. Most of the changes in window depth could thereby be eliminated. From these plots, a first impression of variations in sea floor morphology,

sediment coverage and sedimentation patterns along the ship's track could be gained. To improve the signal-to-noise ratio, the echogram sections were filtered with a wide band pass filter. In addition, the data were normalized to a constant value much smaller than the average maximum amplitude, to amplify especially deeper and weaker reflections.

During the entire cruise, the combined Parasound/PARADIGMA system worked without significant problems. The storage procedure with exchangeable hard discs worked successfully and reliably and avoided previously more frequent alert situations due to errors of magnetic tape recording.

The multibeam echosounder Hydrosweep on R/V Sonne was routinely used during the cruise and serviced by the Parasound operator during a 24-hour watch. Sounding 59 pre-formed beams over an opening angle of 90 degrees, the hull-mounted system provides an image of the sea floor topography with a path width of twice the water depth. The system operates at a frequency of 15.5 kHz. To compress refraction effects on the outer beams, the system uses a calibration mode to compare depth values of the central and outer beams in order to calculate a mean sound velocity by producing the best fit between both values. This configuration minimizes residual errors to values smaller than 0.5% of the water depth [Grant and Schreiber, 1990].

During the whole cruise GPS and DGPS were available and provided navigation data of satisfactory quality.

2.4.1.3 High-Resolution Multichannel Reflection Seismics

2.4.1.3.1 Methods and Instruments

Multichannel seismic surveying was carried out in all three study areas of Cruise M49/2. With the GeoB high-resolution multichannel seismic equipment, small scale sedimentary structures and closely spaced layers can be imaged on a meter to sub-meter scale, which can usually not be resolved with conventional seismic systems. The alternating operation of a small chamber watergun (0.16 L; 200 – 1600 Hz), a GI airgun with reduced chamber volume (0.4 L; 100 – 500 Hz), and a GI airgun with normal chamber volume (1.7 L; 30 – 200 Hz) yields three seismic data sets simultaneously. Guns with larger chamber volume are of greater penetration into the sea floor, revealing the larger scale structural framework, whereas guns with smaller chamber volume are of higher resolution, revealing finer details of the upper 200-400 m of the sediment cover beyond the penetration of the PARASOUND sediment echosounder (50-100 m). Figure 2.2 gives an outline of the system setup as it was used during R/V Meteor Cruise M49/2.

All multichannel seismic profiling activities are accompanied by a continuous operation of the two hydro-acoustic systems (Parasound sediment echosounder and Hydrosweep swath sounder) to determine the sea floor morphology, to characterize and analyze sediment deposition processes and structures in the uppermost 10 - 60 m, and to provide detailed very-high resolution information for site selection of gravity coring. Both hydro-acoustic data sets were acquired digitally.

Additionally, at locations where Cenozoic sediment sequences pinch out, deeper layers were sampled by gravity cores in order to achieve information on the stratigraphy of the sediment column (cf. chapter 4.2). These locations were selected on basis of the Parasound sediment echosounder data, the seismic online records and the brutestacks of the multichannel seismic data produced by onboard processing.

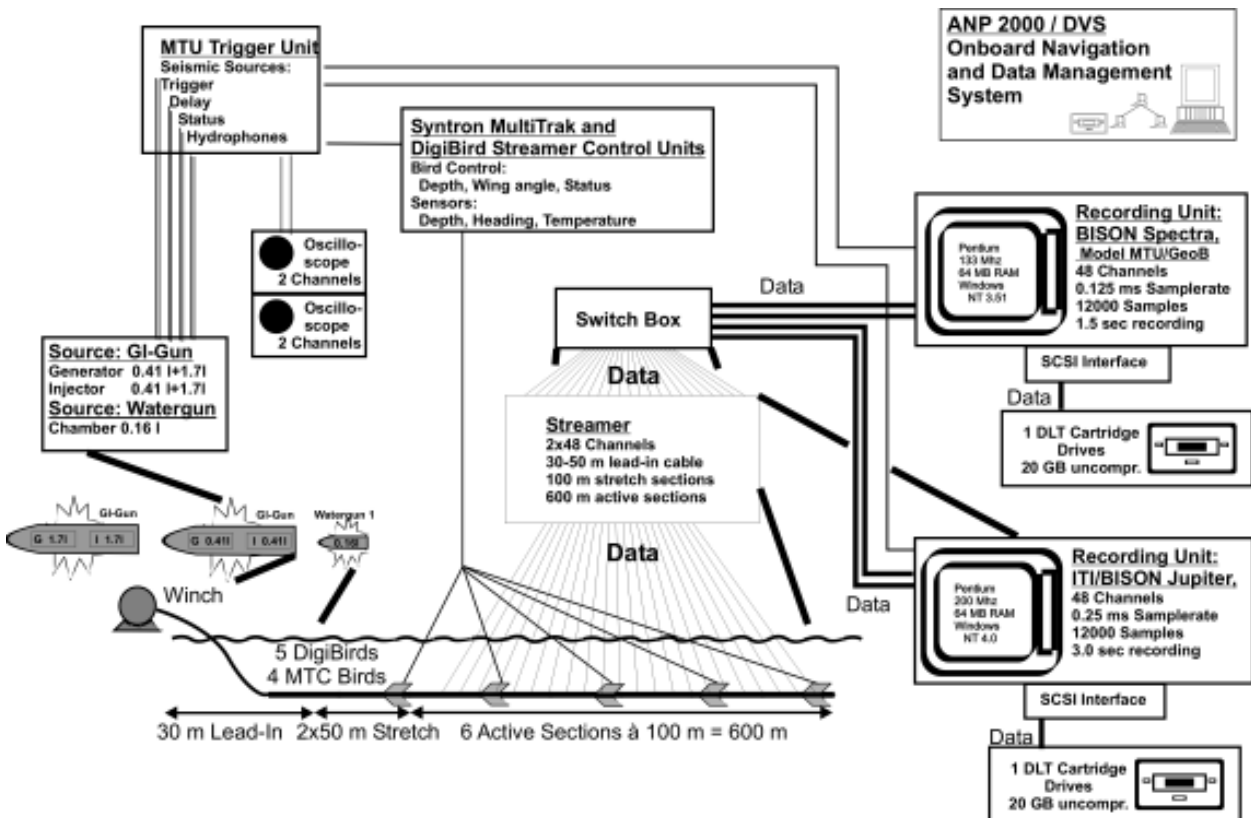


Fig. 2.2: Multichannel seismic instrumentation used during R/V METEOR Cruise M49/2

2.4.1.3.2 Seismic Sources and Compressor

During seismic surveying, three different seismic sources, two GI-Guns and one watergun, were triggered in an alternating mode at a time interval between 9 and 11.5 s (cf. Trigger Unit). Owing to an average ship speed of 6.0 - 6.5 kn, a shot distance of approximately 30 to 38 m was thus obtained for the alternating mode operation, corresponding to a shot point distance of 60 - 76 m for the same GI-Gun type and 30 - 38 m for the watergun (cf. Trigger Unit).

Each source type was shot more than 65'000 times at an air pressure of about 150 bar. Due to rough weather, the systems were temporarily operating under heavy conditions and pressure lines were broken several times. Complete data gaps, however, could be avoided, since only one of the sources had to be turned off at a time.

The geometry of source and receiver systems during the measurements is shown in Figure 2.3. Ship velocity during deployment and retrieval was between 2.5 and 3.5 kn, respectively, depending on weather conditions and surface currents.

The standard GI-Gun (Generator-Injector Gun; Sodera) with normal chamber volume (2 x 1.7 L) was towed by a wire, which was separate from the Meteor rope holding the umbilical of the gun about 17 m behind the ship's stern and 7 - 8 m portside of the streamer and the ship's axis. The towing wire was connected to a bow with the GI-Gun hanging on two chains 0.4 m beneath. An elongated buoy, which stabilized the gun in a horizontal position at a water depth of about 1.2 m, was connected to the bow by two rope loops. The injector was triggered with a delay of 50 ms with respect to the generator signal, which basically eliminated the bubble signal.

The second GI-Gun with reduced chamber volumes (2×0.41 L) was towed by the wire of the starboard side crane, set off perpendicular to the starboard side. Distance to the ship's stern was about 13 m, starboard distance to the streamer and ship's axis about 14 - 15 m. The towing wire was again connected to a bow with the GI-Gun hanging on two chains 0.4 m beneath. An elongated buoy, which stabilized the gun in a horizontal position at a water depth of about 1.2 m, was connected to the bow by two rope loops, as well. The injector was triggered with a delay of 30 ms with respect to the generator signal, which basically eliminated the bubble signal.

The third source was an S15 watergun (Sodera) with 0.16 L volume. It was towed by a wire which ran over a roll at starboard side and which was separate from the Meteor rope holding the umbilical of the gun about 15 m behind the ship's stern and about 4 - 5 m starboard side of the streamer and ship's axis. A steel frame held the watergun in a tight position parallel to the elongated buoy in a depth of approximately 0.6 m.

High-pressure air of 150 bar for gun operation was provided by the LMF compressor set up in an oversized container on the working deck and maintained by the ship's engineers. Only minor technical problems occurred. Due to the improved noise damping which was particularly achieved by re-routing the surplus air - which is about 90% of the total air production in case of our small volume guns - into the water by a hose close to the pulser station at portside, the noise level could significantly be reduced compared to our first R/V METEOR cruise M46/3 with this compressor container in 2000 [Bleil et al., 2001].

2.4.1.3.3 Streamer

The multichannel seismic streamer (SYNTRON) includes a tow-lead, two stretch sections of 50 m and six active sections of 100 m length each. A 100 m long Meteor rope with a buoy at the end was connected to the tail swivel. A 30 m long deck cable connected the streamer to the recording system. The winch location on the working deck is shown in Figure 2.3. During operations, the streamer (tow lead) was fixed with two Meteor ropes. The tow lead was laid out approximately 30 - 33 m.

Active sections are subdivided in 16 hydrophone groups of 6.25 m length (Figure 2.4). Each of these 6.25 m long hydrophone groups is subdivided into 5 subgroups of different length. One of the subgroups is a high-resolution hydrophone with preamplifier. A programming module distributes the subgroups of 4 hydrophone groups, i.e. a total of 20 groups, to 5 channels. As illustrated in Figure 2.4, every second 6.25 m hydrophone subgroup was completely used with all 13 hydrophones, whereas the two additional channels were reduced in length and number of hydrophones to 2.45 m (6 hydrophones) and 3.35 m (9 hydrophones), respectively. Midpoint locations of individual hydrophone groups are listed in Table 2.1.

A switch box connects the streamer via deck cable with the seismograph and allows the assignment and optional stacking of streamer hydrophone subgroups to individual recording channels. The incoming 120 channels (96 hydrophone groups and 24 single hydrophones) were distributed to the output channels of the recording system(s) with the same pattern during the whole cruise. Output channels 1 to 48 were connected to the Jupiter recording system (alternating mode of small- and large-chamber GI-Gun) (Table 2.2a), channels 49 to 96 to the Spectra recording system (watergun) (Table 2.2b). Single hydrophones (streamer channels 97 to 120) were not recorded.

Deployment and retrieval lasted approximately 45 minutes including installation of the ten Remote Bird Units (RUs; see below).

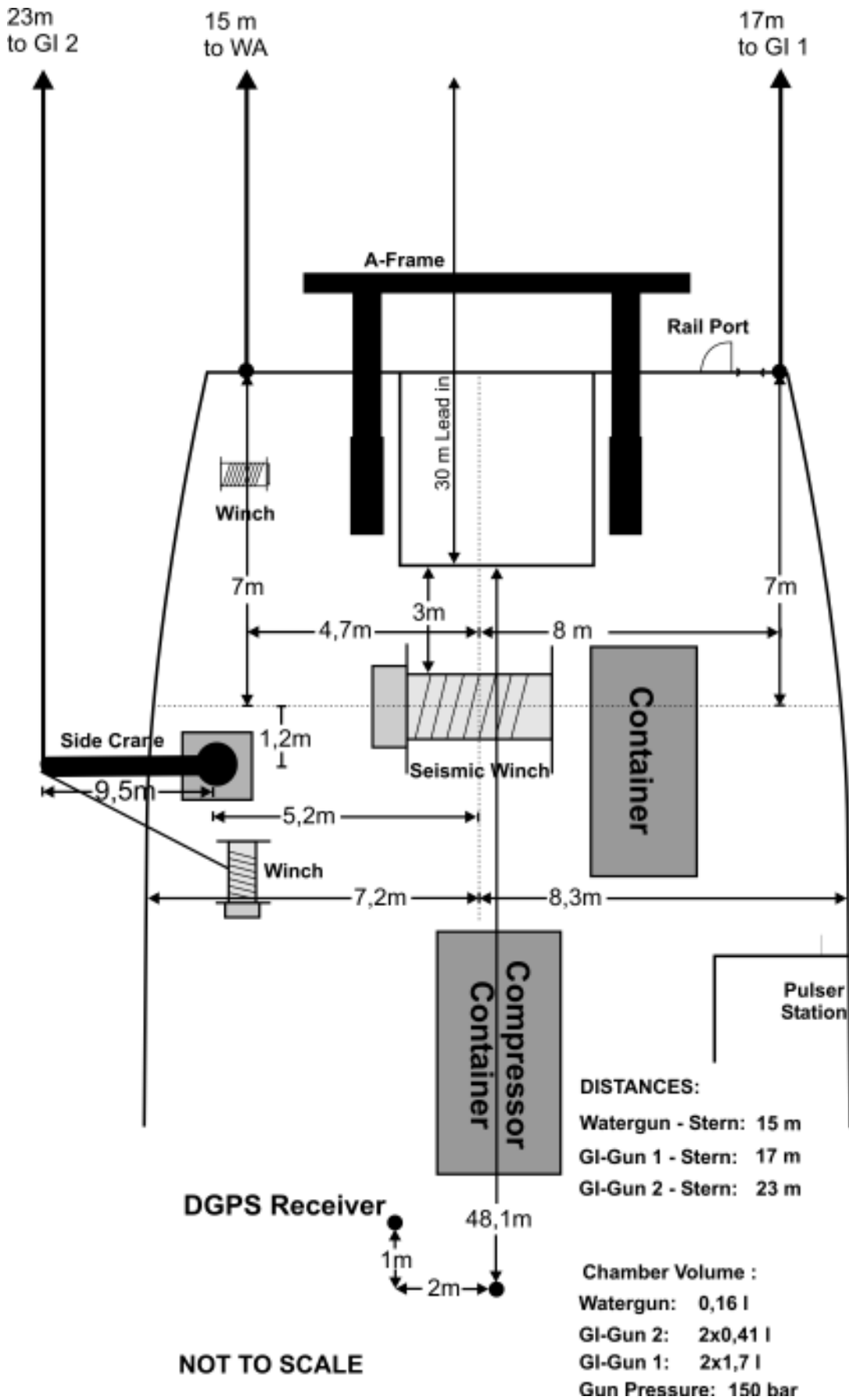


Fig. 2.3: Seismic working deck setting during R/V METEOR Cruise M49/2.

2.4.1.3.4 MultiTrak Controller, DigiBird Controller

In operation, 5 MultiTrak and 5 DigiBird Remote Units (RUs) were attached to the streamer. Each RU includes a depth and a heading sensor as well as adjustable wings. The RUs are controlled by two separate controllers in the seismic lab, the MultiTrak and the DigiBird controller. Controllers and RUs communicate via communication coils nested within the streamer. A twisted pair wire within the deck cable connects controllers and coils.

Each shot trigger started the bird scan of water depth, wing angle and heading data (delay 0.0 s, duration 1.0 s). The current location of the streamer can be displayed as a depth or heading profile on a monitor. All parameters are digitally stored on the controller PC, together with shot number, date and time.

There are two ways of controlling the streamer depth. The most common way is to send an operating depth range to the RUs (3 m during R/V Meteor Cruise M49/2). The RUs try to force the streamer to the predefined depth by adjusting the wing angles accordingly. Another option is to set a predefined wing angle or depth before deployment. This is useful if communication problems with RUs arise and was partially applied during this cruise. Depth and wing angle statistics help to set appropriate parameters.

Table 2.1: Channel assignment and midpoint distances of hydrophone groups from begin of each active section.

Segments of 25 m length	Hydrophone Group No.	Channel No. in Section	Midpoint Distance
A (0-25 m)	1	1	3.1 m
A	2	2	11.3 m
A	3	3	15.6 m
A	4	4	23.3 m
B (25-50 m)	1	5	28.1 m
B	2	6	36.3 m
B	3	7	40.6 m
B	4	8	48.3 m
C (50-75 m)	1	9	53.1 m
C	2	10	61.3 m
C	3	11	65.6 m
C	4	12	73.3 m
D (75-100 m)	1	13	78.1 m
D	2	14	86.3 m
D	3	15	90.6 m
D	4	16	98.3 m

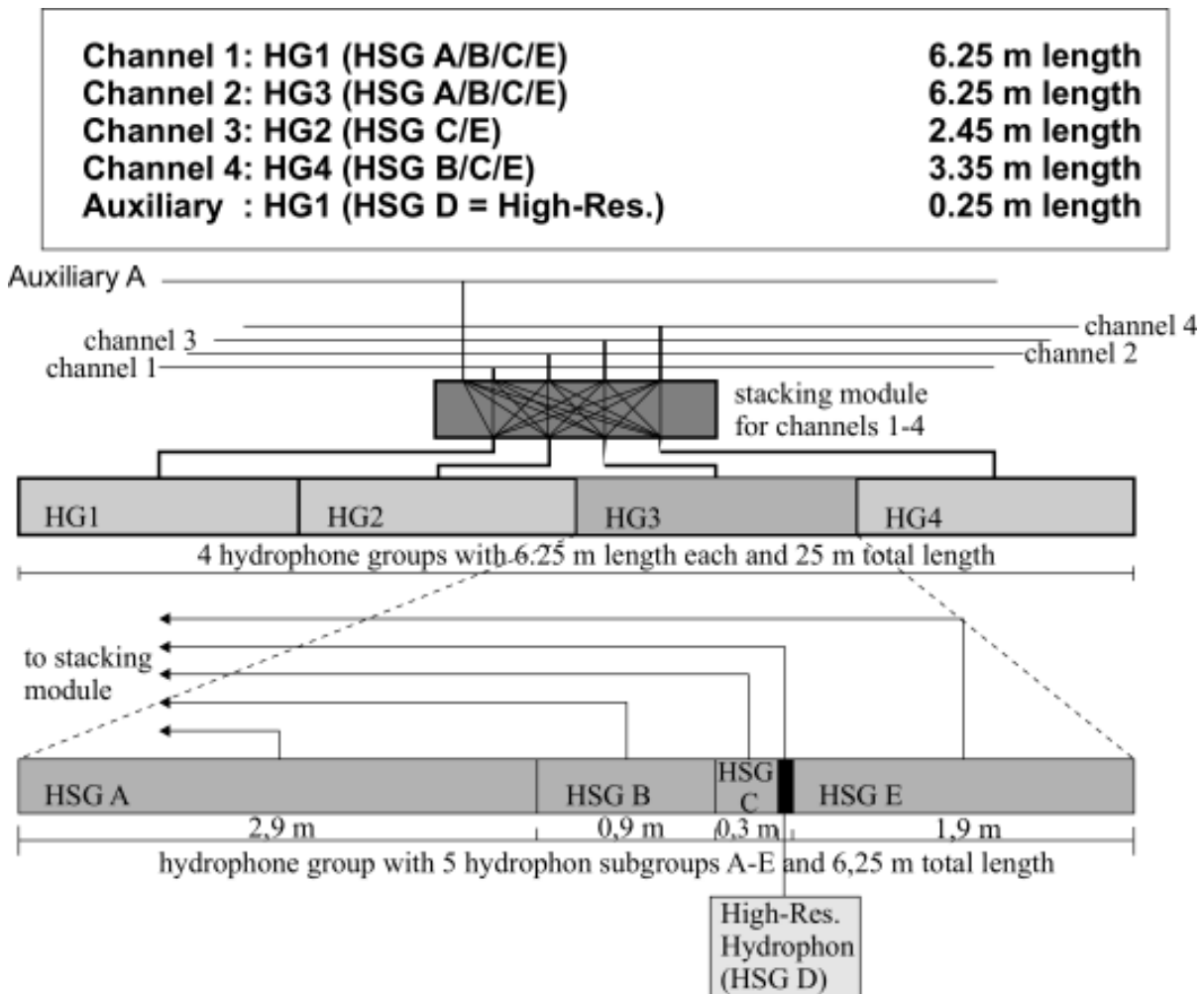


Fig. 2.4: Multichannel streamer design used during R/V METEOR Cruise M49/2.

Due to shark bites in the streamer during the preceding R/V METEOR Cruise M49/1 (Spieß et al., in prep.) and possibly induced seawater communication problems between the controllers in the seismic lab and the birds attached to the streamer occurred, i.e. more and more depth and heading values were lost. These problems could partially be solved by an appropriate positioning of the RUs along the streamer. Tables 2.3a-c describe the distribution of RUs during R/V METEOR Cruise M49/2 along the different profile lines. Possible depth variations of the streamer could be checked later during preliminary data processing, and despite of the communication problems, depth control appeared to be successful. In addition, the position of the tail buoy was frequently checked from the bridge to provide information about the heading of the streamer. In general, no sideward drift was observed.

2.4.1.3.5 Data Acquisition System

Two recording systems were used to acquire the multichannel seismic data, one for the GI-Gun data, a second for the wateregun data.

The first system is a 48 channel JUPITER/ITI/BISON seismograph, which allows a maximum sample frequency of 4 kHz at 24 bit resolution. It is based on a PENTIUM PC (200 MHz; 64 MB RAM) with a WINDOWS NT 4.0 operating system. The seismograph allows online data display (shot gather), online demultiplexing and storage in SEG-Y format on a DLT 4000 cartridge tape with 20 GByte uncompressed capacity. The GI-Gun data were recorded at a sample frequency of 4 kHz over an interval of 3 s, resulting in 48 x 12'000 samples of 4 bytes per shot. Preamplifiers were set to 48 dB, low cut filters to 4 Hz for each channel.

Table 2.2a: Streamer channel 1 to 48 assignment to output channels for Jupiter recording system (GI-Gun).

Input Channel	Output Channel	Hydrophone Group	Number of Hydrophones per Group	Hydrophone Group Length [m]	Hydrophone Group Distance [m]
1	1	HG1	13	6.25	12.5
2	2	HG3	13	6.25	12.5
5	3	HG1	13	6.25	12.5
6	4	HG3	13	6.25	12.5
9	5	HG1	13	6.25	12.5
10	6	HG3	13	6.25	12.5
13	7	HG1	13	6.25	12.5
14	8	HG3	13	6.25	12.5
17	9	HG1	13	6.25	12.5
18	10	HG3	13	6.25	12.5
21	11	HG1	13	6.25	12.5
22	12	HG3	13	6.25	12.5
25	13	HG1	13	6.25	12.5
26	14	HG3	13	6.25	12.5
29	15	HG1	13	6.25	12.5
30	16	HG3	13	6.25	12.5
33	17	HG1	13	6.25	12.5
34	18	HG3	13	6.25	12.5
37	19	HG1	13	6.25	12.5
38	20	HG3	13	6.25	12.5
41	21	HG1	13	6.25	12.5
42	22	HG3	13	6.25	12.5
45	23	HG1	13	6.25	12.5
46	24	HG3	13	6.25	12.5
49	25	HG1	13	6.25	12.5
50	26	HG3	13	6.25	12.5
53	27	HG1	13	6.25	12.5
54	28	HG3	13	6.25	12.5
57	29	HG1	13	6.25	12.5
58	30	HG3	13	6.25	12.5
61	31	HG1	13	6.25	12.5
62	32	HG3	13	6.25	12.5
65	33	HG1	13	6.25	12.5
66	34	HG3	13	6.25	12.5
69	35	HG1	13	6.25	12.5
70	36	HG3	13	6.25	12.5
73	37	HG1	13	6.25	12.5
74	38	HG3	13	6.25	12.5
77	39	HG1	13	6.25	12.5
78	40	HG3	13	6.25	12.5
81	41	HG1	13	6.25	12.5
82	42	HG3	13	6.25	12.5
85	43	HG1	13	6.25	12.5
86	44	HG3	13	6.25	12.5
89	45	HG1	13	6.25	12.5
90	46	HG3	13	6.25	12.5
93	47	HG1	13	6.25	12.5
94	48	HG3	13	6.25	12.5

Table 2.2b: Streamer channel 49 to 96 assignment to output channels for Spectra recording system (watergun).

Input Channel	Output Channel	Hydrophone Group	Number of Hydrophones per Group	Hydrophone Group Length [m]	Hydrophone Group Distance [m]
3	49	HG2	6	2.45	12
4	50	HG4	9	3.35	13
7	51	HG2	6	2.45	12
8	52	HG4	9	3.35	13
11	53	HG2	6	2.45	12
12	54	HG4	9	3.35	13
15	55	HG2	6	2.45	12
16	56	HG4	9	3.35	13
19	57	HG2	6	2.45	12
20	58	HG4	9	3.35	13
23	59	HG2	6	2.45	12
24	60	HG4	9	3.35	13
27	61	HG2	6	2.45	12
28	62	HG4	9	3.35	13
31	63	HG2	6	2.45	12
32	64	HG4	9	3.35	13
35	65	HG2	6	2.45	12
36	66	HG4	9	3.35	13
39	67	HG2	6	2.45	12
40	68	HG4	9	3.35	13
43	69	HG2	6	2.45	12
44	70	HG4	9	3.35	13
47	71	HG2	6	2.45	12
48	72	HG4	9	3.35	13
51	73	HG2	6	2.45	12
52	74	HG4	9	3.35	13
55	75	HG2	6	2.45	12
56	76	HG4	9	3.35	13
59	77	HG2	6	2.45	12
60	78	HG4	9	3.35	13
63	79	HG2	6	2.45	12
64	80	HG4	9	3.35	13
67	81	HG2	6	2.45	12
68	82	HG4	9	3.35	13
71	83	HG2	6	2.45	12
72	84	HG4	9	3.35	13
75	85	HG2	6	2.45	12
76	86	HG4	9	3.35	13
79	87	HG2	6	2.45	12
80	88	HG4	9	3.35	13
83	89	HG2	6	2.45	12
84	90	HG4	9	3.35	13
87	91	HG2	6	2.45	12
88	92	HG4	9	3.35	13
91	93	HG2	6	2.45	12
92	94	HG4	9	3.35	13
95	95	HG2	6	2.45	12
96	96	HG4	9	3.35	13

The second system, a 48 channel seismograph (BISON Spectra), was specially designed for the University of Bremen. It allows a continuous operation mode to acquire very high resolution seismic data with a sample rate up to 20 kHz. The seismograph (PENTIUM PC; 133 MHz; 64 MB RAM) is a predator of the above mentioned Jupiter system, runs under WINDOWS NT 3.51 and reveals basically the same features. It allows online data display (shot gather), online demultiplexing and storage in SEG-Y format on DLT 4000 cartridge tapes of 20 GByte uncompressed capacity. Sample frequency was 8 kHz for the watergun data, record length 1.5 s, resulting again in 48 x 12'000 samples of 4 bytes per shot. Preamplifiers were set to 60 dB, i.e. a multiplier of 1000, to ensure an optimum voltage range for digitizing the incoming signals. Analog low- and high-cut filters were set to 16 and 2000 Hz, respectively.

On both systems, the recording delay was controlled and adjusted to the current water depth by the trigger unit (cf. Trigger Unit).

Table 2.3a: RU positions along the seismic streamer for lines GeoB01-089 to GeoB01-131.

RU (No.)	Type	Position	Distance to Tow-Lead
-	-	End of Stretch Section No.1	48 m
3	MultiTrak	End of Stretch Section No. 2	98 m
11	DigiBird	Mid of Active Section No. 1	145 m
12	DigiBird	End of Active Section No. 1	189 m
-	-	Mid of Active Section No. 2	245 m
4	MultiTrak	End of Active Section No. 2	289 m
13	DigiBird	Mid of Active Section No. 3	345 m
6	MultiTrak	End of Active Section No. 3	389 m
-	-	Mid of Active Section No. 4	445 m
14	DigiBird	End of Active Section No. 4	489 m
-	-	Mid of Active Section No. 5	545 m
5	MultiTrak	End of Active Section No. 5	589 m
2	MultiTrak 1	Mid of Active Section No. 6	645 m
15	DigiBird	End of Active Section No. 6	689 m

¹ RU No. 2 with defect compass

Table 2.3b: RU positions along the seismic streamer for lines GeoB01-132 to GeoB01-146.

RU (No.)	Type	Position	Distance to Tow-Lead
-	-	End of Stretch Section No.1	48 m
3	MultiTrak	End of Stretch Section No. 2	98 m
11	DigiBird	Mid of Active Section No. 1	145 m
12	DigiBird	End of Active Section No. 1	189 m
-	-	Mid of Active Section No. 2	245 m
5	MultiTrak	End of Active Section No. 2	289 m
13	DigiBird	Mid of Active Section No. 3	345 m
6	MultiTrak	End of Active Section No. 3	389 m
-	-	Mid of Active Section No. 4	445 m
4	MultiTrak	End of Active Section No. 4	489 m
-	-	Mid of Active Section No. 5	545 m
14	DigiBird	End of Active Section No. 5	589 m
2	MultiTrak1	Mid of Active Section No. 6	645 m
15	DigiBird	End of Active Section No. 6	689 m

¹ RU No. 2 with defect compass

Table 2.3c: RU positions along the seismic streamer for lines GeoB01-147 to GeoB01-158.

RU (No.)	Type	Position	Distance to Tow-Lead
-	-	End of Stretch Section No. 1	48 m
3	MultiTrak	End of Stretch Section No. 2	98 m
11	DigiBird	Mid of Active Section No. 1	145 m
2	MultiTrak 1	End of Active Section No. 1	189 m
4	MultiTrak	Mid of Active Section No. 2	245 m
5	MultiTrak	End of Active Section No. 2	289 m
13	DigiBird	Mid of Active Section No. 3	345 m
6	MultiTrak	End of Active Section No. 3	389 m
-	-	Mid of Active Section No. 4	445 m
12	DigiBird	End of Active Section No. 4	489 m
-	-	Mid of Active Section No. 5	545 m
14	DigiBird	End of Active Section No. 5	589 m
-	-	Mid of Active Section No. 6	645 m
15	DigiBird	End of Active Section No. 6	689 m

¹ RU No. 2 with defect compass

2.4.1.3.6 Trigger Unit

The custom trigger unit controls seismic sources, seismographs, remote unit (bird) controllers, online-plotter with separate filter and digital scope (near-field hydrophones). The unit is set up on an IBM compatible PC with a Windows NT 4.0 operating system and includes a real-time controller interface card (SORCUS) with 16 I/O channels, synchronized by an internal clock. The unit is connected to an amplifier unit and a gun amplifier unit. The PC runs a custom software, which allows to define arbitrary combinations of trigger signals, which were used to optimize the available recording time for three seismic sources and to minimize the shot distance.

Trigger times can be changed at any time during the survey. Through this feature, the recording delay can be adjusted to water depth without interruption of data acquisition. The amplifier unit converts the controller output to positive or negative TTL levels. The gun amplifier unit, which generates a 60V / 8 A trigger level, controls the magnetic valves of the individual seismic sources. It was placed in the pulser station close to the gun pressure controls for immediate shutdown of gun operation.

Table 2.4 shows the trigger scheme(s) used during the surveys for the two recording systems, the three different source types, the two RU controllers and the EPC online recorder. Two trigger intervals were used in an alternating mode, one controlling the watergun and the GI-Gun with smaller chamber volume, the second controlling the same watergun and the GI-Gun with larger chamber volume. Each trigger interval usually has a length of 9 s, which has to be later extended up to 11.5 s at greater water depth and to avoid interference between the primary signal of one source with the first or second multiple of another source. Each source type was recorded on a separate tape, one on the Bison Spectra for the watergun source and one on the Bison Jupiter for the GI-Gun sources. Recording and data storage occurred parallel on both systems. In this mode, an additional processing step of splitting records from different sources is required for the GI-Gun data prior to standard seismic data processing. As a consequence of the parallel recording, acquisition parameters could be adjusted on each system according to the frequency content and signal penetration achieved for each source type.

Table 2.4: Trigger scheme for GI-Guns, watergun, GI-Guns and watergun recording systems, *MultiTrak* and *DigiBird* (RU) controllers and *EPC* online recorder used during R/V METEOR Cruise M49/2.

Depth [m]	TWT [ms]	Delay [ms]	Shot Time Watergun [ms]	Shot Time GI Gun [ms]	Recording Time Watergun [ms]	Recording Time GI Gun (BISON-2) [ms]	DigiBird Controller [ms]	MTC-Controller [ms]	EPC Online Recording [ms]	Total Trigger Period [ms]
0	0	0	0	1500	0 - 1500	1500 - 4500	5000	5500	0	9000
375	500	500	0	2000	500 - 2000	2500 - 5500	6000	6500	2500	9000
750	1000	1000	0	2500	1000 - 2500	3500 - 6500	7000	7500	3000	9000
1125	1500	1500	0	3000	1500 - 3000	4500 - 7500	3300	0	4500	9000
1500	2000	2000	0	3500	2000 - 3500	5500 - 8500	0	500	5000	9000
1875	2500	2500	0	4000	2500 - 4000	6500 - 9500	0	500	6500	9500
2250	3000	3000	0	1500	3000 - 4500	4500 - 7500	0	500	4000	9000
2625	3500	3500	0	1500	3500 - 5000	5000 - 8000	0	500	5000	9000
3000	4000	4000	0	1500	4000 - 5500	5500 - 8500	0	500	5000	9000
3375	4500	4500	0	1500	4500 - 6000	6000 - 9000	0	500	6000	9000
3750	5000	5000	0	1500	5000 - 6500	6500 - 9500	0	500	6000	9500
4125	5500	5500	0	1500	5500 - 7000	7000 - 10000	0	500	7000	10000
4500	6000	6000	0	1500	6000 - 7500	7500 - 10500	0	500	7000	10500
4875	6500	6500	0	1500	6500 - 8000	8000 - 11000	0	500	8000	11000
5250	7000	7000	0	1500	7000 - 8500	8500 - 11500	0	500	8000	11500

2.4.1.4 Seismic Data Processing Onboard

For an immediate evaluation of the data quality brutestacks of the GI-Gun data were produced for each multichannel seismic line. Processing was done with custom software and with the public domain package Seismic Un*x [Stockwell, 1997] on a SUN Enterprise 250 workstation. For all lines GeoB01-089 to GeoB01-158 the near field traces 2 - 4 were chosen for the brutestacks in order to avoid time-consuming NMO corrections. After application of a bandpass filter of 55/110 - 600/800 Hz, which suppresses a sometimes strong ringing of 50 Hz and concentrates the frequency content of both GI-Guns to approximately the same band, these three traces were simply added up for the brutestacks. An occasionally occurring, up to now undefined short offset in the trigger time of both GI-Guns sometimes produces slightly smeared reflection horizons in the seismogram sections displayed in chapters 2.4.1.5 - 2.4.1.7.

A complete listing of the multichannel seismic lines acquired during R/V Meteor Cruise M49/2 is given in Table 2.5. Track charts displayed in chapters 2.4.1.5 - 2.4.1.7 are produced with the public domain software package GMT [Wessel and Smith, 1998].

The digital Parasound data displayed in chapters 2.4.1.5 - 2.4.1.7 were bandpass filtered between 2 and 6 kHz and displayed in 8 gray scales, after application of a routine which suppresses the negative flanks of the envelopes of the wiggle traces. These image traces are normalized to a constant (voltage) value in order to achieve and display a maximum penetration of 20 - 60 m. In all figures displaying Parasound recordings the two-way traveltime is converted to a Parasound depth by dividing through a P-wave velocity of 1500 m/s.

Based on the seismic GI-Gun brutestacks potential drilling sites were selected. In the following chapters 2.4.1.5 - 2.4.1.7 the seismic line, the (nearest) crossing line and a Parasound record across each proposed drill site is presented together with a detailed track chart of each survey area. The proposed drill sites of each survey area A - C are summarized in a table in Table 2.6 together with the (shot) date and time, the preliminary values for longitude and latitude, the nearest crossing line, an information if a gravity core is available at or close to the site and a keyword characterizing the location. These proposed drill sites themselves as well as their latitude and longitude are preliminary and have to be checked and adapted to CDP numbers after final processing of the multichannel seismic data. Additionally, if possible we tried to define a preliminary (seismo-) stratigraphy based either on biostratigraphic ages estimated and extrapolated from the gravity cores or from changes in seismic reflection pattern.

2.4.1.5 Southern Argentine Continental Margin at 44°S (Survey Area A)

2.4.1.5.1 Geologic Setting, Goals and Site Survey Strategy

The southernmost survey area A is located between about 43° - 46°S and 57° - 60°W. According to Lonardi and Ewing [1971] and data collected during R/V Meteor Cruises M29/1 [Segl et al., 1994] and M46/3 [Bleil et al., 2001] the continental margin here is rather steep, shaped by strong contour currents originating from the northward flowing Antarctic Bottom Water (AABW), the southward flowing North Atlantic Deep Water (NADW) and shallow water masses (e.g. Antarctic Intermediate Water (AAIW)), and dissected by several canyons deeply incised into the sediment cover. Most of the smaller canyons are considered to be tributaries to a large canyon, the Almirante Brown Transverse Canyon, running almost parallel to the bathymetric contours of the Argentine continental margin in about 4000 - 4500 m water depth.

Table 2.5: Multichannel seismic lines collected during R/V METEOR Cruise M49/2.

Profile	Start			End			Date	Time (UTC)	Course	Number of shots	Length [nm]
	Latitude	Longitude		Latitude	Longitude	Date					
GeoB01-089	43° 08.22' S	59° 47.35' W		44° 37.44' S	57° 05.86' W	16.02.01	18:58	125	8903	145	
GeoB01-090	44° 36.60' S	57° 05.68' W		44° 42.07' S	57° 06.78' W	16.02.01	17:33	190	321	8	
GeoB01-091	44° 42.81' S	57° 08.43' W		43° 49.35' S	58° 52.30' W	17.02.01	18:39	305	5645	92	
GeoB01-092	43° 50.60' S	58° 54.43' W		44° 00.23' S	58° 50.89' W	17.02.01	09:28	165	614	10	
GeoB01-093	44° 00.64' S	58° 48.44' W		43° 49.13' S	58° 12.86' W	17.02.01	11:18	65	1714	28	
GeoB01-094	43° 49.19' S	58° 11.71' W		43° 51.59' S	58° 06.87' W	17.02.01	15:42	125	319	5	
GeoB01-095	43° 52.99' S	58° 06.53' W		44° 08.42' S	58° 49.54' W	17.02.01	16:39	245	2144	35	
GeoB01-096	44° 05.78' S	58° 51.75' W		43° 52.83' S	58° 14.05' W	18.02.01	22:42	65	1501	31	
GeoB01-097	43° 52.06' S	58° 13.95' W		43° 45.20' S	58° 20.18' W	18.02.01	03:45	290	251	5	
GeoB01-098	43° 51.36' S	58° 22.79' W		44° 04.59' S	58° 34.34' W	18.02.01	05:14	215	974	18	
GeoB01-099	44° 05.76' S	58° 33.89' W		44° 13.40' S	58° 19.50' W	18.02.01	07:53	125	125	13	
GeoB01-100	44° 13.02' S	58° 17.90' W		43° 56.86' S	58° 08.81' W	18.02.01	10:04	20	1085	18	
GeoB01-101	43° 56.07' S	58° 06.86' W		43° 59.70' S	58° 01.76' W	18.02.01	13:01	130	294	5	
GeoB01-102	44° 00.38' S	58° 01.59' W		44° 33.13' S	58° 20.76' W	18.02.01	13:52	205	2220	36	
GeoB01-103	44° 33.13' S	58° 20.76' W		44° 51.89' S	58° 52.97' W	18.02.01	19:26	230	1819	23	
GeoB01-104	44° 52.69' S	58° 53.41' W		45° 31.64' S	59° 03.14' W	19.02.01	00:07	190	2472	41	
GeoB01-105	45° 33.19' S	59° 05.46' W		45° 30.18' S	59° 27.30' W	19.02.01	06:38	280	963	16	
GeoB01-106	45° 28.90' S	59° 28.60' W		45° 17.18' S	59° 24.09' W	19.02.01	09:18	10	739	13	
GeoB01-107	45° 17.18' S	59° 24.09' W		44° 08.77' S	57° 27.65' W	20.02.01	11:09	50	6526	107	
GeoB01-108	44° 08.51' S	57° 26.51' W		44° 16.90' S	57° 12.58' W	20.02.01	04:04	130	761	13	
GeoB01-109	44° 18.33' S	57° 12.99' W		44° 31.08' S	57° 52.19' W	20.02.01	06:19	245	1874	31	
GeoB01-110	44° 13.21' S	58° 31.42' W		44° 07.10' S	58° 43.25' W	21.02.01	04:56	305	702	11	
GeoB01-111	44° 59.50' S	58° 43.50' W		43° 43.99' S	58° 24.53' W	21.02.01	06:50	30	1577	26	
GeoB01-112	43° 43.08' S	58° 22.32' W		43° 43.11' S	58° 19.20' W	21.02.01	11:06	90	140	1	

Table 2.5: continued

GeoB01-113	43° 43.77' S	58° 17.78' W	21.02.01	11:40	43° 52.10' S	58° 17.81' W	21.02.01	12:56	180	508	9
GeoB01-114	43° 52.81' S	58° 17.81' W	21.02.01	12:56	43° 49.84' S	58° 06.72' W	21.02.01	14:38	135	676	11
GeoB01-115	43° 49.84' S	58° 06.72' W	21.02.01	14:38	44° 08.17' S	58° 04.05' W	21.02.01	15:57	165	531	9
GeoB01-116	44° 08.76' S	58° 04.05' W	21.02.01	16:09	43° 55.40' S	58° 30.50' W	21.02.01	19:48	305	1467	22
GeoB01-117	41° 00.00' S	57° 18.46' W	23.02.01	05:34	41° 00.01' S	55° 03.78' W	23.02.01	21:18	90	6260	102
GeoB01-118	40° 53.95' S	55° 03.04' W	23.02.01	22:38	39° 44.56' S	55° 59.10' W	24.02.01	11:09	330	4911	82
GeoB01-119	39° 44.44' S	56° 00.85' W	24.02.01	11:23	40° 03.41' S	56° 17.97' W	24.02.01	14:57	215	1423	22
GeoB01-120	40° 04.10' S	56° 17.90' W	24.02.01	15:04	41° 01.66' S	55° 39.86' W	25.02.01	01:05	150	3977	65
GeoB01-121	41° 02.60' S	55° 38.99' W	25.02.01	01:15	41° 17.50' S	55° 55.80' W	25.02.01	04:16	220	1208	19
GeoB01-122	41° 17.60' S	55° 57.60' W	25.02.01	04:31	40° 50.20' S	56° 43.42' W	25.02.01	11:18	310	2735	44
GeoB01-123	40° 49.12' S	56° 43.42' W	25.02.01	11:29	40° 38.37' S	56° 32.52' W	25.02.01	13:35	40	837	14
GeoB01-124	40° 36.10' S	56° 30.64' W	25.02.01	13:50	41° 03.99' S	55° 46.78' W	25.02.01	20:18	125	2588	42
GeoB01-125	41° 05.30' S	55° 45.50' W	25.02.01	20:37	41° 14.07' S	56° 31.54' W	26.02.01	02:18	253	2257	35
GeoB01-126	41° 12.90' S	56° 32.28' W	26.02.01	02:35	40° 44.96' S	56° 04.43' W	26.02.01	08:33	37	2342	38
GeoB01-127	40° 42.47' S	55° 58.73' W	26.02.01	09:02	41° 01.13' S	55° 60.00' W	26.02.01	12:03	6	1188	19
GeoB01-128	41° 01.55' S	56° 01.23' W	26.02.01	12:14	41° 00.11' S	56° 05.33' W	26.02.01	12:47	297	219	4
GeoB01-129	40° 59.33' S	56° 05.81' W	26.02.01	12:55	40° 51.53' S	56° 05.68' W	26.02.01	14:07	0	471	7
GeoB01-130	40° 50.81' S	56° 04.12' W	26.02.01	14:23	40° 44.60' S	55° 57.90' W	26.02.01	15:30	129	444	6
GeoB01-131	40° 55.80' S	55° 58.30' W	26.02.01	15:34	40° 51.80' S	56° 17.50' W	26.02.01	17:56	286	948	15
GeoB01-132	38° 52.83' S	54° 45.42' W	27.02.01	14:52	38° 13.25' S	53° 56.00' W	27.02.01	23:34	43	3469	55
GeoB01-133	38° 13.00' S	53° 56.21' W	27.02.01	23:45	38° 25.73' S	53° 38.49' W	28.02.01	02:28	130	1079	17
GeoB01-134	38° 28.92' S	53° 37.79' W	28.02.01	02:40	38° 42.10' S	53° 45.30' W	28.02.01	04:57	219	895	16
GeoB01-135	38° 42.70' S	53° 47.00' W	28.02.01	05:11	38° 05.00' S	55° 20.32' W	28.02.01	18:03	296	4881	82
GeoB01-136	38° 03.20' S	55° 21.78' W	28.02.01	18:26	37° 58.03' S	55° 16.69' W	28.02.01	19:41	33	428	7
GeoB01-137	37° 57.68' S	55° 15.26' W	28.02.01	19:42	38° 10.98' S	54° 17.86' W	01.03.01	03:09	105	3375	47
GeoB01-138	38° 10.72' S	54° 16.54' W	01.03.01	03:21	37° 17.93' S	53° 38.65' W	01.03.01	14:51	28	4603	61
GeoB01-139	37° 16.91' S	53° 39.48' W	01.03.01	15:03	37° 10.69' S	54° 31.17' W	01.03.01	21:30	277	2569	42
GeoB01-140	37° 11.11' S	54° 32.38' W	01.03.01	21:40	37° 21.59' S	54° 43.40' W	01.03.01	23:49	220	858	13

Table 2.5: continued

GeoB01-141	37°22.27 S	54°43.23 W	02.03.01	00:00	37°53.68 S	53°27.51 W	02.03.01	10:27	119	4173	68
GeoB01-142	37°53.08 S	53°26.29 W	02.03.01	10:42	37°38.53 S	53°24.73 W	02.03.01	13:13	4	1017	15
GeoB01-143	37°37.80 S	53°25.20 W	02.03.01	13:22	37°19.76 S	54°09.40 W	02.03.01	19:37	297	2489	33
GeoB01-144	37°20.70 S	54°10.80 W	02.03.01	19:50	38°07.84 S	54°39.11 W	03.03.01	03:59	204	3259	53
GeoB01-145	38°08.44 S	54°39.10 W	03.03.01	04:04	38°28.60 S	54°33.20 W	03.03.01	07:19	167	1281	20
GeoB01-146	38°29.38 S	54°31.85 W	03.03.01	07:30	38°21.03 S	54°40.93 W	03.03.01	09:52	298	943	10
GeoB01-147	36°32.79 S	53°12.80 W	04.03.01	08:18	36°18.10 S	51°18.70 W	04.03.01	23:00	80	5892	94
GeoB01-148	36°18.90 S	51°18.00 W	04.03.01	23:18	36°23.43 S	51°25.49 W	05.03.01	00:39	230	535	7
GeoB01-149	36°23.24 S	51°27.04 W	05.03.01	00:53	36°16.87 S	51°36.17 W	05.03.01	02:32	309	659	10
GeoB01-150	36°15.85 S	51°35.58 W	05.03.01	02:45	35°15.50 S	51°29.09 W	05.03.01	03:34	85	320	6
GeoB01-151	36°16.20 S	51°28.07 W	05.03.01	03:47	36°28.04 S	51°39.53 W	05.03.01	06:46	219	1142	14
GeoB01-152	36°28.23 S	51°40.77 W	05.03.01	06:59	36°01.82 S	53°25.50 W	05.03.01	14:11	306	2827	44
GeoB01-153	36°12.24 S	53°14.24 W	05.03.01	20:32	36°32.90 S	52°57.60 W	06.03.01	00:??	147	1667	24
GeoB01-154	36°34.07 S	52°57.81 W	06.03.01	00:52	36°39.35 S	53°03.71 W	06.03.01	01:57	221	439	7
GeoB01-155	36°39.47 S	53°05.45 W	06.03.01	02:12	36°19.64 S	53°27.06 W	06.03.01	06:20	317	1648	27
GeoB01-156	36°18.03 S	53°26.09 W	06.03.01	06:37	36°18.73 S	53°22.42 W	06.03.01	07:15	103	248	4
GeoB01-157	36°18.73 S	53°22.42 W	06.03.01	07:15	36°29.50 S	53°08.50 W	06.03.01	09:40	133	965	15
GeoB01-158	36°29.90 S	53°07.20 W	06.03.01	09:51	36°05.15 S	53°03.20 W	06.03.01	13:40	8	1533	24
									Total	131'867	2111

Based on this given hydrography and morphology which facilitate downslope sediment transport processes and cause erosional surfaces and hiatuses at the sea floor and in the sediment column our site survey focused on locations where sedimentation was protected or enhanced. From R/V Meteor Cruise M46/3 [Bleil et al., 2001] it was known that such locations could possibly be found in the vicinity of large canyons where drift sediments occurred on both canyon flanks. Though such deposits might not only reflect the in-situ sedimentation at this location but are possibly mixed with sediment components transported to this location either from southern or northern latitudes by bottom-currents (e.g. AABW or NADW) or from shallower water depths by suspension currents, they potentially provide much more complete sedimentary sections than could be achieved in other locations at this latitude.

2.4.1.5.2 Preliminary Results, Stratigraphy and Proposed Drill Sites

Figure 2.5 displays the track chart of R/V Meteor Cruise M49/2 in survey area A, Figure 2.6 a blow-up of the detailed survey grid around an unnamed "Channel 1".

Based on the global seafloor bathymetry data set of Smith and Sandwell [1997] data was first collected along two parallel NW-SE oriented lines GeoB01-089 and GeoB01-091 along a part of the continental margin which seemed to descend more gentle than adjacent areas and which crosses the Almirante Brown Canyon in about 4500 m water depth, in order to get an overview on the sediment structures in this area.

Figure 2.7 presents the brutestack of the GI-Gun data along the complete line GeoB01-089. After a very steep continental slope follows a part between 1.6 - 3.0 s TWT (about 1200 - 2250 m) water depth which descends more gentle, but is dissected by several smaller canyons and furrows. Indications of strong erosion both at the sea floor and 0.25 - 0.5 s TWT (about 190 - 375 m) beneath it can be observed, as well as thick interbedded slump deposits. Further downslope, an about 700 - 800 m deep canyon, which we called "Channel 1", was crossed. Particularly at the northwestern canyon flank a very thick, obviously undisturbed sediment package occurs. On the southeastern flank, a similar sediment drift is deposited which, however, is of lesser extent and quickly changes to a sequence with pronounced, current-controlled, wavy internal structures. This deposit again is followed by a part with almost parallel subbottom layers pinching out at the northwestern flank of the Almirante Brown Canyon. In contrast, sediments deposited southeast of the Almirante Brown Canyon seem to be more disturbed. Additionally, southeast of "Channel 1" and also southeast of the Almirante Brown Canyon a strongly reflecting erosional surface occurs about 0.8 - 1.0 s TWT (about 600 - 750 m) below sea floor. This erosional surface seems to be characteristic for this area and might indicate a stratigraphic event, because it was also observed along line GeoB01-091, as well as along lines recorded further north at about 41°S.

Some seismic lines (GeoB01-103 to GeoB01-107) to the southern part of survey area A, where bathymetric contours show at least two other large canyons at about 44°45' and 45°25'S (Figure 2.5), exhibit a sharp transition from sediment deposition northeast of the northerly canyon to pure erosion towards southwest in lines GeoB01-103 and GeoB01-107, so that no suitable drilling targets could be defined here.

Hence, a dense grid of seismic lines was recorded particularly in the area of „Channel 1“ (GeoB01-089, GeoB01-091 to GeoB01-102, GeoB01-110 to GeoB01-116) and around the Almirante Brown Canyon (GeoB01-089 to GeoB01-091, GeoB01-107 to GeoB01-109) (Figure 2.6) in order to map out the regional extent and sedimentation pattern of the drift deposits on the channel and canyon flanks, to

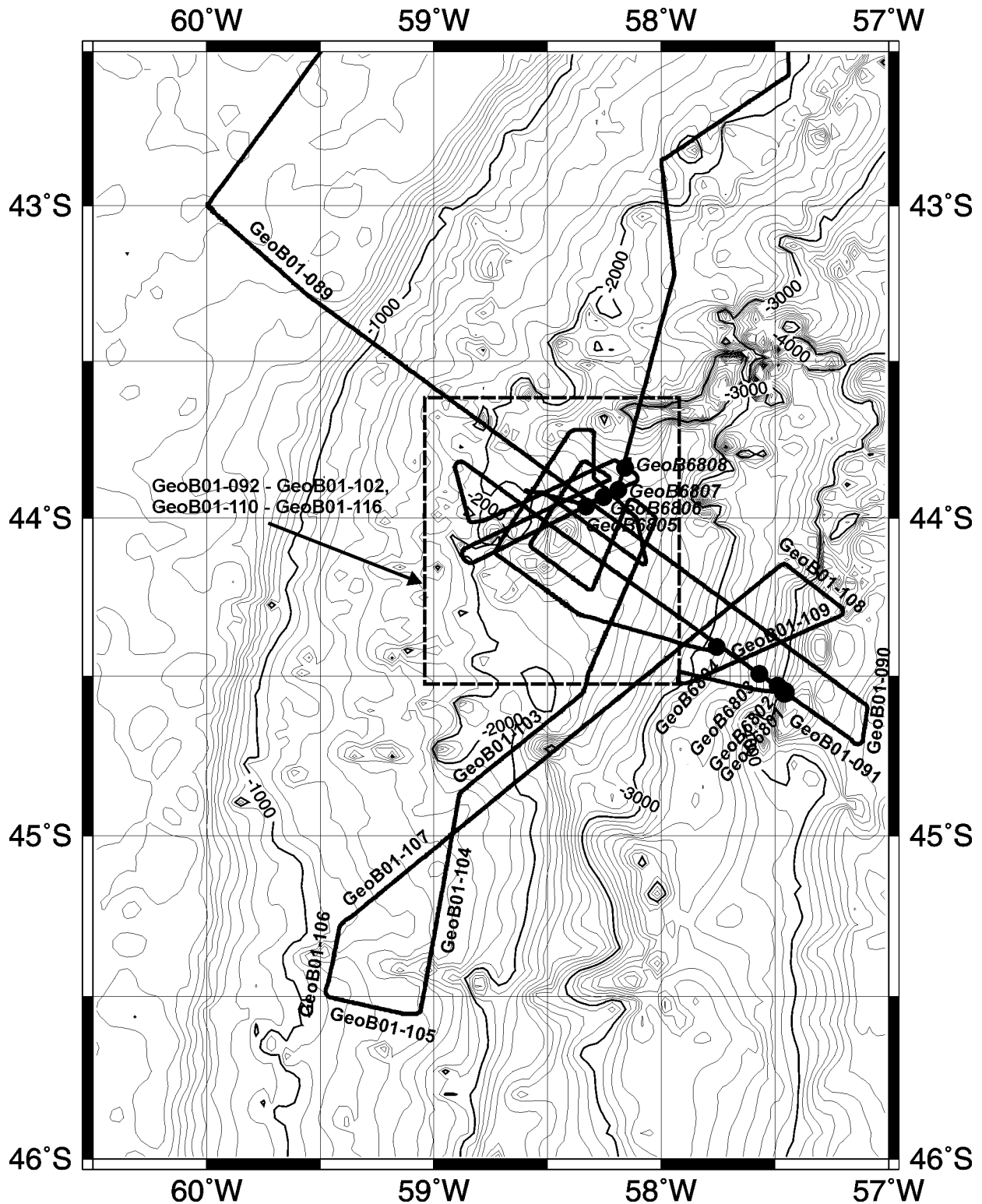


Fig. 2.5: Track chart and gravity core positions of R/V Meteor Cruise M49/2 on the southern Argentine continental margin at 44°S (Survey Area A).

define reflectors of regional significance, to collect the data base to trace them spatially and to define suitable drilling locations. Additionally, four gravity cores (GeoB6801-1 to GeoB6804-1) were taken on the northwestern flank of the Almirante Brown Canyon along line GeoB01-091 and four gravity cores (GeoB6805-1 to GeoB6808-1) on the northeastern flank of „Channel 1“ along line GeoB01-095 so that layers from successively greater depth outcropping at the canyon and channel flanks could be sampled and possibly provide (bio-)stratigraphic information (cf. chapter 2.4.2).

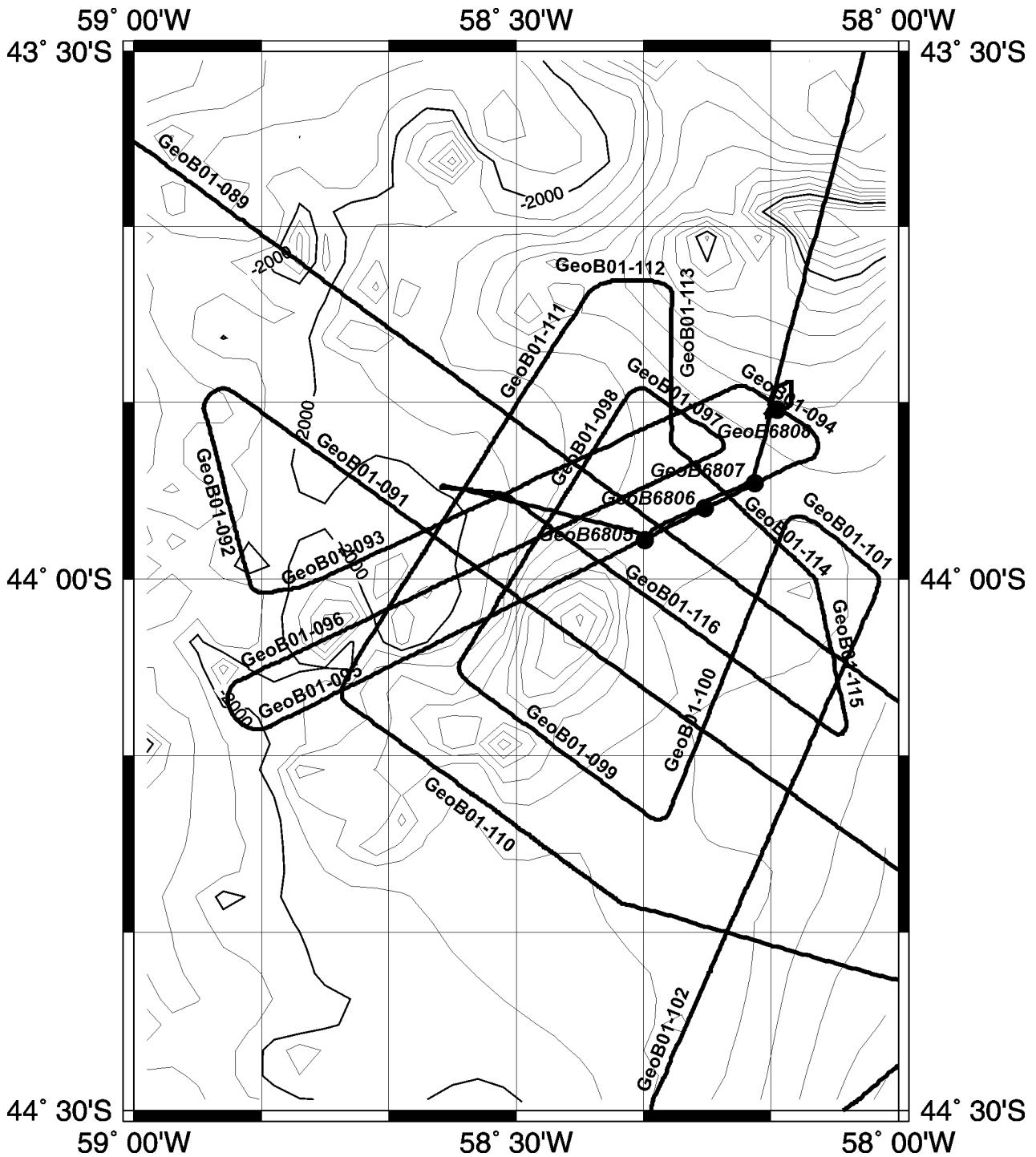


Fig. 2.6: Detailed track chart of the area around unnamed „Channel 1“.

Two drilling locations are defined on the drift deposits of „Channel 1“ in about 2000 - 2200 m water depth along line GeoB01-089. Site SAM-1 is located upslope of „Channel 1“ on top of a large sediment package with almost parallel subbottom layers that lie on top of an erosional unconformity limiting seismic signal penetration (Figure 2.8). Site SAM-1 is intended to drill an almost complete record from Holocene to Pliocene or Miocene age, depending on the sedimentation rates. The nearest crossing line GeoB01-095 about 2.5 km southeast of Site SAM-1 indicates that this drift deposit extends at least 15 km to both northeast and southwest, where it is limited by the loop of another canyon (Figure 2.9).

Gravity cores taken on line GeoB01-095 mainly consist of diatom-bearing foraminifer-nannofossil ooze on the top and consolidated siliceous muddy sand (GeoB6806-1) or siliceous nannofossil ooze

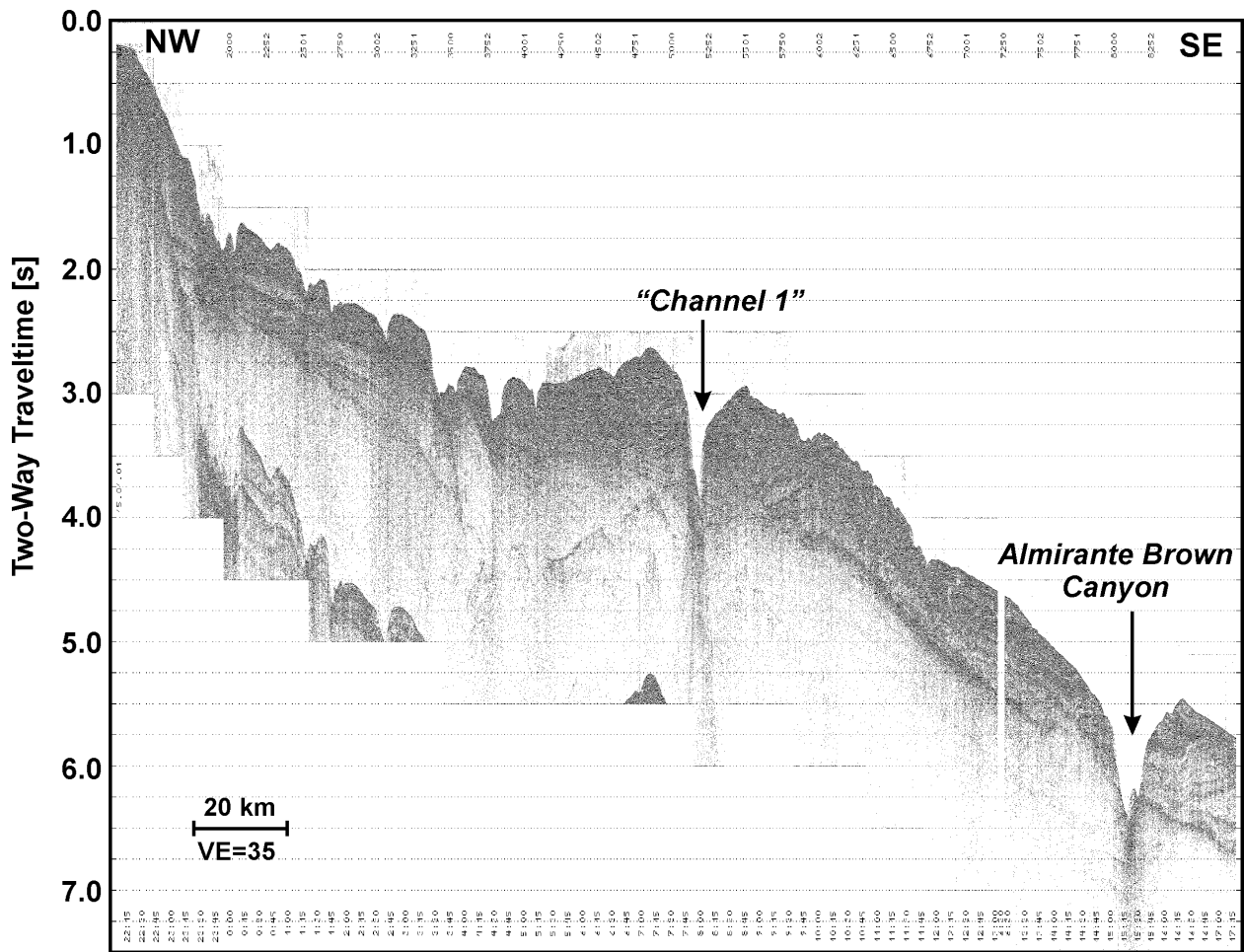


Fig.2.7: Multichannel seismic line GeoB01-089 on the southern Argentine continental margin.

(GeoB6807-1) below (cf. chapter 2.4.2). A preliminary dating of the diatoms found in core GeoB6807-1 yields a biostratigraphic age of about 4 Ma in 2.5 m core depth. An extrapolation of the reflection horizon outcropping at this gravity core location to the proposed Site SAM-1 leads to an age of 4 Ma about 0.5 s TWT (about 375 m) below sea floor, resulting in a preliminary average sedimentation rate of about 90 m/Ma, provided that the sampled reflector is defined and traced correctly, Holocene is at the top and biostratigraphic age estimation is correct. Similarly, if this preliminary average sedimentation rate could be extrapolated downwards, an approximate age of about 8 - 10 Ma would be reached at the erosional unconformity that limits seismic signal penetration.

The Parasound record along line GeoB01-089 and across Site SAM-1 illustrates that the drilling location was not chosen directly at the top of the drift deposit but slightly southeastwards, because the uppermost sediment layer seems to be more complete here (Figure 2.10). Erosionally truncated reflectors occur northwest of Site SAM-1 and can be observed in both multichannel seismic and Parasound data. Additionally, an inspection of the other seismic lines upslope of „Channel 1” yields that erosion of the uppermost sediment layers increases towards southwest and northwest, so that we hope to find the highest, undisturbed sedimentation rates at the proposed drilling location.

Site SAM-2 is located downslope of „Channel 1“ on top of a rather small sediment cap deposited on a sequence with wavy pattern and erosional truncations at the sea floor (Figure 2.11). Seismic signal penetration is again limited by an unconformity, which is probably the same as upslope of „Channel 1“, and which appears as strongly reflecting erosional surface further downslope between „Channel 1“ and Almirante

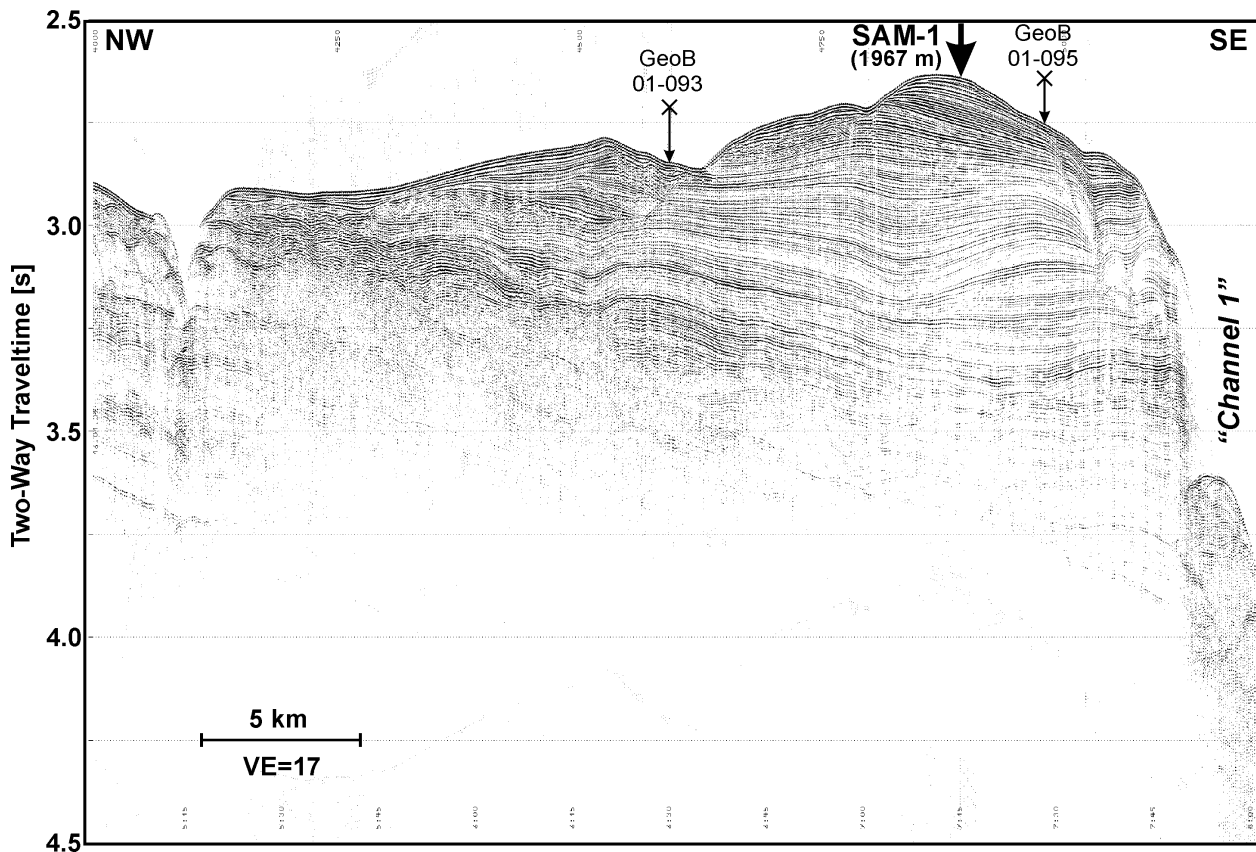


Fig. 2.8: Part of multichannel seismic line GeoB01-089, upslope of „Channel 1“, across Site SAM-1. Arrows with a cross at the top indicate the intersections with lines GeoB01-093 and GeoB01-095.

Brown Canyon, as discussed above (cf. Figure 2.7). Site SAM-2 is intended to provide a very high-resolution Holocene and Pleistocene record possibly included in the small sediment cap, whereas below at least two hiatuses might be present about 0.2 and 0.4 s TWT (about 150 and 300 m) below sea floor, where sedimentation pattern changes across unconformities. However, the nearest crossing line GeoB01-100 about 4 km northwest of Site SAM-2 indicates that the sequence beneath the small sediment cap extends rather continuously over more than 20 km to the southwest, though some indications of current control like wavy pattern, locally variable sedimentation rates and erosional truncations within the sequence are present (Figure 2.12). Nevertheless, drilling this sequence below the sediment „hat“ might reveal an at least partially complete record that can possibly supplement and complete the record from Site SAM-1. No stratigraphic information or age dating from gravity cores is available here, unless the erosional surface at the bottom of the sequence is the same as upslope so that its age estimation can be extrapolated downslope.

The Parasound record across Site SAM-2 illustrates the extraordinary position of this proposed drilling locating on top of the small sediment cap with erosional truncations at both sides (Figure 2.13). Additionally, an inspection of both parallel lines GeoB01-116 and GeoB01-091 yields that erosion increases towards southwest, so that the sediment cap is almost completely eroded on these lines.

A transect of 5 drilling locations SAM-3 to SAM-7 is proposed for the large drift deposit northwest of the Almirante Brown Canyon between about 3200 and 4100 m water depth, along line GeoB01-091 (Figure 2.14). The sea floor in this region is shaped by erosional currents leading to truncations and reflectors outcropping at the canyon flank. The transect is intended to drill successively older sediments, so that a combination of these 5 overlapping records could produce a long record from Holocene to Pliocene or Miocene times, depending on sedimentation rates. The parallel subbottom layers of the drift deposit are

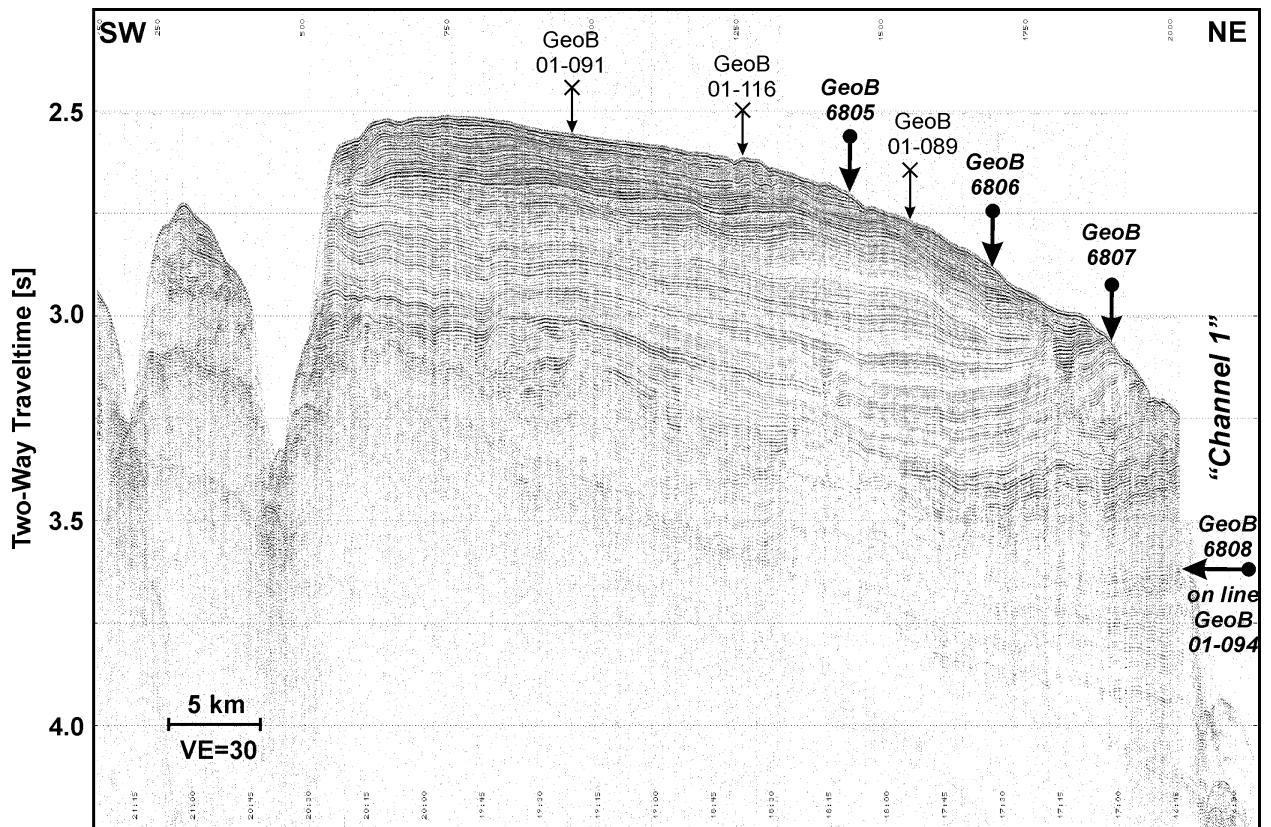


Fig. 2.9: Part of multichannel seismic line GeoB01-095 upslope of „Channel 1“ with gravity core positions GeoB6805-1 to GeoB6808-1. Line GeoB01-095 is the crossing line to Site SAM-1 on line GeoB01-089. Arrows with a cross at the top indicate the intersections with lines GeoB01-089, GeoB01-091, GeoB01-116.

truncated by an unconformity in about 0.4 s TWT (about 300 m) below sea floor. The reflection pattern below this unconformity is rather diffuse, and seismic signal penetration ends at a strongly reflecting rough surface supposed to be an erosional surface, as discussed above (cf. Figure 2.9).

The four gravity cores GeoB6801-1 to GeoB6804-1 recovered at or between the proposed drilling locations SAM-3 to SAM-7 mainly consist of soft diatom mud including various amounts of foraminifer tests and nannofossil placoliths at the top and slightly consolidated mud with varying amounts of biosiliceous components interrupted by few centimeters thick sandy turbidite or slump deposits below (cf. chapter 2.4.2). They were taken to sample and date deeper layers pinching out here. However, up to now no (bio-)stratigraphic information is available.

The crossing line GeoB01-109 illustrates that the parallel-bedded drift deposit as well as the unconformity in about 0.4 s TWT below sea floor and the strongly reflecting rough erosional surface extend several kilometers southwest- and northeastward (Figure 2.15). In this line the sequence between the unconformity and the erosional surface about 0.4 to 0.8 s TWT below sea floor, seems to exhibit a wavy depositional pattern which indicates an interaction between bottom currents and sediment deposition during this time interval.

The Parasound record across Sites SAM-3 to SAM-7 clearly shows the erosional truncations at the canyon flank, but also some slump deposits which were widely avoided at the proposed drill sites (Figure 2.16).

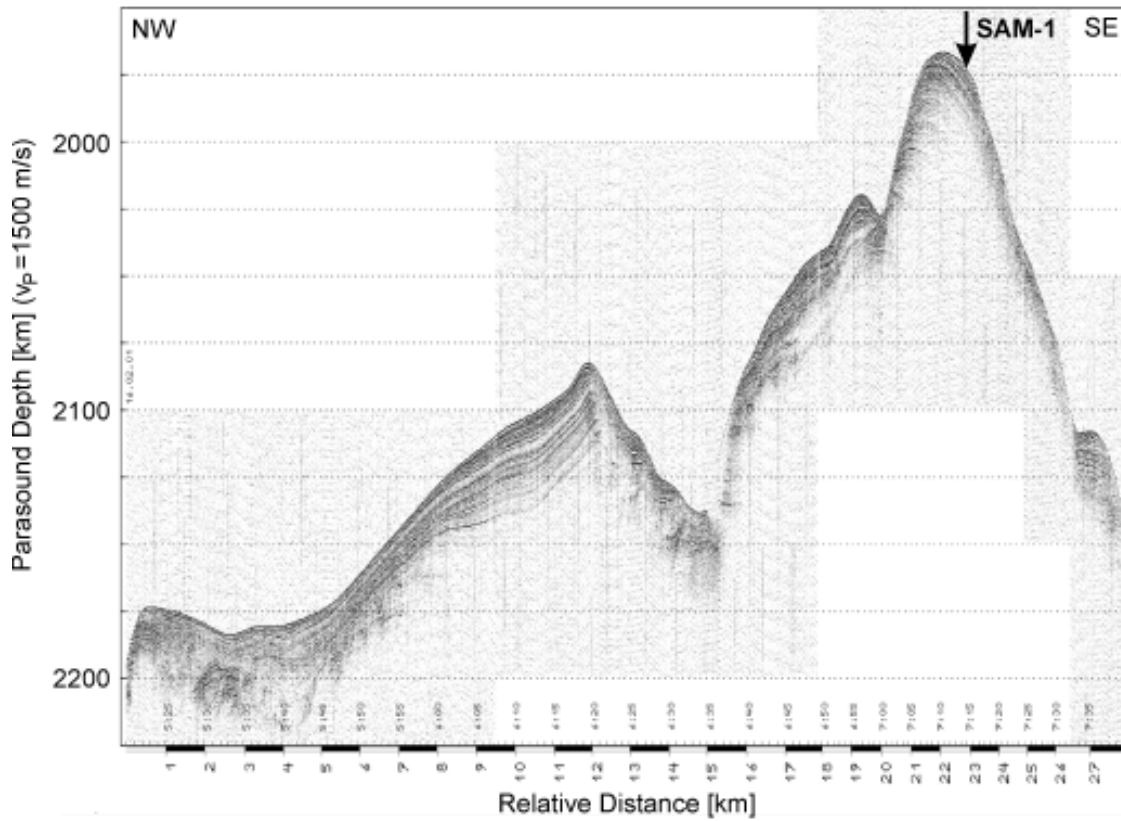


Fig. 2.10: PARASOUND example recorded along line GeoB01-089 across Site SAM-1.

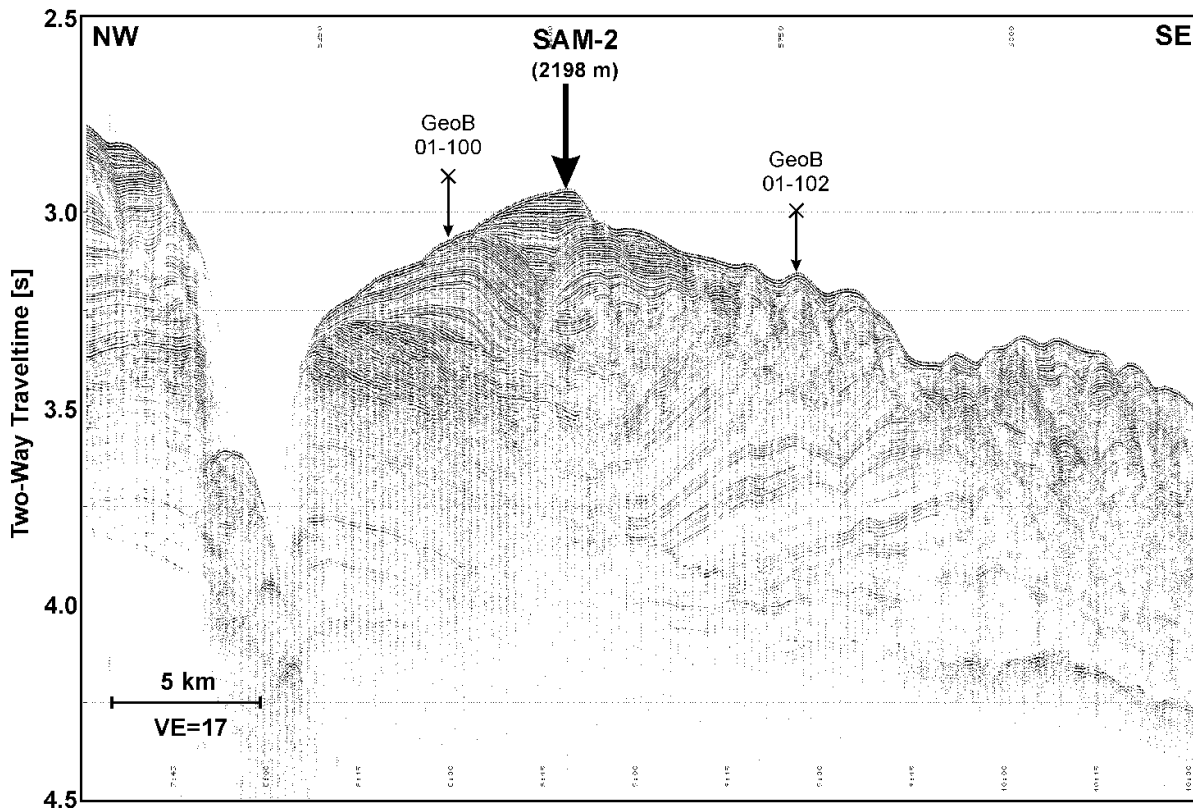


Fig. 2.11: Part of multichannel seismic line GeoB01-089, downslope of „Channel 1“, across proposed Site SAM-2. Arrows with a cross at the top indicate intersections with lines GeoB01-100 and GeoB01-102.

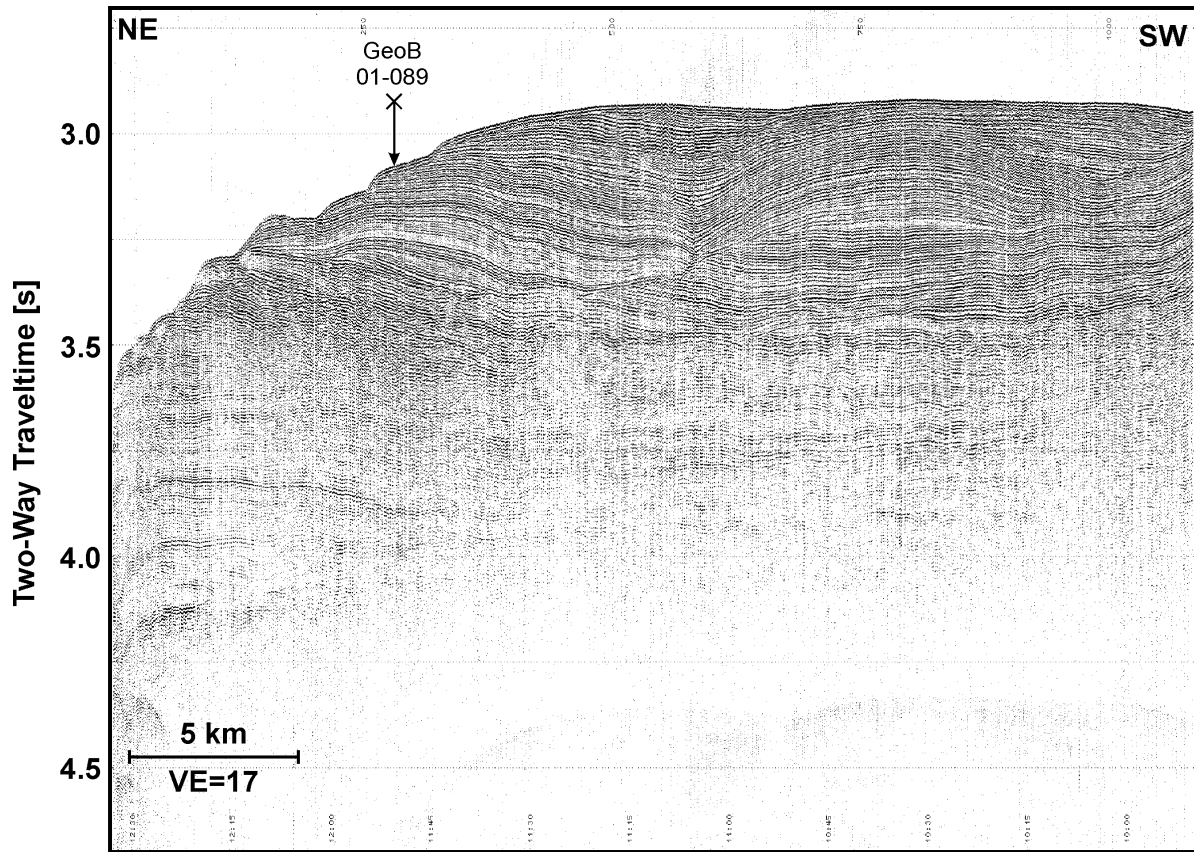


Fig. 2.12: Part of multichannel seismic line GeoB01-100, downslope of „Channel 1“. Line GeoB01-100 is the crossing line to Site SAM-2 on line GeoB01-089. Their intersection is marked by an arrow with a cross at the top.

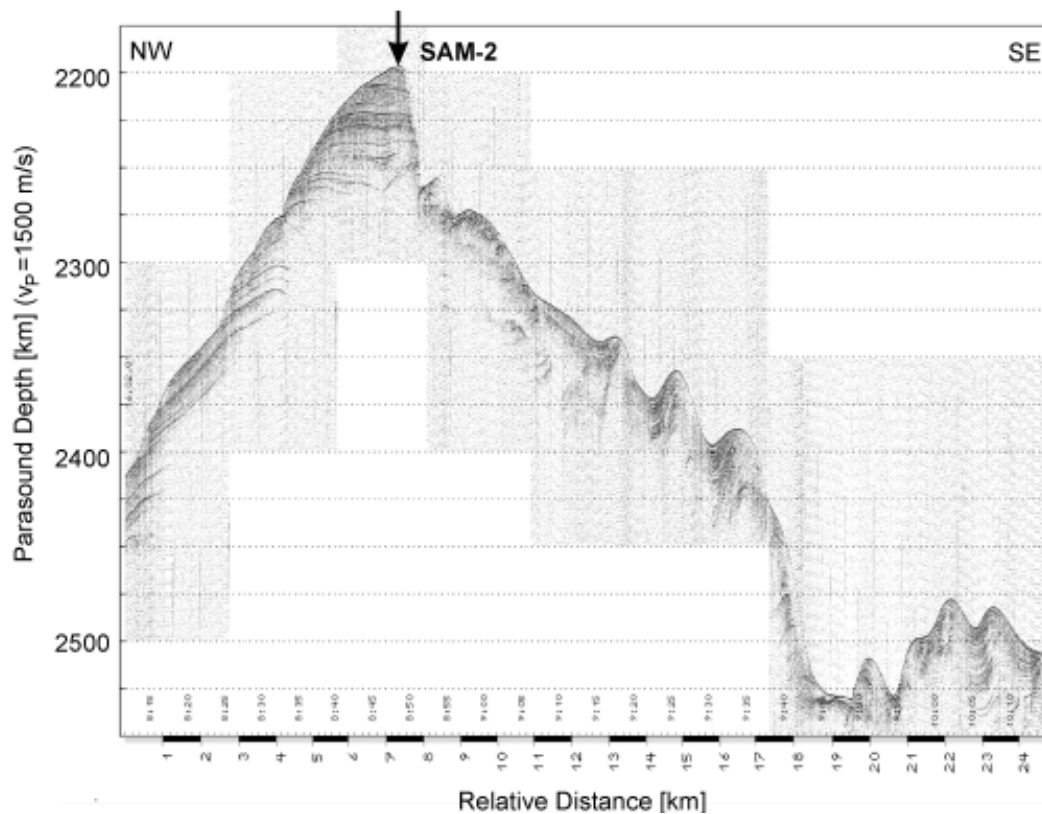


Fig. 2.13: PARASOUND example recorded along line GeoB01-089 across Site SAM-2.

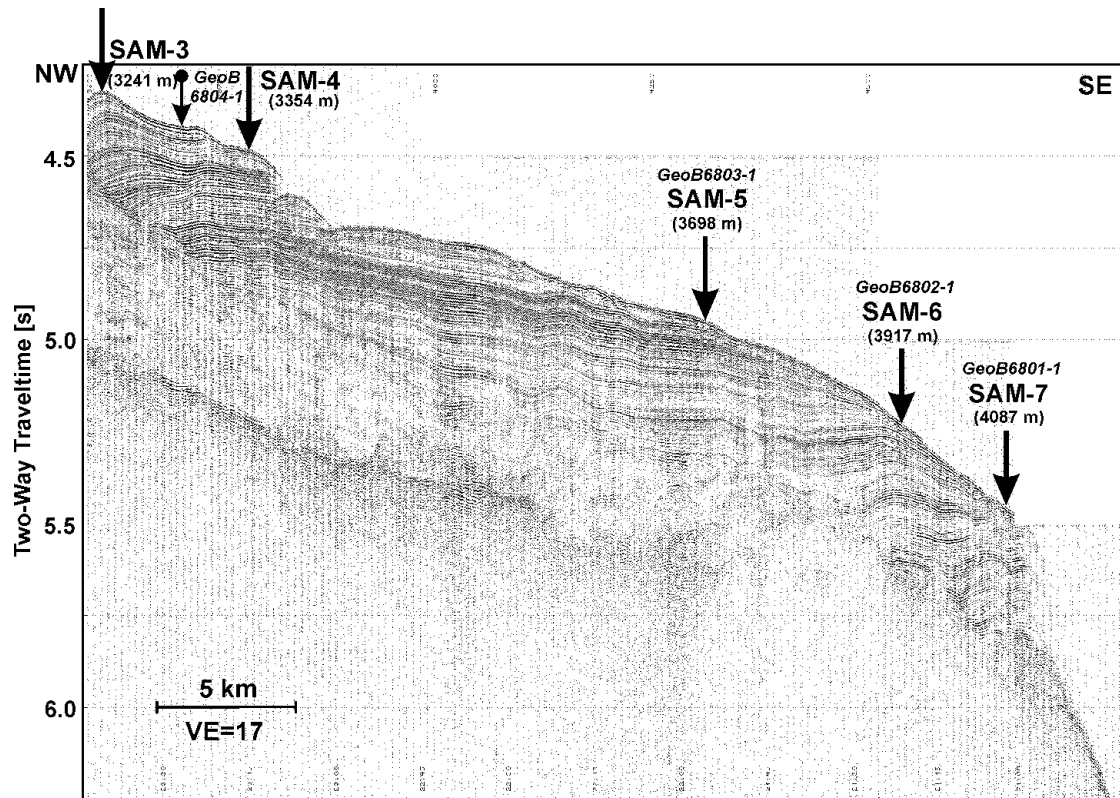


Fig. 2.14: Part of multichannel seismic line GeoB01-091 on the northwestern flank of the Almirante Brown Canyon, across proposed Sites SAM-3, SAM-4, SAM-5, SAM-6, SAM-7 and gravity core positions GeoB6801-1 to GeoB6804-1.

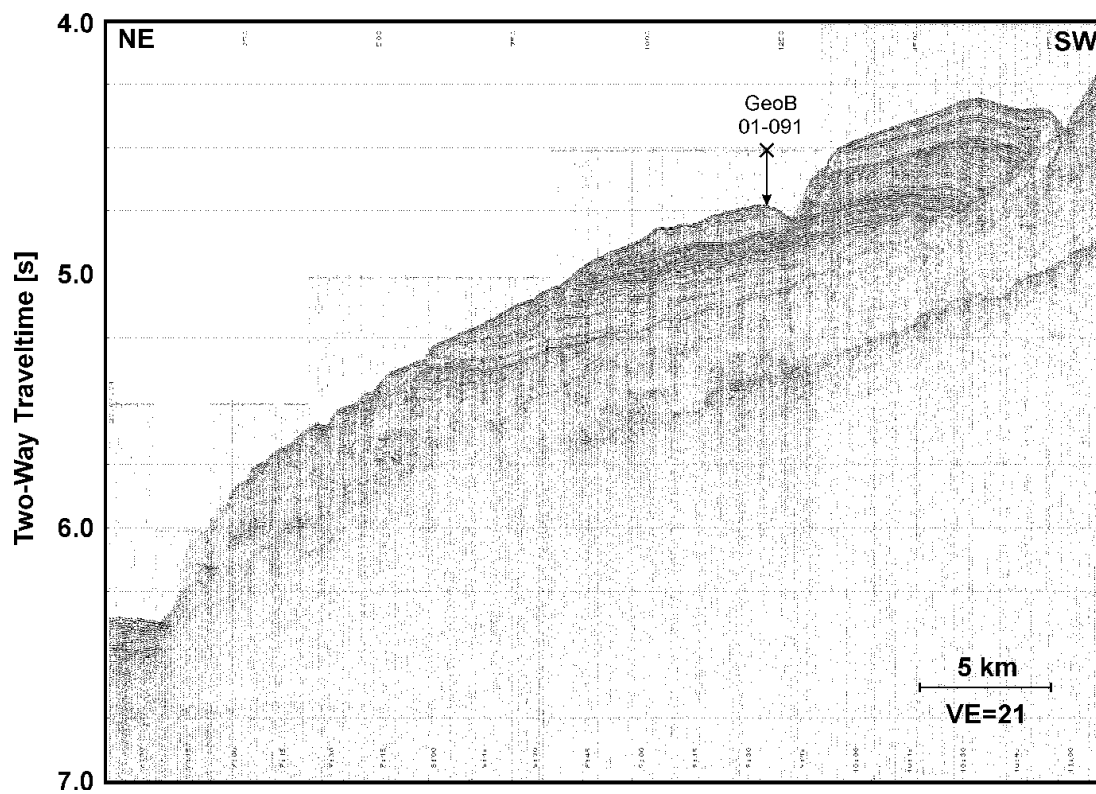


Fig. 2.15: Part of multichannel seismic line GeoB01-109, close to the Almirante Brown Canyon. Line GeoB01-109 is the crossing line to Sites SAM-3 to SAM-7 on line GeoB01-091. Their intersection is marked by an arrow with the cross at the top.

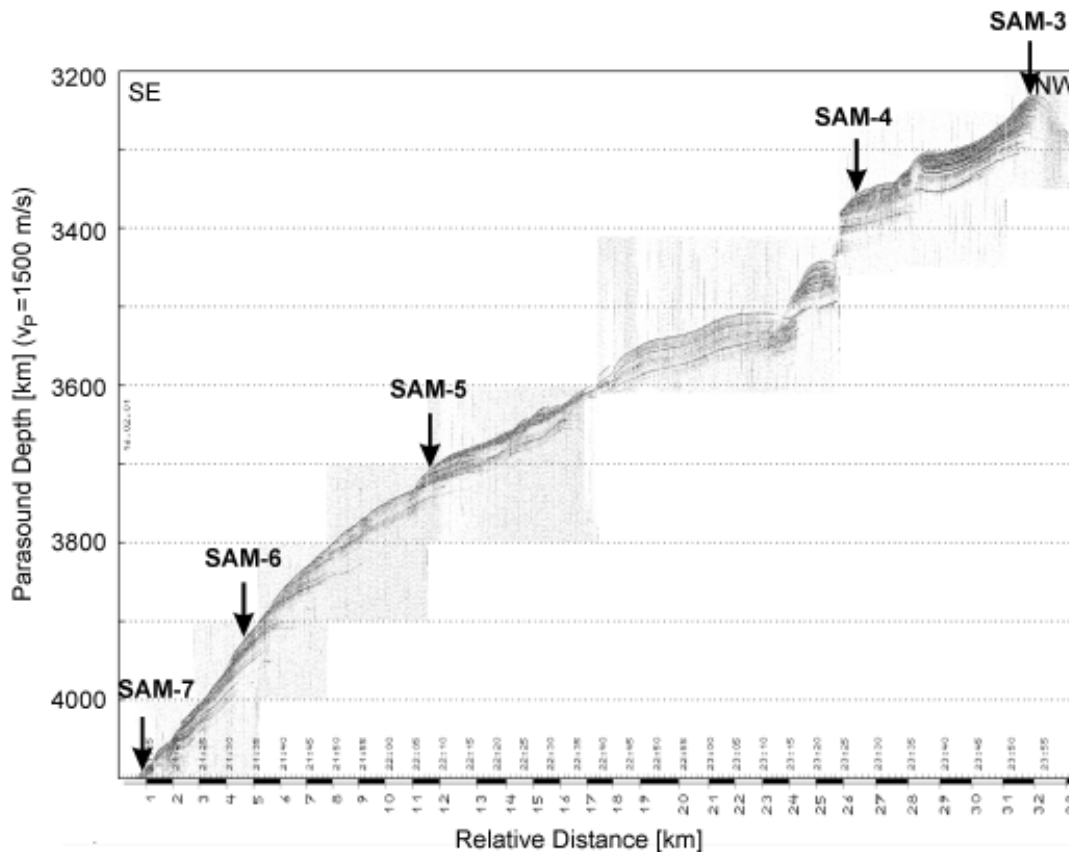


Fig. 2.16: PARASOUND example recorded along line GeoB01-091 across Sites SAM-3 to SAM-7. Note that the orientation is opposite to the seismic line (Figure 14).

2.4.1.6 Central Argentine Continental Margin at 41°S (Survey Area B)

2.4.1.6.1 Geologic Setting, Goals and Site Survey Strategy

Survey area B on the central Argentine continental margin is located between about 39°30' - 41°30'S and 55°00' - 57°30'W. It is still very steep and dissected by several canyons. It was chosen as part of a latitudinal transect necessary to drill in order to reach the goals of the proposal which are a reconstruction of the cold (Falkland/Malvinas current) and warm water (Brazil current) confluence near the coast and their evolution through geologic time as well as their impact on biologic productivity and depositional style.

In order to find suitable sites with almost undisturbed continuous sediment deposition we tried to follow the same strategy as in survey area A, where we tried to find locations in the vicinity of large canyons with a protected and enhanced deposition of drift sediments.

2.4.1.6.2 Preliminary Results, Stratigraphy and Proposed Drill Sites

However, in fact, this area proved to reveal an even steeper morphology than further south in area A. The seismic recordings (cf. track chart in Figure 2.17) are characterized by extensive slump deposits with wavy depositional structures, wedge shaped units and erosional unconformities. Figure 2.18 shows the brutestack of the GI-Gun data of line GeoB01-117 as example. Generally, the sediment units are much thinner and erosional features are more pronounced than in survey area A, so that we had difficulties to define any suitable drilling location in this area.

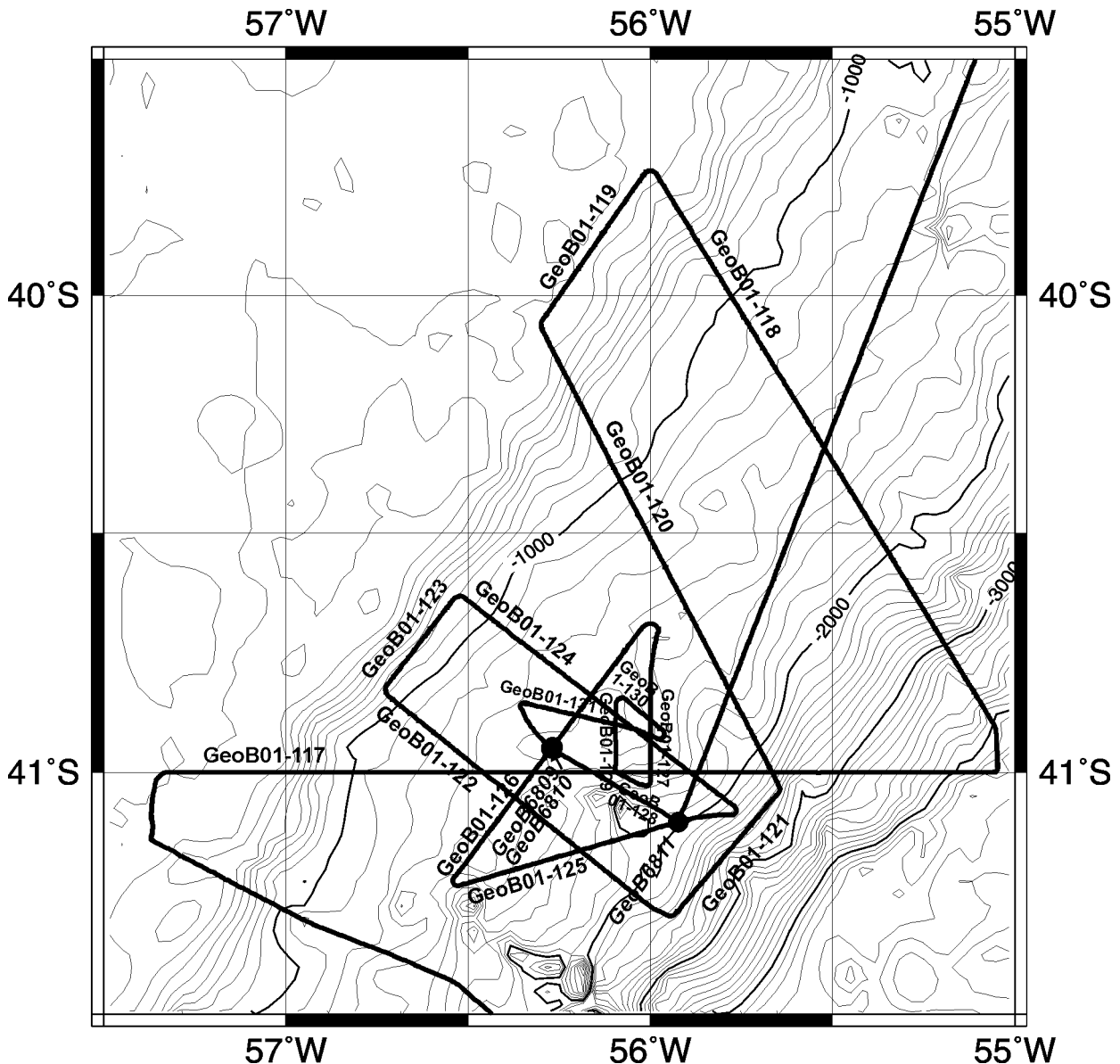


Fig. 2.17: Track chart and gravity core positions of R/V Meteor Cruise M49/2 on the central Argentine continental margin at 41°S (Survey Area B).

2.4.1.7 Northern Argentine and Uruguayan Continental Margin between 39° - 34°S (Survey Area C)

2.4.1.7.1 Geologic Setting, Goals and Site Survey Strategy

As no suitable drilling sites could be identified in survey area B survey area C was extended to the south to an area close to the Mar del Plata Canyon, where the Argentine colleagues had recently carried out a seismic survey. So now, survey area C extends from about 36° - 39°S and 51°00' - 55°30'W and actually comprises two survey sub-areas, a southern one close to the Mar del Plata Canyon between 37 - 39°S on the northern Argentine continental margin, and a northern one northeast off the Rio de la Plata river mouth between 36° - 37°S on the Uruguayan continental margin.

The Mar del Plata Canyon reveals steep flanks of more than 1000 m height and is located seaward of the Rio del la Plata river mouth. In its vicinity sedimentation rates are expected to be significantly higher than elsewhere in this area. In contrast, southwest of this canyon large areas of older sediments are

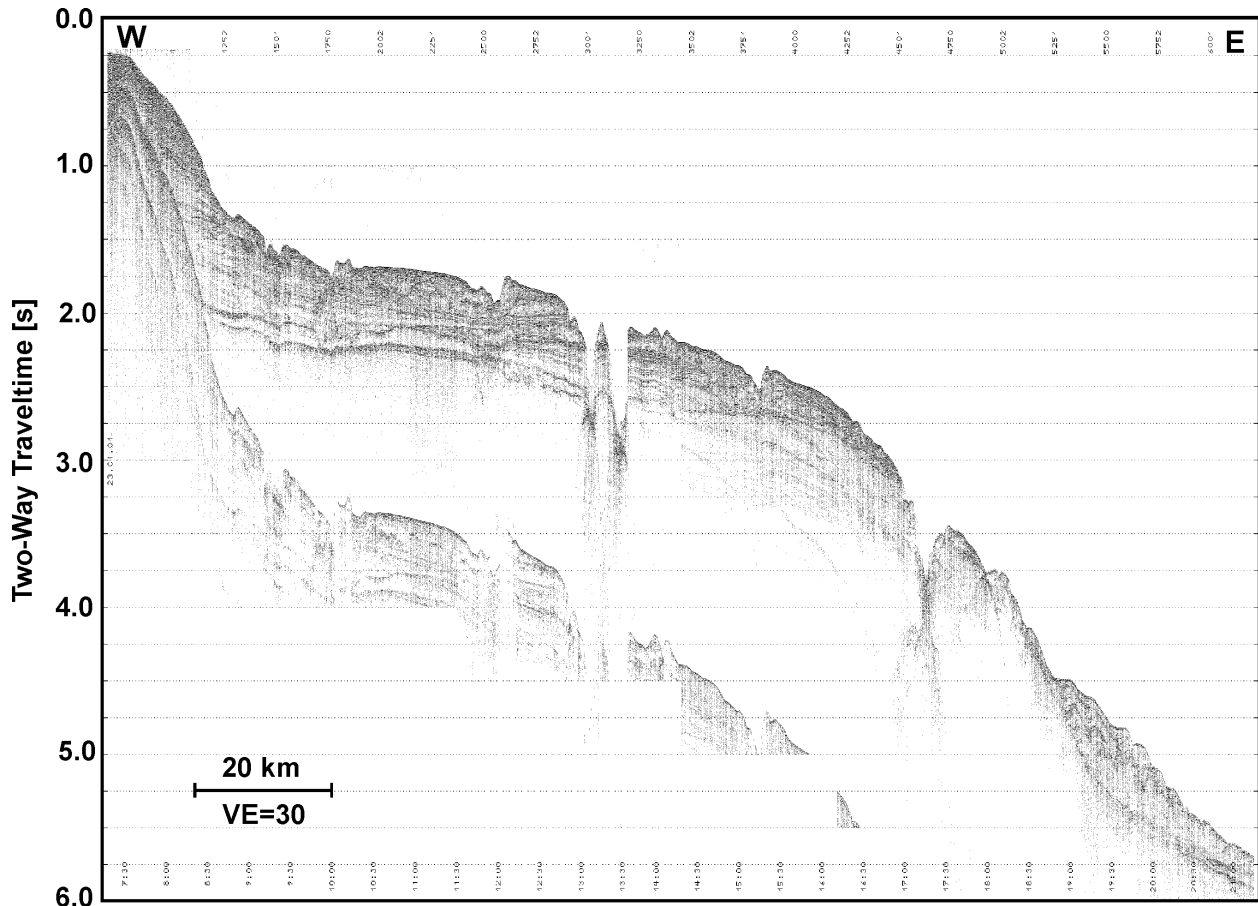


Fig. 2.18: Multichannel seismic line GeoB01-117 on the central Argentine continental margin.

exposed partly caused by massive slumping and partly by strong erosive currents in medium water depths, as shown by the results of the seismic survey of the Argentine colleagues. Additionally, McCoy and Zimmermann [1977] described earlier gravity and piston core sampling campaigns mainly of the Lamont Doherty Observatory which - among others - recovered one core from this eroded area which was composed of sediments of Miocene age.

The Uruguayan continental slope is less steep than the southern and central Argentine continental slope [Lonardi and Ewing, 1971]. It receives a huge amount of terrigenous sediments from the Rio de la Plata river, which is transported northward by coastal currents and deposited on the continental slope. However, the high water content and low rigidity of this almost suspended material facilitates downslope sediment transport and mass wasting processes in this area.

The site survey strategy in the two subareas was (1) to identify suitable drilling locations with high sedimentation rates on one or both flanks of the Mar del Plata Canyon and to provide stratigraphic information from the eroded area where outcrops of Tertiary sediments are expected and, (2) to find locations on the Uruguayan margin where downslope mass transport is reduced, possibly again in the vicinity of large or small canyons.

2.4.1.7.2 Preliminary Results, Stratigraphy and Proposed Drill Sites

Figure 2.19 presents the track chart of R/V Meteor cruise M49/2 in survey area C in the vicinity of the Mar del Plata Canyon (at about 37°55'S 54°W) and on the Uruguayan continental margin (at about 36°30'S 53°W).

Line GeoB01-135 was acquired to get an overview on the depositional pattern in the eroded area south of the Mar del Plata Canyon. The brutestack of the GI-Gun data shows a broad terrace with an about 0.5 s thick sediment sequence of almost parallel, slightly undulating subbottom layers deposited in 0.7 - 1.5 s TWT (about 500 to 1100 m) water depth above a seaward dipping unconformity (Figure 2.20). This parallel-bedded depositional pattern changes to deformed, wavy structures southeastwards until they steeply dip seawards below 1.6 s TWT (about 1100 m) water depth. Below the unconformity occur several other wedge-shaped units with parallel-bedded, diffuse or sigmoidal seaward dipping reflection pattern, bounded by unconformities each. The uppermost parallel-bedded sequence is strongly eroded so that deeper layers outcrop along the gentle slope of a broad terrace. We attempted to sample these outcrops by five gravity cores (GeoB6812-1 to GeoB6816-1) in order to get an age estimate of this sequence. Due to the hardness of the sediment, they recovered only very short (< 2 m) sequences of

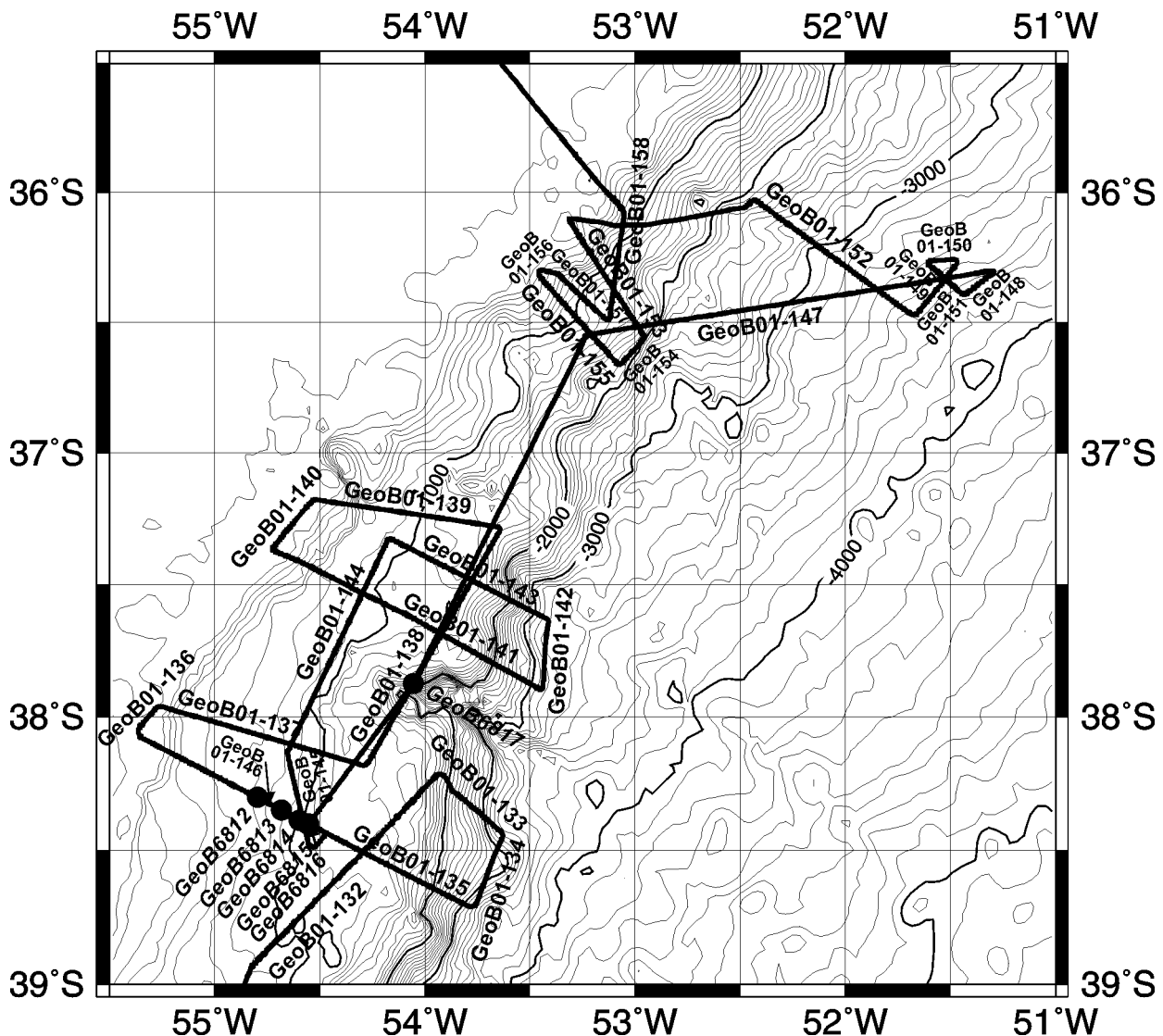


Fig. 2.19: Track chart and gravity core positions of R/V Meteor Cruise M49/2 on the northern Argentine and Uruguayan continental margin between 36° and 39°S and 51°W (Survey Area C).

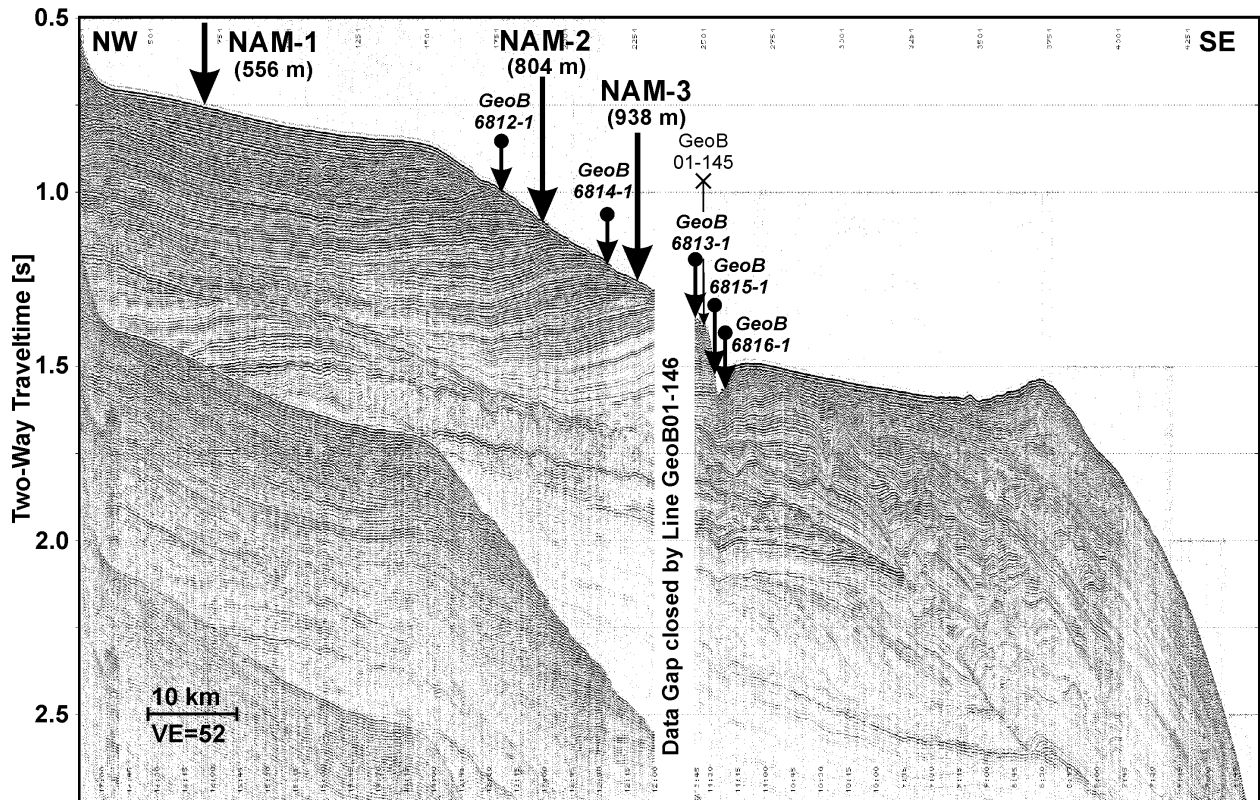


Fig. 2.20: Multichannel seismic line GeoB01-135 across Sites NAM-1, NAM-2, NAM-3 with gravity core positions GeoB6812-1 to GeoB6816-1. The intersection with line GeoB01-145 is marked by an arrow with a cross at the top.

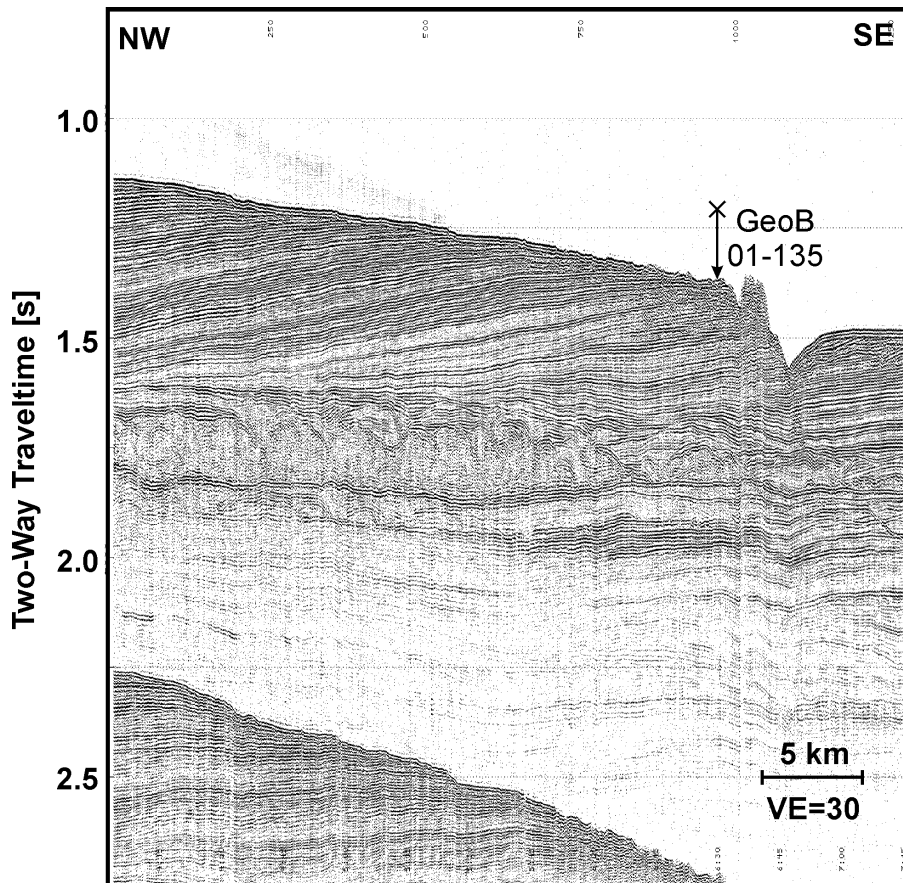


Fig. 2.21: Multichannel seismic line GeoB01-145, which is the crossing line to Sites NAM-1 to NAM-3 on line GeoB01-135. Their intersection is marked by an arrow with a cross at the top.

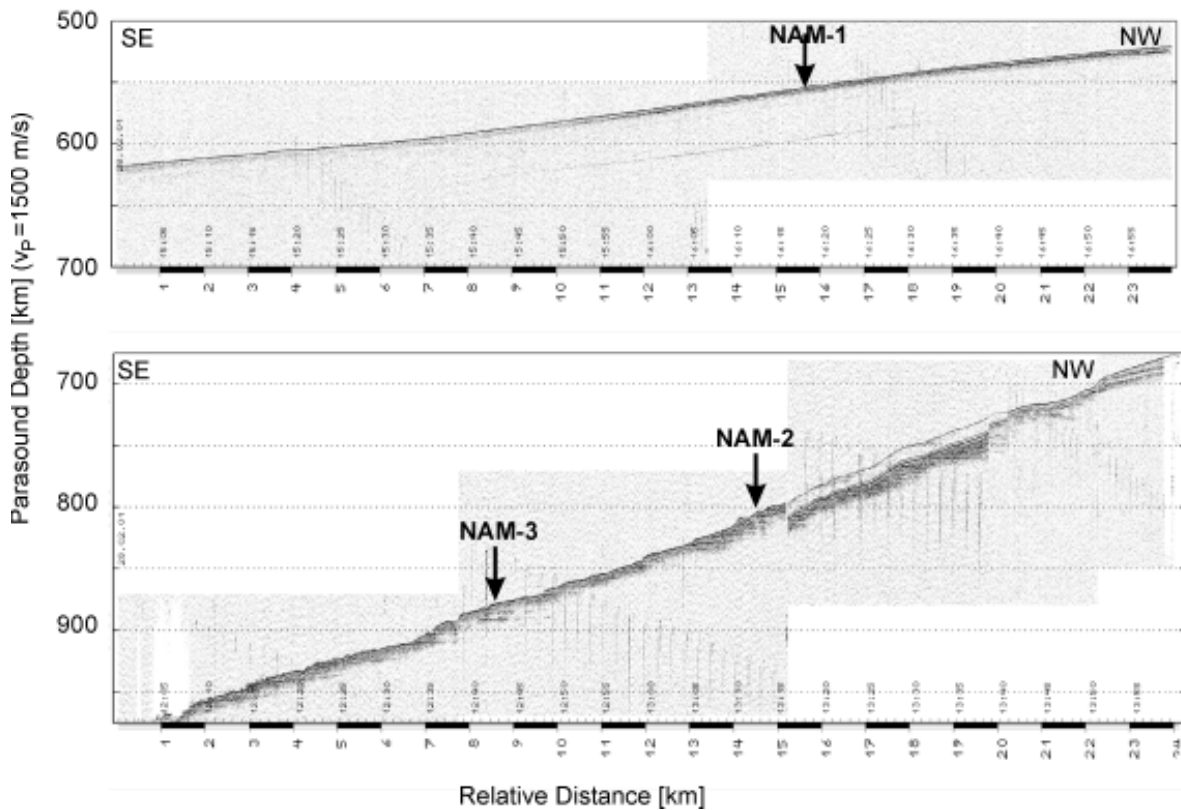


Fig. 2.22: PARASOUND example recorded along line GeoB01-135 across Sites NAM-1 to NAM-3. Note that the orientation is opposite to the seismic line (Figure 20).

sediments which mainly consist of soft sandy mud with small amounts of biogenic siliceous components at the top and very consolidated silty mud almost barren of biogenic components below (cf. chapter 2.4.2). The crossing line GeoB01-145 yields that the erosional zone extends at least 30 - 35 km to the northwest almost parallel to the shelf edge, with northwestward dipping layers in the uppermost sequence (Figure 2.21).

A transect of three drilling locations NAM-1 to NAM-3 located on line GeoB01-135 between about 550 and 930 m water depth is proposed (Figure 2.20) with the intention to recover successively older sediments so that a combination of all three overlapping records can produce a long record of the regional paleoceanography in medium water depths. A preliminary dating of the diatoms found in core GeoB6815-1 yields a biostratigraphic age of about 2 - 4 Ma in 0.35 m core depth. Lateral tracing of the reflector sampled here and adding of the top sequence missing at gravity core location GeoB6815 leads to a preliminary average sedimentation rate of more than 150 m/Ma, provided that the sampled reflector is identified and traced correctly, sequences are vertically added correctly, Holocene is at the top and biostratigraphic age estimation is right.

The Parasound record across Sites NAM-1 to NAM-3 reveals a very strong sea floor reflection in the vicinity of NAM-1 and a rough sea floor with reflectors pinching out near NAM-2 and NAM-3 (Figure 2.22). Generally, signal penetration is very low indicating a rather hard sea floor probably due to erosion.

A fourth drilling location NAM-4 is defined on line GeoB01-113 in about 1900 m water depth (Figure 2.23). Though unfortunately it is located close to a data gap in the seismic record caused by problems with the power supply of the trigger system, it was chosen as deeper site in order to have one location that can be used for a latitudinal transect to the south where only sites in water depths greater than 2000 m could be

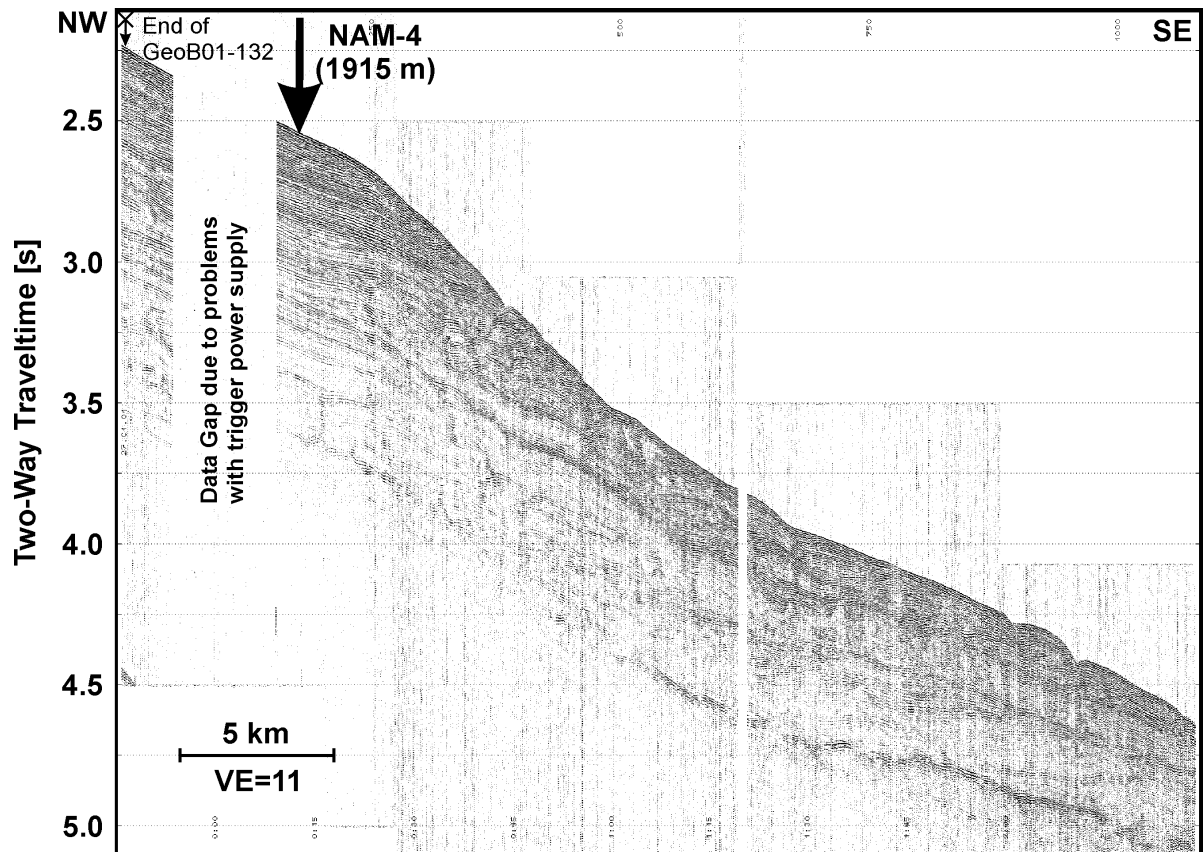


Fig. 2.23: Multichannel seismic line GeoB01-133 across Site NAM-4.

identified for the reconstruction of the confluence. Site NAM-4 is located on top of a parallel-bedded sequence with obviously very limited extent. Further downslope mass wasting is evident, whereas the „crossing“ line GeoB01-132 again shows several stacked, wedge-shaped sequences with wavy, current-controlled depositional pattern, bounded by unconformities each (Figure 2.24). The corresponding Parasound profile yields a rather diffuse reflection pattern without any indication of layering or mass wasting and with only low signal penetration (Figure 2.25).

Three possible drilling locations were identified on the northern flank of the Mar del Plata Canyon, two again in a medium water depth of 1100 m and one in a greater water depth of 2200 m for the latitudinal reconstruction of the confluence. Together they form a transect similar to those proposed in the southern eroded area. Site NAM-5 is located on line GeoB01-138 crossing the Mar del Plata Canyon, on top of an about 0.4 s TWT (about 300 m) thick sequence with almost parallel subbottom layers (Figure 2.26). The crossing line GeoB01-143 about 2 km southwest of Site NAM-5 shows that this sequence was deposited on top of an unconformity which pinches out in the northwestern part of this line, about 1 - 2 km southeast of Site NAM-6 (Figure 2.27). Hence, Site NAM-6 is located such that the sequence below the unconformity could be drilled, and Site NAM-7 is defined in order to sample almost parallel-bedded layers in a greater water depth.

The corresponding Parasound records clearly indicate that Site NAM-5 lies on top of an undisturbed sequence which is eroded and deformed further southwestwards, and Site NAM-6 will sample the older layers dipping towards the southeast (Figures 2.28, 2.29).

The seismic lines acquired in the northern sub-area off Uruguay are characterized by extensive slump and debris flow deposits caused by the large amount of terrigenous material delivered by the Rio de la Plata river, so that it was difficult to define any suitable drilling location here.

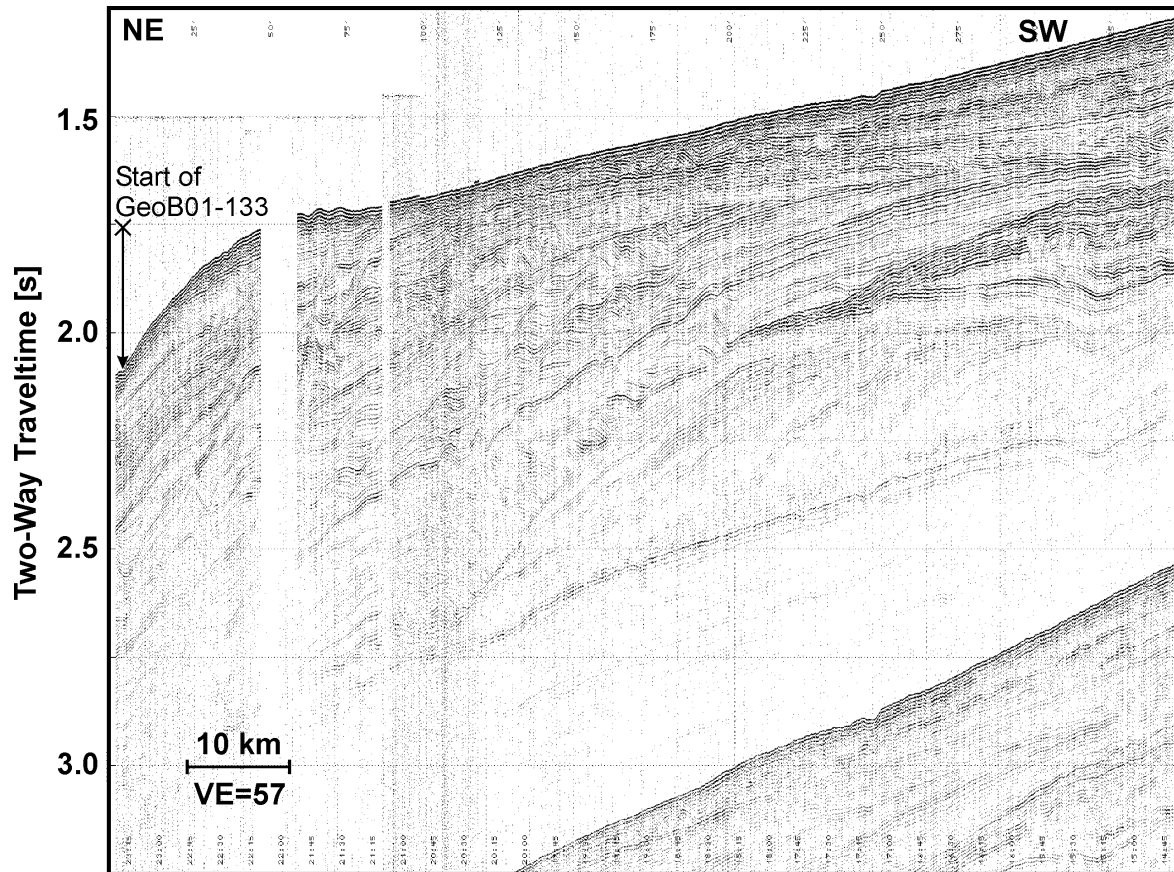


Fig. 2.24: Multichannel seismic line GeoB01-132, which is the crossing line to Site NAM-4 on line GeoB01-133.

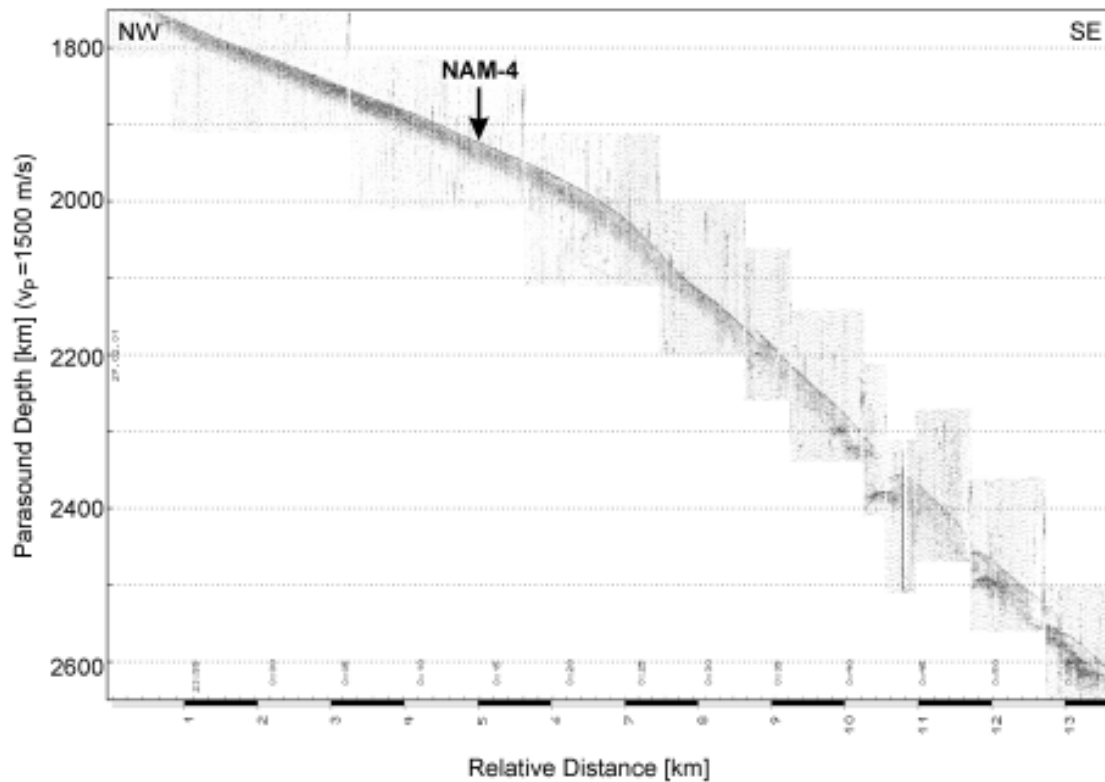


Fig. 2.25: PARASOUND example recorded along line GeoB01-133 across Site NAM-4.

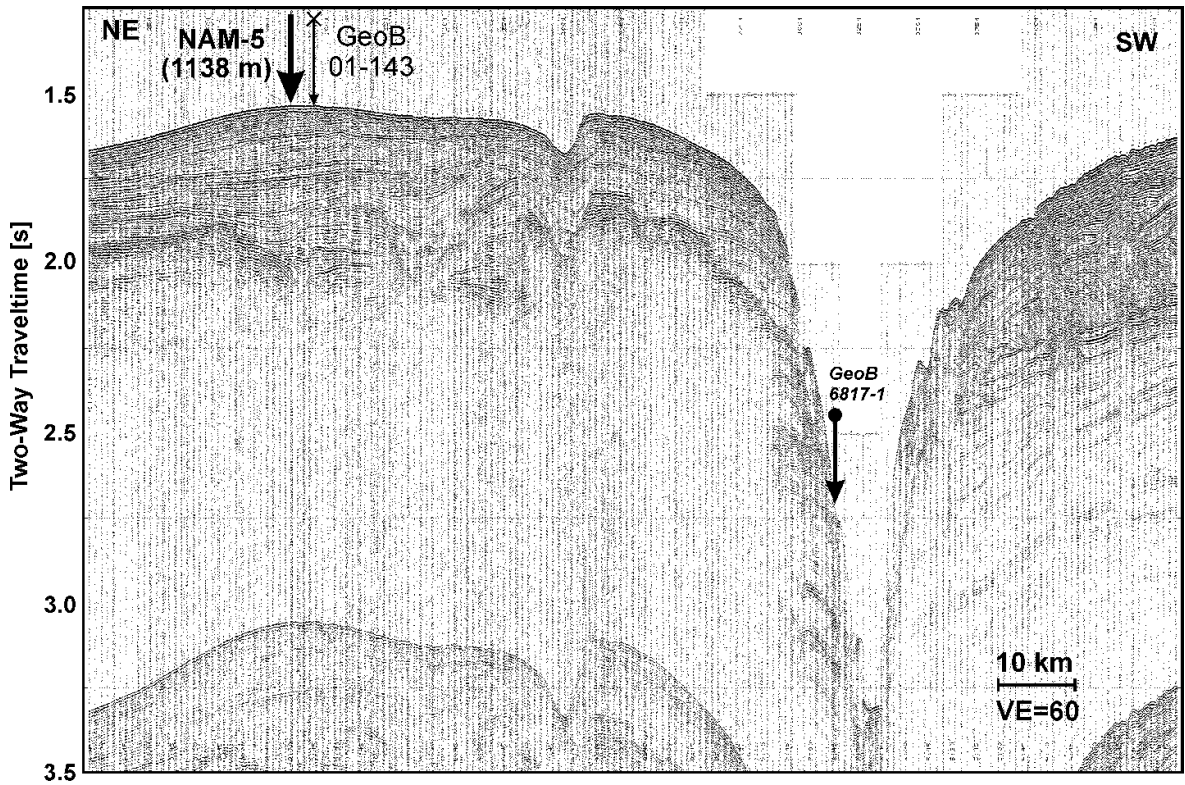


Fig. 2.26: Multichannel seismic line GeoB01-138 across Site NAM-5 on the northeastern flank of the Mar del Plata Canyon with gravity core position GeoB6817-1. The intersection with line GeoB01-143 is marked by an arrow with a cross at the top).

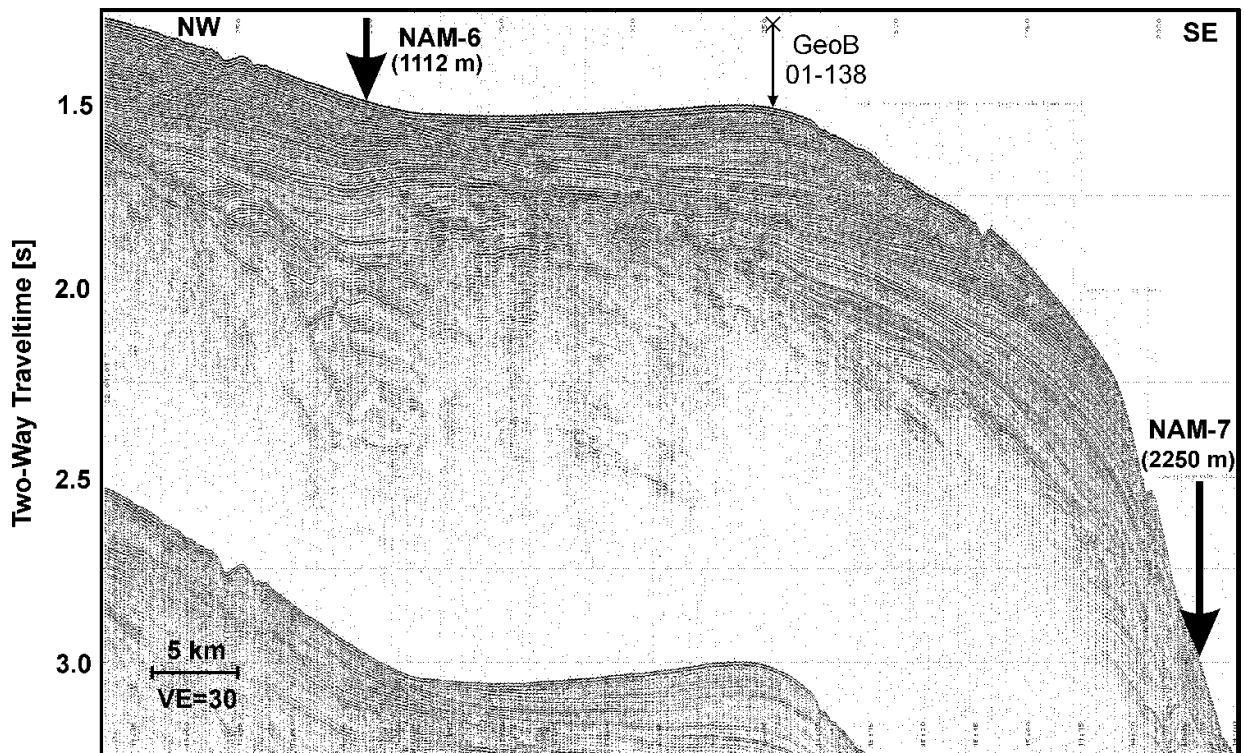


Fig. 2.27: Multichannel seismic line GeoB01-143 across Sites NAM-6 and NAM-7. Line GeoB01-143 is also crossing line to Site NAM-5 on line GeoB01-138. Their intersection is marked by an arrow with a cross at the top.

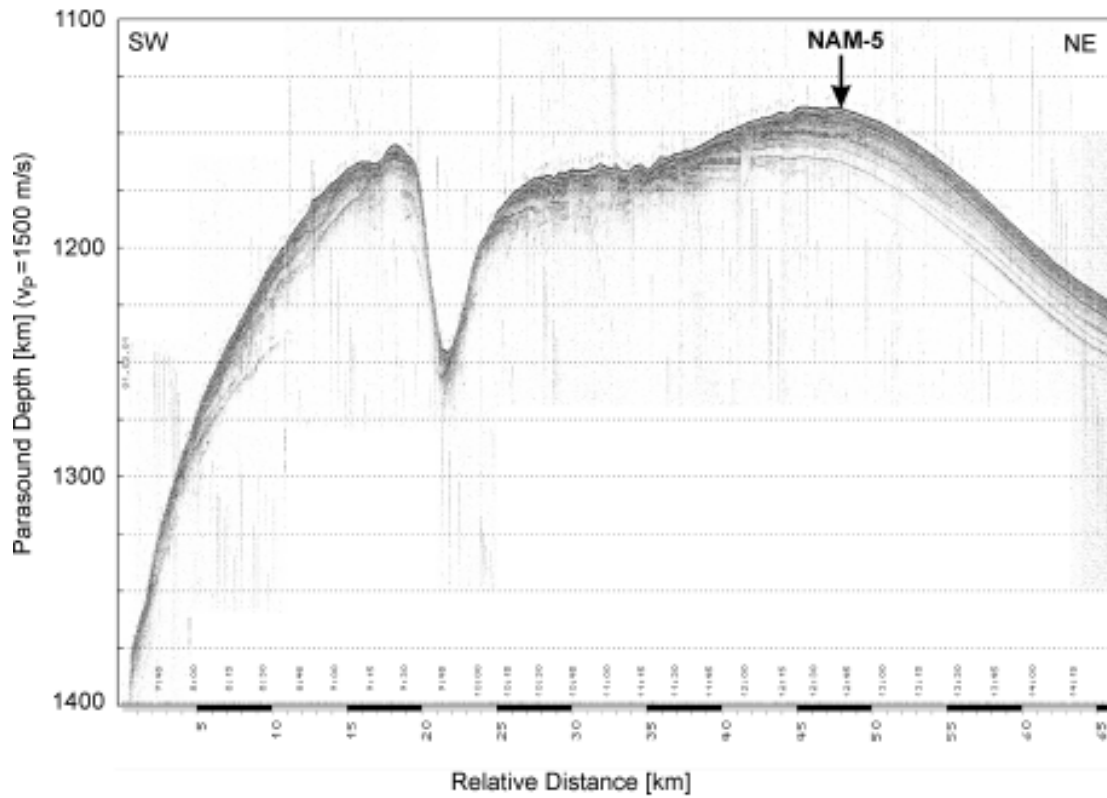


Fig. 2.28: PARASOUND example recorded along line GeoB01-138 across Site NAM-5. Note that the orientation is opposite to the seismic line (Figure 26).

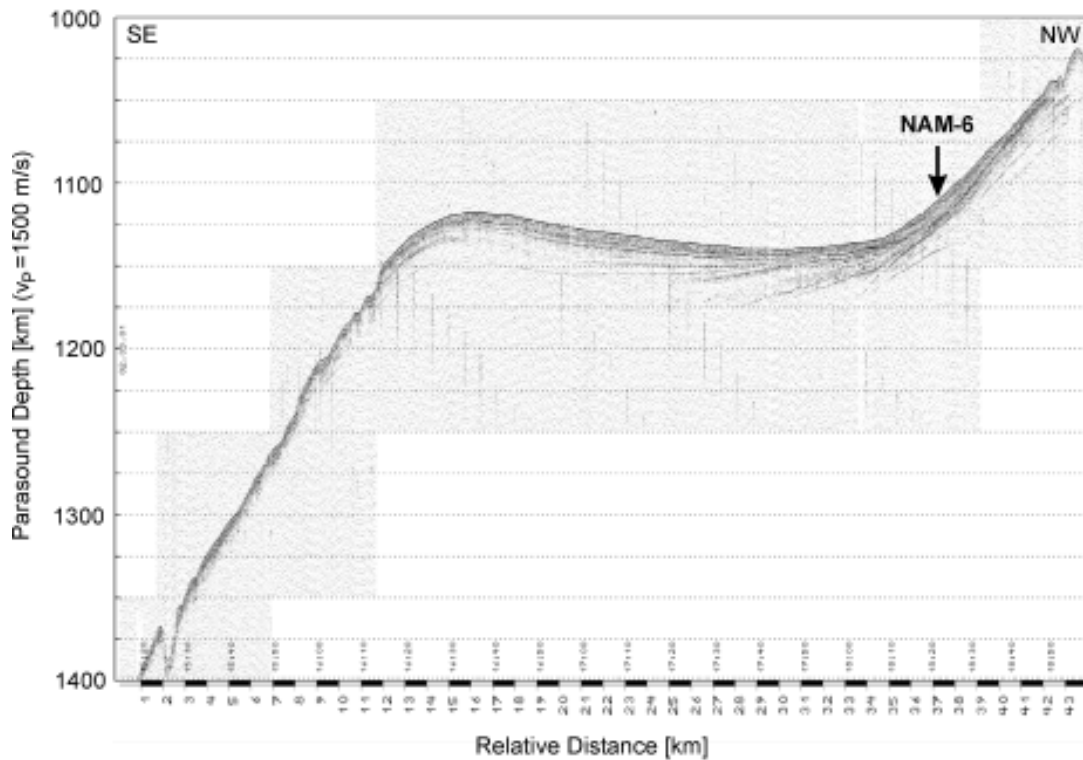


Fig. 2.29: PARASOUND example recorded along line GeoB01-143 across Sites NAM-6 and NAM-7. Note that the orientation is opposite to the seismic line (Figure 27).

Table 2.6: Proposed drill sites (preliminary) for survey areas A and C along the Argentine and Uruguayan continental margins.

Area A - Southern Argentine Continental Margin at 44°S

Site	Latitude	Longitude	Seismic Line	Date	Time	Water Depth	Gravity Core	Location
	Site/ Crossing	Site/ Crossing	/Crossing Line	Site/ Crossing	Site/ Crossing	Site/ Crossing		
SAM-1	43°56.372'S	58°20.034'W	GeoB01-089	16.02.01	07:15	1974 m	appx. GeoB6805-1 to GeoB6808-1	Channel 1, upslope
	43°57.225'S	58°18.446'W	GeoB01-095	17.02.01	18:10	2058 m		
SAM-2	44°02.316'S	59°08.772'W	GeoB01-089	16.02.01	08:48	2198 m		Channel 1, downslope
	44°01.152'S	58°10.982'W	GeoB01-100	16.02.01	08:30	2290 m		
SAM-3	44°23.447'S	57°46.238'W	GeoB01-091	16.02.01	23:52	3241 m	appx. GeoB6804 to GeoB6804	Almirante Brown Canyon, upslope
	44°26.965'S	57°39.291'W	GeoB01-109	20.02.01	09:36	3532 m		
	44°21.687'S	57°50.103'W	GeoB01-107	20.02.01	00:48	3090 m		
SAM-4	44°25.038'S	57°43.124'W	GeoB01-091	16.02.01	23:28	3354 m	appx. GeoB6801 to GeoB6804	Almirante Brown Canyon, upslope
	44°26.965'S	57°39.291'W	GeoB01-109	20.02.01	09:36	3532 m		
SAM-5	44°29.646'S	57°34.033'W	GeoB01-091	16.02.01	22:09	3698 m	GeoB6803-1	Almirante Brown Canyon, upslope
	44°26.965'S	57°39.291'W	GeoB01-109	20.02.01	09:36	3532 m		
SAM-6	44°33.866'S	57°29.732'W	GeoB01-091	16.02.01	21:34	3917 m	GeoB6802-1	Almirante Brown Canyon, upslope
	44°26.965'S	57°39.291'W	GeoB01-109	20.02.01	09:36	3532 m		
SAM-7	44°33.052'S	57°27.380'W	GeoB01-091	16.02.01	21:15	4087 m	GeoB6801-1	Almirante Brown Canyon, upslope
	44°26.965'S	57°39.291'W	GeoB01-109	20.02.01	09:36	3532 m		

Table 2.6: continued

Area C - Northern Argentine and Uruguayan Continental Margins between 39° - 34°S

Site	Latitude	Longitude	Seismic Line	Date	Time	Water Depth	Gravity Core	Location
	Site/Crossing	Site/Crossing	/Crossing Line	Site/ Crossing	Site/ Crossing	Site/ Crossing		
NAM-1	38°10.209'S 38°23.719'S	55°07.558'W 54°34.652'W	GeoB01-135 appx. GeoB01-145	28.02.01 03.03.01	16:18 06:30	556 m 1023 m	appx. GeoB6812-1 to GeoB6816-1	Lamont Core
NAM-2	38°19.438'S 38°23.719'S	54°44.833'W 54°34.652'W	GeoB01-135 appx. GeoB01-145	28.02.01 03.03.01	13:13 06:30	804 m 1023 m	appx. GeoB6812-1 to GeoB6816-1	Lamont Core
NAM-3	38°21.897'S 38°21.851'S 38°23.719'S	54°38.751'W 54°38.898'W 54°34.652'W	GeoB01-135 GeoB01-146 appx. GeoB01-145	28.02.01 03.03.01 03.03.01	12:23 09:36 06:30	938 m 1023 m	appx. GeoB6812-1 to GeoB6816-1	Lamont Core
NAM-4	38°15.579'S 38°13.311'S	53°52.833'W 53°56.758'W	GeoB01-133 appx. end of line GeoB01-132	28.02.01 27.02.01	00:14 23:34	1915 m 1559 m		
NAM-5	37°28.007'S	53°45.889'W	GeoB01-138 appx. GeoB01-143	01.03.01 02.03.01	12:43 16:22	1138 m	appx. GeoB6817-1	Mar del Plata Canyon
NAM-6	37°23.112'S 37°29.052'S	54°01.244'W 53°46.602'W	GeoB01-143 appx. GeoB01-138	02.03.01 01.03.01	18:22 12:28	1112 m 1137 m		Mar del Plata
NAM-7	37°34.837'S 37°29.052'S	53°32.623'W 53°46.602'W	GeoB01-143 appx. GeoB01-138	02.03.01 01.03.01	14:24 12:28	2250 m 1137 m		Mar del Plata

2.4.1.8 Additional Seismic Surveys

Additional multichannel seismic data, which could possibly serve as pre-site survey data, too, were collected during R/V Meteor Cruise M46/3 [Bleil et al., 2001] in the Argentine Basin. This data was collected with the intention to study the mud wave area and its evolution through time close to the Zapiola Drift.

2.4.2 Sedimentology

2.4.2.1 Sediment sampling

(T. Bickert, U. Gross, R. Violante, T. Westerhold)

A gravity corer was used to recover Neogene sediments at 17 stations at the Argentine continental slope. The main purpose was to sample the outcrops of sediment layers along seismic lines to give the opportunity to describe and date these sediments related to selected seismic reflectors. Detailed information on locations, deployed devices and recovery is summarised in the station list (Table 2.7).

2.4.2.1.1 Gravity Corer

In order to obtain long sediment cores a gravity corer with a pipe of 3 or 6 m length and with a weight of 1.5 tons on top was used. Some 32 m of sediments were recovered with the gravity corer during cruise M49/2. Individual core lengths varied between 12 and 571 cm. Before use all core liners have been marked with a straight line to retain a common azimuthal orientation of the core segments for paleomagnetic purposes. After recovery, the core liners were cut into 1 m long segments, sealed with caps at both ends and inscribed.

The segments were cut along-core into a work and an archive half. Immediately after core opening, digital color reflectance data were routinely recorded at 31 wavelengths in the visible light range (400-700 nm) on the archive halves using a hand-held Minolta CM-2002 spectrophotometer. Prior to every measurement of a core segment at 2-cm intervals, the instrument was adjusted to 100% reflectance by attaching a white calibration cap. The sediment surfaces were carefully scraped to expose a fresh, clean plane and covered with a thin transparent film (Hostaphan) to avoid any contamination. The data files were transferred to a PC. A graphic representation of the percent reflectance at 550 nm wavelength is shown for each core. Also on the archive halves the sediments were described, and smear slide samples were picked from representative horizons.

From the work half one series of syringe samples (10 ccm) was collected at 5 cm depth intervals. These samples will be used for shore-based measurements of physical properties, mineralogy and organic geochemistry. Additional syringe samples were taken from selected horizons of the sediment cores retrieved at the Argentine Slope at 38°S. These samples will be studied for sedimentological and faunal characteristics at the Marine Geology Department of the Servicio di Hidrografia Naval, Buenos Aires (R. Violante). For the determination of the existence of any hydrocarbons in the Neogene sediments (S. Schmidt, BGR, Hannover), 100 ml of the core catcher sediment of each core were sampled and immediately stored at -18°C.

Work and archive halves were then stored at +4°C and shipped to the core repository of the Department of Geosciences, University of Bremen, at this temperature.

Table 2.7: Station list.

GeoB #	Ship #	Device	Date	Time UTC max.depth / bottom contact	Latitude	Longitude	Water depth (m)	Samples / #BEZUG!	Remarks
Working Area 'A' - Argentine Continental Slope									
6801-1	1	SL 6	20.02.	15:35	44°33.07' S	57°27.40' W	4090	469 cm	seismic line 091
6802-1	2	SL 6	20.02.	18:29	44°31.80' S	57°29.20' W	3915	25 cm	seismic line 091
6803-1	3	SL 6	20.02.	21:05	44°29.60' S	57°34.10' W	3696	484 cm	seismic line 091
6804-1	4	SL 6	20.02.	23:38	44°24.50' S	57°45.30' W	3286	571 cm	sed. in weight, seismic line 091
6805-1	5	SL 6	21.02.	22:28	43°57.80' S	58°19.90' W	2027	47 cm	bent tube, seismic line 095
6806-1	6	SL 6	22.02.	00:06	43°56.00' S	58°15.17' W	2155	112 cm	seismic line 095
6807-1	7	SL 6	22.02.	01:41	43°54.58' S	58°11.27' W	2294	275 cm	seismic line 095
6808-1	8	SL 6	22.02.	05:06	43°50.40' S	58°09.50' W	2677	569 cm	sed. in weight, seismic line 094
Working Area 'B' - Argentine Continental Slope									
6809-1	9	SL 6	26.02.	19:59	40°56.80' S	56°16.09' W	1727	-	tube empty, seismic line 126
6810-1	10	SL 6	26.02.	21:08	40°56.97' S	56°16.32' W	1781	few gravels	tube empty, seismic line 126
6811-1	11	SL 6	26.02.	23:20	41°06.18' S	55°55.42' W	2457	115 cm	seismic line 125
Working Area 'C' - Argentine Continental Slope									
6812-1	12	SL 3	03.03.	11:19	38°18.23' S	54°47.74' W	734	186 cm	seismic line 135
6813-1	13	SL 3	03.03.	12:58	38°23.29' S	54°35.96' W	985	128 cm	bent tube, seismic line 135
6814-1	14	SL 3	03.03.	14:15	38°21.06' S	54°40.87' W	888	-	tube empty, seismic line 135
6815-1	15	SL 3	03.03.	15:54	38°24.12' S	54°33.44' W	1156	48 cm	seismic line 135
6816-1	16	SL 3	03.03.	16:40	38°24.22' S	54°33.20' W	1180	12 cm	seismic line 135
6817-1	17	SL 3	03.03.	21:57	37°52.51' S	54°03.33' W	2042	169 cm	seismic line 138

2.4.2.2 Lithologic Core Summary

(T. Bickert, R. Violante, T. Westerhold)

Preliminary lithologic summaries of the gravity cores recovered during cruise M49/2 are shown in Spieß et al. (in prep.). They include the visual descriptions of the representative sediment types, their colors according to the Munsell soil color chart as well as sedimentary structures and unique features, following the ODP conventions (Graham and Mazullo, 1988). Lithological data are primarily based on the investigation of smear slides taken from selected horizons. Smear slides were prepared using Norland Optical Adhesive 61 as mounting medium (refractory index of 1.56), dried with UV light for 10 minutes. Slides were studied at 400x magnification on an Olympus BH-2 petrological microscope along two perpendicular profiles through the central area of the cover slip. Sediment classification followed the ODP terminology. Also displayed is the color reflectance record of the wave length 550 nm.

2.4.2.2.1 Argentine Continental Slope at 44°S (Survey Area A)

Core transects GeoB 6801-1 through 6808-1

Along two transects at 44°S several cores were taken at the Argentine Continental Slope to retrieve Tertiary sediment sequences. The first transect was directed along seismic line GeoB 01-091 at the western flank of the Almirante Brown Travers Canyon, which deeply cuts into the Cenozoic deposits of the deeper Argentine Continental Slope. The core stations were chosen to describe and date the layers between 3286 m and 4090 m water depth (Fig. 2.30). The second transect along seismic lines GeoB 01-095 / 094 tried to sample a sediment drift, which was deposited in top of the Cenozoic sequence along the another traverse canyon in water depth between 2027 and 2677 m (Fig. 2.31).

The deeper sites (GeoB 6801-1, 6802-1, 6803-1, 6804-1, 6808-1) consist mostly of two lithologic units. On top of these cores there is usually a few centimeter thick layer of soft diatom mud with varying amounts of foraminifer tests and nannofossil placoliths. Below, the sediment column consists of slightly consolidated olive gray to gray mud with varying amounts of biogenic siliceous components, i.e. diatoms, radiolarians, and silicoflagellates. The terrigenous material which dominates the slope sediments consists of clay and silt-sized grains of quartz, feldspar, rock fragments. The sediments of this second unit are relatively uniform from top to the bottom, interrupted by several few-cm thick layers or lenses of fine sand, which indicate turbidite deposits. Core 6803-1 penetrated a slump deposit below 2.23 m depth.

At the shallower sites (GeoB 6805-1, 6806-1, 6807-1), located at the northern slope of the drift deposit, surface sediments were recovered which consist mainly of greenish gray to gray diatom-bearing foraminifer-nannofossil ooze. This carbonate-bearing layer spans only the uppermost 28 to 71 cm. This pattern might belong to the increased carbonate dissolution during pre-Holocene times, which prevent foraminifer preservation in sediments of the late Pleistocene. Nevertheless, the smear slide study revealed mostly well preserved diatoms assemblages, which are worth to study the opal productivity in the frontal zone of the Malvinas Confluence. Below the surface layer, a greenish-grey siliceous muddy sand (GeoB 6806-1) as well as an olive grey siliceous nannofossil ooze (GeoB 6807-1) are consolidated and might belong to one of the seismic reflectors indicated in seismic line GeoB 01-095.

2.4.2.2.2 Argentine Continental Slope at 41°S (Survey Area B)

Core transect GeoB 6809-1 through 6811-1

In a second area at the Argentine Continental Slope further stations were selected to retrieve Neogene sediment sequences along the seismic lines GeoB 01-125 and 01-126 at about 41°S. Unfortunately, two

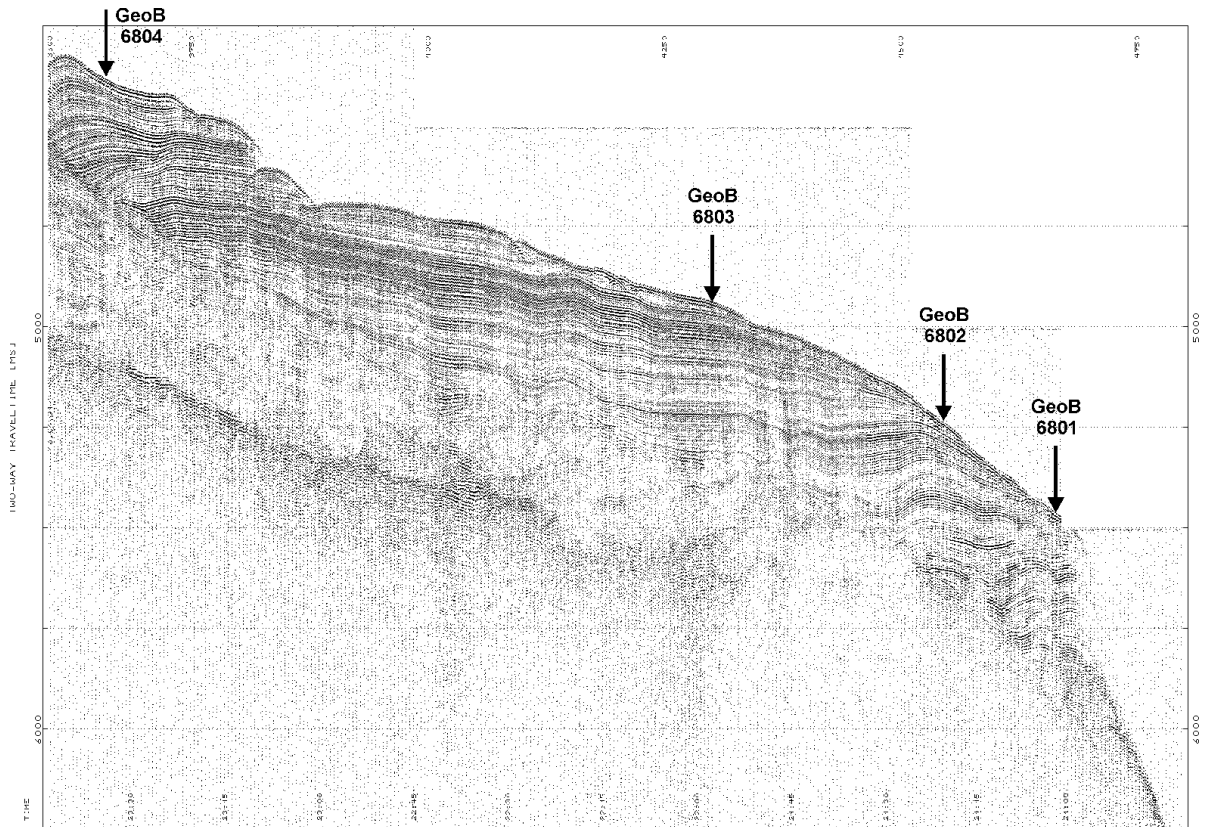


Fig. 2.30: Digital seismogram crossing core positions GeoB 6801-1 through GeoB 6804-1, recorded along GeoB seismic line 01-091.

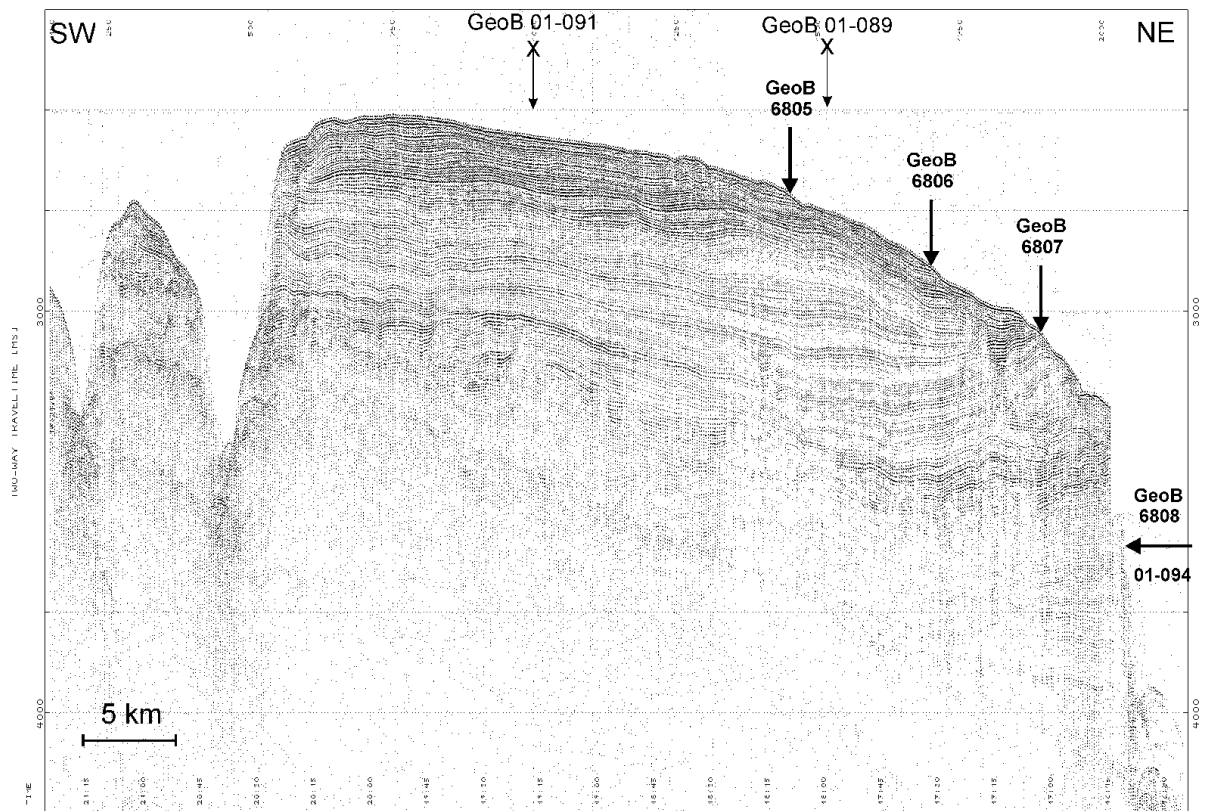


Fig. 2.31: Digital seismogram crossing core positions GeoB 6805-1 through GeoB 6808-1, recorded along seismic line GeoB 01-095.

gravity cores failed to penetrate the seafloor, probably due to a seafloor covered by coarse gravels. Core GeoB 6811-1 located at 2457 m water depth at the flank of a deep canyon recovered a short sequence of olive grey silty mud with diatoms and a few percent foraminifers in the uppermost layer of the sediment column. However, the frequent occurrence of mud clasts in this core characterises a typical canyon deposit rather than a section of the older strata cut by the deep erosional structure.

2.4.2.2.3 Argentine Continental Slope at 38°S (Survey Area C)

Core transect GeoB 6812-1 through 6816-1

At 44°S a further transect of several cores was positioned along seismic line GeoB 01-135 at the Argentine Continental Slope to retrieve Tertiary sediment sequences. The core stations were chosen to describe and date some of the seismic layers between 734 m and 1180 m water depth, which outcrop along the gentle slope of a broad terrace extending parallel to the shelf edge (Fig. 2.32).

Due to the hardness of the sediments, the gravity cores (GeoB 6812-1, 6813-1, 6815-1, 6816-1) recovered only very short sequences of sediments. However, most of them consisted of two lithologic units. On top of these cores there is usually a few centimeter thick layer of soft sandy mud with small amounts of biogenic siliceous components, i.e. diatoms, radiolarians, and silicoflagellates. Below, the sediment column consists of very consolidated olive gray to greenish gray silty mud which is almost barren of biogenic components, i.e. diatoms. Nevertheless, these consolidated layers might represent some early Neogene deposits which form the seismic horizons.

Core GeoB 6817-1

Core GeoB 6817-1 was recovered on the north eastern flank of the Mar del Plata Canyon. This site has been chosen to date the deep reflectors of the seismic section GeoB 01-138 (Fig. 2.33), which connects the seismic surveys south and north of the canyon. However, due to the steepness of the slopes, the gravity corer was not able to penetrate the envisioned sections. The sediments recovered consisted mainly of young sediments of diatom-bearing silty mud. Only the consolidated nannofossil mud pebble at 158 cm core might indicate the composition of an old layer.

2.4.2.3 Preliminary stratigraphy

(T. Bickert)

A main purpose of METEOR cruise M 49/2 was the sampling and dating of reflectors that occurred in the seismic profiles of the Cenozoic sediment sequences along the continental slope off Argentina. Several cores retrieved older sediment layers that gave the opportunity to date the seismic horizons (e.g. GeoB 6807, 6815, 6816). These sediments were dated by using diatom biostratigraphic events. Planktonic as well as benthonic foraminifer events could not be used as stratigraphic tool due to the sparse occurrence of carbonatic shells within the recovered sediments which are mostly dominated by terrigenous and siliceous sediment constituents.

2.4.3 Water and Plankton Studies

2.4.3.1 Pumped water samples for oxygen isotope measurements

(U. Gross)

At 27 stations water samples from about 3 m water depths for the analysis of stable oxygen isotopes were taken from the shipboard membrane pump (Tab. 2.9). About 50 ml of water were filled into a glass bottle,

Table 2.8: Sediment constituents, grain size estimates and sediment classification results based on smear slide investigation.

GeoB	Depth (cm)	Abiogenic components										Biogenic components					Grain size			Sediment name	
		Quartz	Feldspar	Rock fragments	Mica	Clay	Volcanic glass	Inorganic calcite	Accessory minerals	Micronodules	Pyrite	Foraminifers	Nannofossils	Diatoms	Radiolarians	Sponge spicules	Silicoflagellates	Sand	Silt		Clay
6801-1	5	8	acc		acc	55					2	5	25	5		acc	40	60		diatom mud	
	70	12	acc		acc	80				acc			5	3		acc	20	80		siliceous mud	
	154	3			1	85	1			1		1	8	2		acc	15	85		siliceous mud	
	332	40	10		5	20	5			15			3	2			70	10	20	pyritized sand layer	
6802-1	5	5	2			65				2		15	10	1		acc	5	15	80	diatom-b. nannofossil mud	
	20	10	4		acc	80				acc			5	1			5	15	80	diatom-bear. mud	
6803-1	5	5	1		1	15	1				20	40	15	1		1	15	30	55	diatom. foram nannof. ooze	
	170	10	1			72				5			10	2		acc	3	25	72	diatom-bear. mud	
	332	40	10		5	20	5			15			3	2			70	10	20	pyritized sand layer	
6804-1	40	5			acc	75	acc						18	2					25	75	diatom mud
6805-1	20	15	1		2	10	acc				25	35	10	1	1		35	20	45	diatom-b. foram nannof. ooze	
6806-1	10	15	1		1	10					20	40	10	2	1		30	20	50	diatom-b. foram nannof. ooze	
	90	55	2		2	30			1				10				45	25	30	siliceous muddy sand	
6807-1	8	15	1		2	10							1	1			30	20	50	sandy foram. nannof. ooze	
	112	8				10				2	2	55	12	10		1	10	25	65	siliceous nannofossil ooze	
	230	15			2	45				3		5	25	5			15	35	50	diatom mud	
6808-1	55	20			1	65				5			7	2			5	30	65	diatom-bear. mud	
	59	30	1		1	40				2			25	1			20	40	40	diatom mud	
	200	10				68				2			18	2	acc		2	30	68	diatom mud	
6811-1	8	35	2	2	1	20					25	10	2	2	1		40	30	30	foraminifer mud	
	80	35		15		40				2			7	1			30	30	40	silty mud w. diatoms	
6812-1	5	40	2	15	10	30								2	1		50	30	20	sandy mud	
	40	30	2	10	3	50				2			2	1			20	30	50	silty mud	
	140	40	2	8	3	45				2				acc			25	30	45	silty mud	
6813-1	20	35	2	25	2	35	1							acc			40	25	35	sandy mud	
	60	30	2	25	2	40				1			acc	acc			30	30	40	sandy mud	
	120	35	2	8	2	50				2			1	acc			10	30	50	silty mud	
6815-1	7	20		2	1	60							15	2					40	60	diatom-b. silty mud
	40	15	1	5	2	60				1			15	1			40	60		diatom-b. silty mud	
6816-1	3	30	1	25	3	40	1						acc	acc			30	30	40	sandy mud	
	13	25	1	8	2	60				2			2	acc			40	60		silty mud	
6817-1	120	25	1		1	60				2			10	1			5	35	60	diatom-b. silty mud	
	mud clast	156	15		2	2	40						35	5	1		5	20	75	nannofossil mud	

but were not poisoned. The samples will be used for calibrating the oxygen isotope composition of seawater as a basic parameter for applying oxygen isotopes as a proxy parameter in reconstructing surface water temperatures and salinities in past times. This is especially important in the area of fresh water influx of the Rio de la Plata River to the South Atlantic Ocean. Accordingly, the additional measurements of the thermosalinograph gave a wide range of temperatures (9.4° to 25°C) and salinities (29.5 to 34 psu).

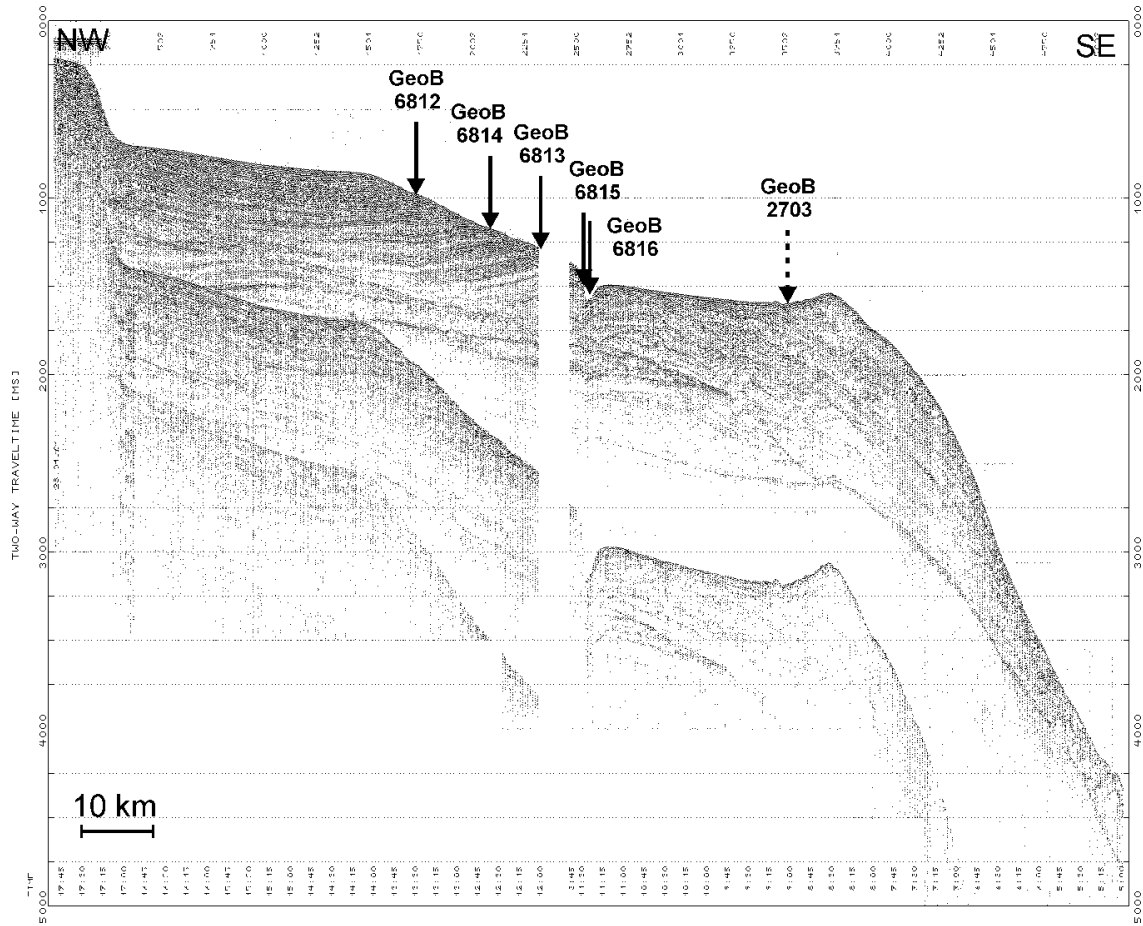


Fig. 2.32: Digital seismogram crossing core positions GeoB 6812-1 through GeoB 6816-1, recorded along seismic line GeoB 01-135

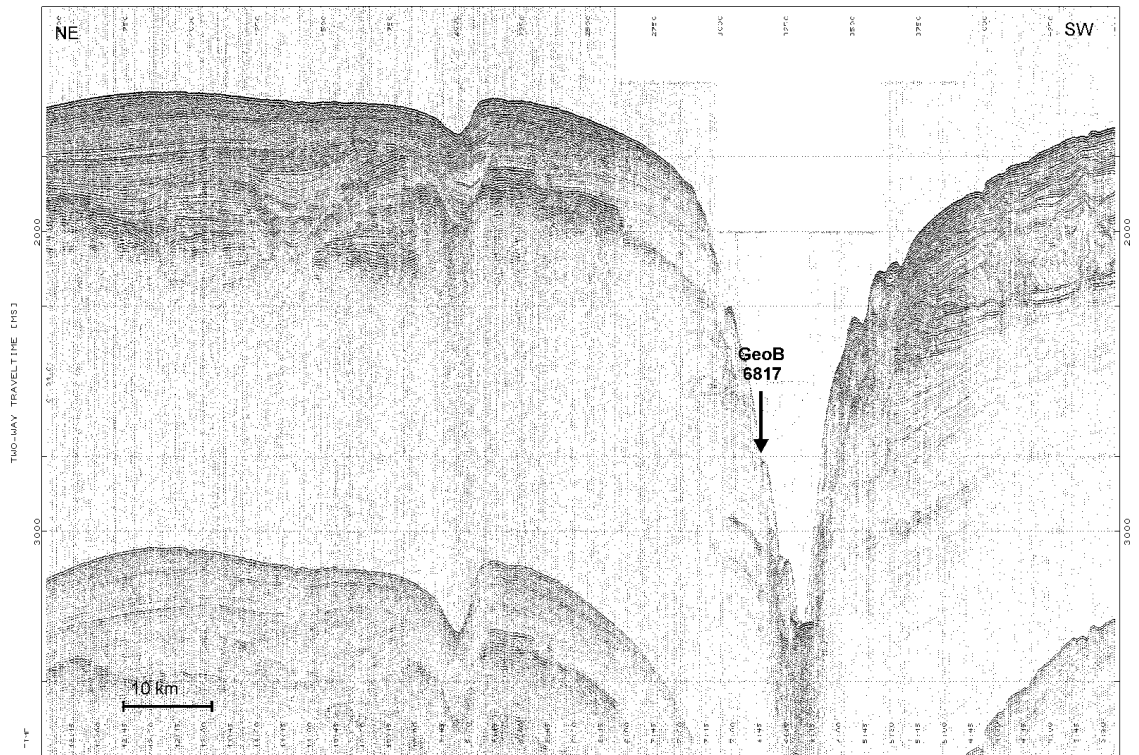


Fig. 2.33: Digital seismogram crossing core position GeoB 6817-1, recorded along seismic line GeoB 01-138.

Table 2.9: Locations of surface water samples for oxygen isotope measurements.

No.	Date 2000	Local Time (UTC = L.T.+ 3 h)	Latitude South	Longitude West	SST [°C]	SSS [‰]	Remarks
1	13.2.01	17:08	35°18.16	55°00.96	22.4	29.4788	
2	14.2.01	14:19	39°07.34	57°09.16	18.3	33.6161	
3	14.2.01	16:40	39°32.11	57°24.80	18.1	33.6659	
4	14.2.01	20:15	40°08.19	57°47.71	17.2	33.7494	
5	15.2.01	15:08	42°47.91	57°47.85	15.2	33.7218	
6	15.2.01	16:27	43°10.29	59°44.16	15.5	33.8024	
7	15.2.01	20:15	43°25.95	59°17.14	13.1	33.9849	
8	16.2.01	9:49	44°17.88	57°39.28	13.9	34.0793	
9	17.2.01	10:18	43°55.02	58°31.56	13.5	34.1369	
10	18.2.01	10:32	43°58.70	58°03.35	13.4	34.0771	
11	19.2.01	11:05	45°00.96	58°57.37	9.4	34.0892	
12	20.2.01	9:58	44°30.70	57°46.20	13.3	34.0829	
13	22.2.01	13:12	42°14.14	57°26.45	12.4	34.0389	
14	23.2.01	19:43	40°53.61	55°03.76	13.8	34.1140	
15	24.2.01	17:11	40°33.23	55°58.24	12.9	33.9851	
16	25.2.01	13:01	40°46.86	56°15.82	12.7	33.8826	
17	26.2.01	9:47	41°00.08	56°05.42	11.4	34.0010	
18	27.2.01	14:07	38°42.64	54°32.67	16.2	33.7769	
19	28.2.01	3:22	38°39.81	53°54.75	17.9	33.8468	
20	28.2.01	8:57	38°23.20	54°35.64	17.9	33.7424	
21	28.2.01	14:22	38°07.18	55°14.97	16.9	33.6262	
22	1.3.01	0:05	38°10.87	54°18.30	18.9	33.6960	
23	1.3.01	11:20	37°20.28	53°40.38	23.3	29.4786	
24	2.3.01	11:27	37°34.65	53°33.10	23.5	33.1145	
25	3.3.01	14:25	38°24.22	54°33.21	19.6	33.7988	
26	4.3.01	15:32	36°22.68	51°53.12	25.0	32.0325	
27	5.3.01	9:11	36°09.51	52°12.75	24.7	31.5404	

2.4.3.2 Pumped water samples for alkenone analysis

(U. Gross)

The alkenone method provides a tool for reconstructing past sea surface temperatures (SSTs). Certain Haptophyte algae, especially coccolithophores of the species *Emiliania huxleyi*, synthesize long-chain (C₃₇-C₃₉) unsaturated ketones (alkenones) in different proportions, depending on the temperature of ambient seawater during growth of the algae (Marlowe 1984). Brassell et al. (1986) introduced the temperature-dependent alkenone unsaturation index U^K₃₇ which, in a simplified form (U^{K'}₃₇), uses the di- and triunsaturated C₃₇ alkenones only (Prahl and Wakeham 1987):

$$U^{K'}_{37} = [C_{37:2}] / [C_{37:2} + C_{37:3}]$$

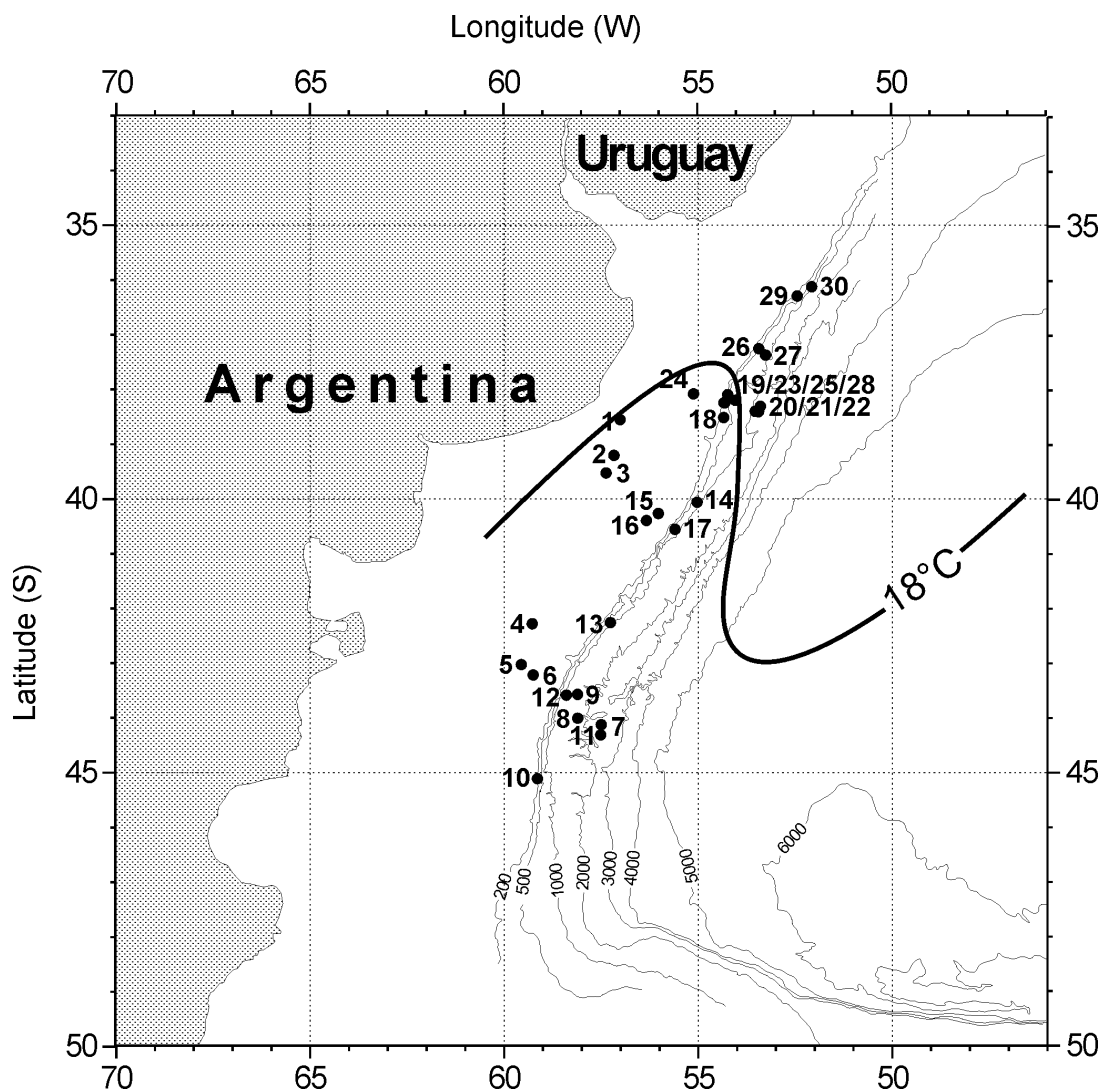


Fig. 2.34: Locations of water samples for alkenone analysis according to Table 9. The 18°C isotherm roughly gives the location of the Brazil-Malvinas Confluence as obtained from satellite-derived sea surface temperatures on February 09, 2001.

Benthien and Müller (in press) have compared alkenone-derived SSTs obtained from surface sediments along the southern Argentine continental slope and deep basin, between 35° and 48° S, to modern atlas temperatures of overlying surface waters (Levitus and Boyer, 1994) using the global core top calibration of Müller et al. (1998) to convert $U^{K'}_{37}$ ratios into temperatures. They found that sediments from the region of the Brazil-Malvinas Confluence (35-39°S) and the Argentine continental slope between 41° and 48°S generally show lower alkenone temperatures by 3-6°C relative to annual mean atlas SSTs. As the most likely cause for the anomalously low $U^{K'}_{37}$ values Benthien and Müller (in press) suggest lateral displacement of suspended particles and sediments by strong northward surface and bottom currents, benthic storms, and downslope processes.

To further assess the regional SST/ $U^{K'}_{37}$ relationship and possible displacement of particles carrying a cold water $U^{K'}_{37}$ signal of coastal or southern origin, the particulate suspended matter of 30 surface water samples was filtered (Tab. 2.10, Fig. 2.34). At each location 84 to 1000 l of surface water were sampled with the vessel's membrane pump. The water was passed through glass fiber filters (GMF 5, Sartorius AG) to obtain the suspended particulate matter. Before use filters were heated at 400°C for 18 h to remove organic compounds. After filtering all samples were frozen immediately and stored at -20°C for later shore-based analysis.

Table 2.10: Locations of surface water samples for alkenone analysis.

No.	Date 2000	Local Time	(UTC = L.T.+ 3 h)	Latitude South	Longitude West	SST [°C]	SSS [‰]	Liters	Remarks
1	14.2.01	13:12	Beginning	38°55.14	57°01.52	18.4	33.6499	390	
		14:10	End	39°05.38	57°07.90	18.1	33.6415		
2	14.2.01	15:32	Beginning	39°20.35	57°17.36	18.2	33.6344	330	
		16:30	End	39°30.42	57°23.74	18.1	33.6583		
3	14.2.01	18:40	Beginning	39°52.53	57°37.69	17.5	33.7400	650	
		20:11	End	40°07.87	57°47.51	17.2	33.7611		
4	15.2.01	9:57	Beginning	42°27.93	59°27.82	15.9	33.7152	1000	
		12:06	End	42°47.31	59°47.28	15.2	33.7164		
5	15.2.01	14:33	Beginning	43°02.54	59°56.08	15.2	33.7160	650	
		16:19	End	43°09.71	59°45.03	15.4	33.8220		
6	15.2.01	19:10	Beginning	43°21.51	59°25.44	13.9	33.8944	305	
		20:13	End	43°25.55	59°17.86	13.5	33.8652		
7	16.2.01	8:20	Beginning	44°12.15	57°50.12	13.3	34.0990	400	
		9:42	End	44°17.46	57°40.10	13.8	34.0775		
8	17.2.01	9:19	Beginning	43°58.22	58°39.85	13.4	34.1001	370	
		10:17	End	43°55.53	58°31.87	13.5	34.1121		
9	18.2.01	9:12	Beginning	44°00.43	58°10.81	13.3	34.0879	410	
		10:27	End	43°58.35	58°03.87	13.4	34.0738		
10	19.2.01	9:40	Beginning	45°10.83	59°14.37	11.0	34.0824	353	
		11:01	End	45°01.29	58°57.88	9.3	34.0893		
11	20.2.01	8:04	Beginning	44°30.86	57°51.49	13.2	34.0845	516	
		9:53	End	44°30.48	57°47.47	13.2	34.0786		
12	21.2.01	10:54	Beginning	43°56.86	58°11.12	13.3	34.0840	460	
		12:15	End	43°03.77	58°05.37	13.2	34.0870		
13	22.2.01	12:07	Beginning	42°25.80	57°26.46	12.8	34.0928	410	
		13:08	End	42°14.56	57°26.47	12.4	34.0814		
14	23.2.01	17:30	Beginning	40°06.00	55°03.14	14.2	34.1163	523	
		19:32	End	40°54.66	56°02.87	13.8	34.1087		
15	24.2.01	16:01	Beginning	40°26.52	56°02.87	12.9	33.7772	400	
		17:03	End	40°32.50	55°58.77	13.0	33.6555		
16	25.2.01	10:23	Beginning	40°39.39	56°33.51	12.7	33.9045	340	
		12:52	End	40°46.26	56°16.83	12.8	33.8331		
17	26.2.01	8:05	Beginning	40°55.54	55°59.95	12.2	33.9535	573	
		9:40	End	41°00.43	56°04.47	11.4	34.0057		
18	27.2.01	12:10	Beginning	38°51.31	54°34.51	14.3	33.9031	950	
		13:59	End	38°43.21	54°33.39	16.2	33.7598		
19	27.2.01	19:05	Beginning	38°19.84	54°04.55	18.7	33.7317	400	
		20:10	End	38°15.07	53°58.92	19.8	33.6987		
20	28.2.01	0:14	Beginning	38°30.71	53°39.92	21.3	32.6490	500	
		1:11	End	38°37.03	53°42.93	20.1	32.9764		
21	28.2.01	1:46	Beginning	38°40.80	53°44.70	19.1	33.7900	110	
		2:09	End	38°42.69	53°46.45	19.0	33.7393		
22	28.2.01	3:19	Beginning	38°39.94	53°53.39	18.1	33.8229	84	
			End	38°38.81	53°57.19	17.7	33.7807		
23	28.2.01	8:27	Beginning	38°24.67	54°32.02	17.9	33.7304	121	18° confluence boundary
			End	38°23.40	54°35.14	17.9	33.7424		
24	28.2.01	13:58	Beginning	38°08.18	55°12.50	17.0	33.6962	87	
		14:22	End	38°07.18	55°14.97	16.9	33.6262		
25	28.2.01	23:21	Beginning	38°09.49	54°24.16	18.5	33.8044	92	
		0:05	End	38°10.87	54°18.30	18.9	33.6960		
26	1.3.01	10:14	Beginning	37°25.61	53°44.16	23.2	29.5686	208	
		11:09	End	37°21.24	53°41.04	23.3	29.5057		
27	2.3.01	10:34	Beginning	37°37.24	53°26.76	23.2	34.7968	280	
		11:22	End	37°34.90	53°32.47	23.5	33.5064		
28	3.3.01	12:23	Beginning	38°24.30	54°33.94	19.0	33.8606	131	
		14:17	End	38°24.22	54°33.20	19.7	33.7964		
29	4.3.01	8:54	Beginning	36°29.26	52°45.01	22.5	35.6022	441	
		11:39	End	36°26.57	52°23.75	22.2	35.4218		
30	5.3.01	8:23	Beginning	36°12.48	52°07.82	24.5	30.2854	210	
		9:08	End	36°09.05	52°12.40	24.7	31.5406		

2.5 Ship's Meteorological Station

Fair, high pressure influenced weather dominated the transit from Montevideo to area „A“. Weather conditions in study area A itself were more variable. Coldfronts of subpolar lows moved from Patagonia eastward in rapid succession. While at the front the northwest wind periodically increased up to 7, in short times even up to 9 Bft, at the rear a southwesterly wind about 6 Bft occurred. The sea achieved a height of 4 meter for a time. At the intermediate high pressure wedges the wind decreased to 4 Bft.

Air temperatures barely exceeded 15 °C due to the coupling to the water temperature which in turn is dominated by the cold Falkland/Malvinas Current. The same situation was met in study area „B“.

During the works in study area „B“ a long-term change in weather took place. By a laterally extended strong rise in pressure over the southwestern Atlantic a more permanent high was build. It reached a maximum in the middle of the 9th week with more than 1035 hPa. Between this high and lower pressure over Patagonia a northeasterly to northerly air stream of temporarily up to 6 Bft stabilized. A swell of up to 3 meters came from the same direction. At the change of the month a subpolar coldfront moved eastward, was blocked by the high just northeasterly of the working area and caused heavy rain with northerly wind up to 8 Bft at 01.03.2001 for a short time. Consecutive pressure rising build up a ridge of high pressure with variable winds between 2 and 4 Bft which changed in a light to moderate northwesterly air stream at weekend.

The last days before the arrival in Montevideo were marked by slight pressure contrasts. From an airmass border extending from Argentina to southeast weaken thunderstorm lows started off and moved to the sea.

At 21st February an impressive cloud phenomenon could be observed. Lenticularis clouds which are normally observed at the altocumulus-level formed the appearance of the stratocumulus for about one hour. Also rotors, fat mamatus bags and radial cloud scraps could be seen. Gravity waves produced by the Andes could be supposed as the origin.

2.6 Acknowledgements and Concluding Remarks

Almost all of the research goals could be achieved during R/V METEOR Cruise M49/2. This is in particular a great success, when the complex sedimentary environment of the Argentine continental margin is considered.

This success was only possible due to the perfect cooperation and technical assistance of Captain Kull, his officers and crew, which we gratefully acknowledge. We also like to thank the Leitstelle METEOR at the University of Hamburg.

The work was funded by the Deutsche Forschungsgemeinschaft within the scope of the Sonderforschungsbereich 261 at the University of Bremen.

2.7 References

- Benthien, A., Müller, P.J. (in press): Anomalously low alkenone temperatures caused by lateral particle and sediment transport in the Malvinas Current region, western Argentine Basin. *Org. Geochem.*
- Bleil, U. and cruise participants. Report and preliminary results of METEOR-Cruise M 49/3, Montevideo - Salvador, 09.03. - 01.04.2001. Berichte, Fachbereich Geowissenschaften, Universität Bremen, Bremen, in prep.
- Bleil, U. and cruise participants 2001. Report and preliminary results of METEOR-Cruise M 46/3, Montevideo - Mar del Plata, 04.01. - 07.02.2000. Berichte, Fachbereich Geowissenschaften, Universität Bremen, 172, 161 pp., Bremen.
- Brassell, S.C., Eglinton, G., Marlowe, I.T., Pflaumann, U., Sarnthein, M. (1986): Molecular stratigraphy: a new tool for climatic assessment. *Nature* 320, 129-133.
- Ewing, M. and Lonardi, A. G. 1971. Sediment transport and distribution in the Argentine Basin. 5. Sedimentary Structure of the Argentine Margin, Basin, and related provinces. *In* L. H. Ahrens et al. (Eds.) *Physics and Chemistry of the Earth*, 8, 123 - 251, Pergamon Press, Oxford.
- Graham, G., and Mazzullo, 1988. Handbook for shipboard sedimentologists. ODP Technical Note No. 8, p. 67.
- Grant, J. A., and Schreiber, R. 1990. Modern swath sounding and sub-bottom profiling technology for research applications: The Atlas Hydrosweep and Parasound Systems, *Marine Geophysical Researches*, 12, 9 - 19.
- Hinz, K., Neben, S., Schreckenberger, B., Roeser, H. A., Block, M., Goncalves de Souza, K. and Meyer, H. 1999. The Argentine continental margin north of 48°S: sedimentary successions, volcanic activity during breakup, *Marine and Petroleum Geology*, 16, 1 - 25.
- Levitus, S., Boyer, T. (1994): *World Ocean Atlas. 4: Temperatures*, NOAA Atlas NESDIS 4. U.S. Government Printing Office.
- Lonardi, A. G. and Ewing, M. 1971. Sediment transport and distribution in the Argentine Basin. 4. Bathymetry of the continental margin, Argentine Basin and other related provinces, canyons and sources of sediments. *In* L. H. Ahrens et al. (Eds.) *Physics and Chemistry of the Earth*, 8, 79 - 121, Pergamon Press, Oxford.
- McCoy, F. W. and Zimmermann, H. B. 1977. A history of sediment lithofacies in the South Atlantic. *In* Supko, P. R. and Perch-Nielsen, K. (Eds.) *Initial Reports of the Deep Sea Drilling Project*, 39, 1047 - 1079, Washington (U.S. Government Printing Office).
- Marlowe, I.T. (1984): Lipids as paleoclimatic indicators. Ph.D. Thesis, University of Bristol, Bristol, 273 pp.
- Müller, P.J., Kirst, G., Ruhland, G., von Storch, I., Rosell-Melé, A. (1998): Calibration of the alkenone paleotemperature index U^{K}_{37} based on core-tops from the eastern South Atlantic and the global ocean (60°N-60°S): *Geochim. Cosmochim. Acta* 62: 1757-1772.
- Parker, G., Paterlini, M. C., and Violante, R. A. (1997). El fondo marino. *El Mar Argentino y sus recursos pesqueros* 1: 65-87.
- Peterson, R. G. and Stramma, L. 1991. Upper-level circulation in the South Atlantic Ocean. *Prog. Oceanogr.*, 26, 1 - 73.
- Prahl, F.G., Wakeham, S.G. (1987). Calibration of unsaturation patterns in long-chain ketone compositions for paleotemperature assessment. *Nature* 330: 367-396.
- Segl, M. and cruise participants 1994. Report and preliminary results of METEOR-Cruise M 29/1, Buenos-Aires - Montevideo, 17.6. - 13.7.1994. Berichte, Fachbereich Geowissenschaften, Universität Bremen, 58, 94 pp., Bremen.

- Smith, W. H. F., Sandwell, D. T., 1997. Global seafloor topography from satellite altimetry and ship depth soundings. *Science*, 277, 1956 - 1962.
- Spieß, V. and cruise participants. Report and preliminary results of METEOR-Cruise M 49/1, Capetown - Montevideo, 04.01. - 10.02.2001. *Berichte, Fachbereich Geowissenschaften, Universität Bremen, Bremen*, in prep.
- Spieß, V. 1993, *Digitale Sedimentechographie - Neue Wege zu einer hochauflösenden Akustostratigraphie*. *Berichte, Fachbereich Geowissenschaften, Universität Bremen*, 35, 199 pp., Bremen (Habilitationsschrift).
- Stockwell, J. W. 1997. Free software in education: A case study of CWP/SU: Seismic Un*x, *Leading Edge*, 16, 1045-1049.
- Wessel, P. and Smith, W. H. F. 1998. New, improved version of Generic Mapping Tools released, *EOS Transactions, American Geophysical Union*, 79, 579, 1998.